Genetic and Biochemical Analysis of the Mammalian Spindle Assembly Checkpoint

by

Max C. Dobles

B.S. Biology
Swarthmore College, 1991

Submitted to the Department of Biology
In Partial Fulfillment of the Requirements for the Degree of

Doctor of Philosophy in Biology
At the
Massachusetts Institute of Technology

June 2001

Signature of Author: _____
Department of Biology
May 17, 2001

Certified by: _____
Peter K. Sorger
Associate Professor of Biology
Thesis Supervisor

Accepted by: _____
Alan Grossman
Professor of Biology
Chairman, Committee for Graduate Students

Genetic and Biochemical Analysis of the Mammalian Spindle Assembly Checkpoint

by

Max C. Dobles

Submitted to the Department of Biology on May 17, 2001, in Partial Fulfillment of the Requirements for the Degree of Doctor of Philosophy in Biology

ABSTRACT

Chromosome segregation is a key event in the transmission of genetic information. Segregation errors lead to developmental abnormality and have been postulated to play a role in tumorigenesis by increasing genetic instability. The high fidelity of chromosome segregation in eukaryotes is ensured by the spindle assembly checkpoint, a surveillance system that links anaphase initiation to the completion of mitotic spindle assembly. To examine the consequences of loss of spindle checkpoint control in mammalian cells, we have used homologous recombination to delete the spindle checkpoint gene *Mad2* in mice. *Mad2*$^{-/-}$ embryos exhibit widespread apoptosis and die *in utero* approximately six days after conception. Cells from *Mad2*$^{-/-}$ early embryos fail to arrest in response to drug-induced mitotic spindle damage, indicating loss of checkpoint function. *Mad2*$^{-/-}$ embryo cells also exhibit a high rate of chromosome loss even in the absence of exogenously-induced spindle damage, thus demonstrating a requirement for the spindle checkpoint during normal mitosis. *Mad2*$^{+/-}$ mice show a dramatic increase in the development of lung tumors, consistent with a tumor suppressor role for genes that maintain genomic stability. To better understand the molecular events of the spindle checkpoint pathway, we have mapped the Mad2-binding sites of two proteins in the pathway, Mad1 and Cdc20, and shown that both interact with a common site of Mad2. These results demonstrate the consequences of loss of spindle checkpoint function in mammalian cells and provide an understanding of molecular interactions that will aid in the design of mutations for more sophisticated genetic experiments.

Thesis Supervisor: Peter K. Sorger
Title: Associate Professor of Biology

Max Dobles

EDUCATION

1994 -2001 Massachusetts Institute of Technology Cambridge, MA
Ph.D. June 2001. Department of Biology. Thesis: Genetic and Biochemical Analysis of the Mammalian Spindle Assembly Checkpoint

1987-1991 Swarthmore College Swarthmore, PA
B.A. in Biology, 1991

RESEARCH EXPERIENCE

1995-2001 Massachusetts Institute of Technology
Principal Investigator: Peter Sorger

1992-1994 University of California San Diego
Principal Investigator: John Newport

1990 Carnegie Mellon University
Principal Investigator: D. Lansing Taylor

PUBLICATIONS

Michel, LS, Liberal, V, Chatterjee, A, Kirchwegger, R, Pasche, B, Gerald, W, Dobles, M, Sorger, PK, Murty, VV, and Benezra, R. (2001) *MAD2* Haplo-insufficiency Causes Premature Anaphase and Chromosome Instability in Mammalian Cells. *Nature* 409: 355-359.

Dobles, M, and Sorger, PK. (2000) Mitotic Checkpoints, Genetic Instability, and Cancer. *Cold Spring Harbor Symposia on Quantitative Biology. In press.*

Dobles, M, Liberal, V, Scott, ML, Benezra, R, and Sorger, PK. (2001) Chromosome Missegregation and Apoptosis in Mice Lacking the Mitotic Checkpoint Protein Mad2. *Cell* 101: 635-645.

Sorger, PK, Dobles, M, Tournebize, R, and Hyman, AA. (1997) Coupling Cell Division and Cell Death to Microtubule Dynamics. *Current Opinion in Cell Biology* 9: 807-814.

Acknowledgements

I owe a great debt of gratitude to Peter for accepting me into his lab and creating an environment for exciting and productive research. I have greatly valued your guidance in times of my confusion, enthusiastic optimism in times good and bad, and your support and faith through everything.

Thank you to the members of my defense committee for participating in my thesis defense. David and Tyler, your ideas and perspectives have been a great source of support and inspiration. I could not have asked for more enjoyable thesis meetings than those we have had.

Thanks to all the members of the Sorger lab for the years of support, intellectual community, and fun. Especially to Ken Kaplan for being the Answer Man every single day. Our nights in pursuit of knowledge with Steve Earle on 11 remain my best memories of graduate school. And also to Rob Hagan, whose unbridled enthusiasm in regard to every aspect of biology and human existence has been both inspirational and amusing.

Thanks also to all the people throughout the MIT biology department who have helped me continuously on many levels. Most of all to Martin Scott for bringing me into the mouse world, and to Barbara Panning for providing me with an apprenticeship in the analysis of embryos.

I am deeply indebted to all of you who read drafts of this thesis and helped rescue it. Aurora Burds, Chris Espelin, Suzanne Gaudet, Ilya Goldberg, Emily Gillett, Xiangwi He, Kim Mercer, Ulrik Nielson, Annegret Schulze-Lutum, Kim Simons, Alicyn Sconiers, Jessica Tytell – I would be in trouble without you.

Mom, Dad, and Michael, thanks for putting me in position to pursue whatever my heart desires. Your constant support has been invaluable.

I am most grateful to Alicyn, for everything. For keeping me human during what at times felt like an inhuman process. For your patience. For your excitement during successes, and for always giving me reason to believe we're going to have a good life no matter what the next gel looks like.

Table of Contents

Sections of this chapter were adapted, with permission, from Dobles and Sorger, 2001.

Dobles, M, and Sorger, PK. (2001) Mitotic Checkpoints, Genetic Instability, and Cancer. *Cold Spring Harbor Symposia on Quantitative Biology. In press.*

Chapter 1: Introduction

Introduction Outline

A. Mitotic spindle assembly

B. Cell cycle checkpoints

C. The spindle assembly checkpoint

C.1 Players of the spindle assembly checkpoint

C.2 The input and output of the spindle assembly checkpoint signaling pathway

C.3 The spindle assembly checkpoint signaling pathway

C.4 Essential nature of the spindle assembly checkpoint

D. Consequences of chromosome missegregation in metazoans

D.1 Organismic consequences of chromosome missegregation

D.2 Cellular consequences of chromosome missegregation

A. Spindle Assembly

All eukaryotes use a self-assembling mitotic spindle to segregate newly replicated chromosomes to daughter cells. The spindle assembles as microtubules radiating from two poles form three classes of attachments: anti-parallel attachment of microtubules from opposite poles, attachment to the cell cortex, and attachment to chromosomes via kinetochores (Figure 1-1). Segregation of sister chromatids in opposite directions requires that each pair of sister chromatids first forms bivalent attachment to microtubules, that is, the kinetochore of one chromatid attaches to microtubules from one spindle pole, and the kinetochore of the sister chromatid attaches to microtubules from the opposite pole. Achieving bivalent attachment for each pair of sister chromatids does not result from a series of ordered steps, but rather from a stochastic process of chance encounters between microtubules and kinetochores (Hyman and Karsenti 1996; Nicklas 1997). This section describes the process of spindle assembly, focusing on the properties and interactions of

Figure 1-1. Microtubule interactions in mitotic spindle assembly. The mitotic spindle assembles as highly dynamic microtubules radiating from two spindle poles form three classes of attachments. Kinetochore microtubules bind to centromere-localized kinetochores (A) and provide the mechanism to segregate chromosomes pole-ward during anaphase. Microtubules from opposite poles form anti-parallel attachment (B) to help maintain spindle morphology. Astral microtubules form attachments to the cell cortex (C) and serve to orient the spindle.

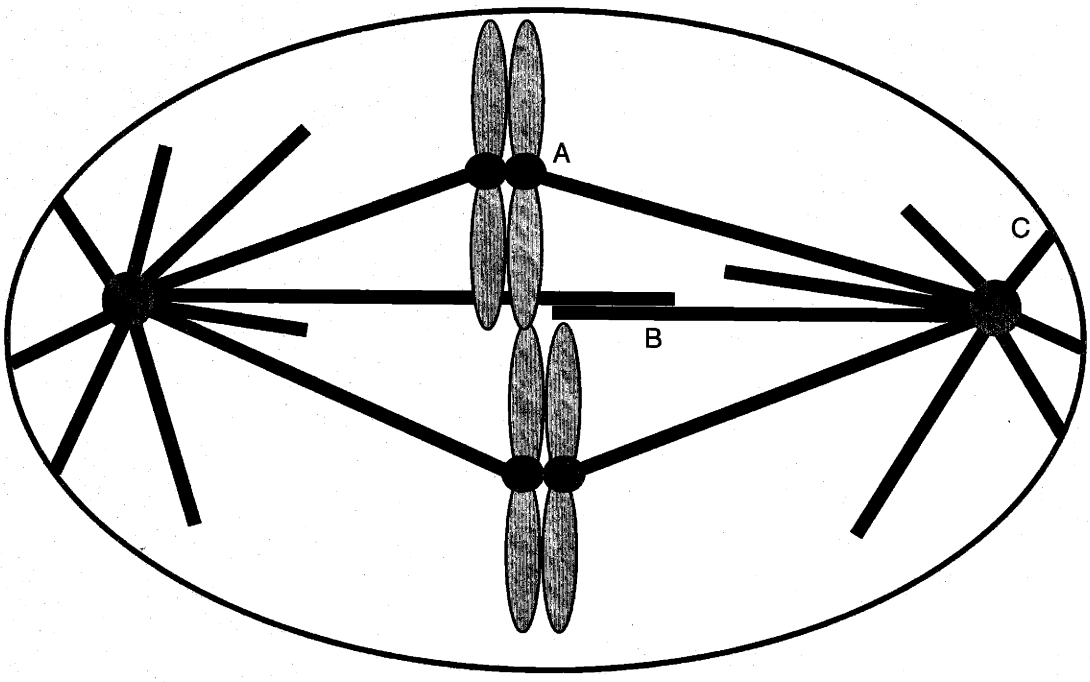
A
B
C

microtubules and kinetochores.

Spindle assembly is dependent on the dynamic nature of microtubules. Microtubules assemble via the GTP-dependent polymerization of αβ-tubulin heterodimers into linear protofilaments arranged to form hollow filaments 25nm in diameter (Amos and Klug 1974; Weisenberg and Deery 1976). The asymmetry of tubulin heterodimers creates an intrinsic microtubule polarity, with the spindle pole-embedded α-tubulin (-) ends being relatively stable, and the β-tubulin (+) ends exhibiting transitions between growth and shrinkage, termed "dynamic instability" (Allen and Borisy 1974; Fan et al. 1996; Mitchison and Kirschner 1984; Mitchison 1993). Microtubule dynamics are based on four factors: rates of polymerization and depolymerization, the catastrophe frequency (the switch from growth to shrinkage), and the rescue frequency (the switch from shrinkage to growth) (Mitchison and Kirschner 1984). As cells transition from interphase to mitosis, an increase in the catastrophe frequency results in an approximately ten-fold increase in microtubule turnover (Belmont et al. 1990; Mitchison et al. 1986; Schulze and Kirschner 1986; Verde et al. 1992). Two proteins have been shown to promote catastrophe in mitosis: KCM1/MCAK, which disrupts the interaction of protofilaments at the (+) ends of microtubules, and Op18/Stathmin, which sequesters tubulin and may also function by a similar mechanism as MCAK (Belmont and Mitchison 1996; Desai et al. 1999; Howell et al. 1999; Walczak et al. 1996). However, *Xenopus* KCM1 exhibits similar activity levels in both interphase and mitosis and it has thus been proposed that the mitotic change in microtubule dynamics occurs by down regulation of the microtubule associated proteins (MAPs) that promote microtubule stability by increasing polymerization rates, suppressing catastrophe, and promoting

rescue (Pryer et al. 1992; Tournebize et al. 2000). This model is supported by the demonstration that the *Xenopus* MAPs XMAP215, 230, and 310 exhibit decreased binding to microtubules in mitotic extracts as compared to interphase extracts, and that the mitotic MAPs are less potent at microtubule stabilization (Andersen 1998). Furthermore, *in vitro* phosphorylation of mammalian MAP4 by the mitotic kinase CDK1 negatively regulates microtubule-stabilizing activity (Ookata et al. 1995). The resulting shift towards increased catastrophe and microtubule turnover creates dense arrays of shorter, more dynamic microtubules that are highly effective in the search for kinetochores (Hayden et al. 1990; Holy and Leibler 1994).

Kinetochores are multi-protein complexes at centromeres that mediate the binding and movement of chromosomes at the dynamic (+) ends of microtubules (Hyman and Sorger 1995). Although the kinetochore proteins that directly interact with microtubules have not been identified, attention has focused on the (-) end-directed microtubule motor protein cytoplasmic dynein, and the kinesin family proteins that exhibit both (+) and (-) end-directed motor activity (McDonald et al. 1990; Paschal and Vallee 1987; Vale et al. 1985b). These proteins use the energy of ATP hydrolysis to translocate along microtubules, and thus can provide both mechanical force for chromosome movement as well as a mechanism for maintaining attachment to the dynamic (+) end of a microtubule (Paschal et al. 1987; Scholey et al. 1989; Vale et al. 1985a). Studies in animal cells have demonstrated the presence of two microtubule motor proteins at kinetochores: dynein and the kinesin protein CENP-E (Pfarr et al. 1990; Steuer et al. 1990; Yen et al. 1992). Antibodies against CENP-E inhibit *in vitro* movement of chromosomes at the (+) end of depolymerizing microtubules (Lombillo et al. 1995), and in human cells microtubule-

kinetochore attachment and chromosome movement are disrupted by injection of anti-CENP-E antibodies, expression of a dominant negative mutant, or antisense expression (Schaar et al. 1997; Yao et al. 2000). Similarly, injection of anti-dynein antibodies in *Drosophila* embryos disrupts microtubule-kinetochore attachment and poleward chromosome movement during anaphase (Sharp et al. 2000). However, this picture is complicated by studies showing that chromosomes attach and move normally in human cells injected with anti-dynein antibodies (Vaisberg et al. 1993), and that in insect spermatocytes most kinetochore dynein is lost soon after microtubule attachment (King et al. 2000). The role of dynein, CENP-E, and other kinetochore proteins in microtubule-kinetochore attachment and the complex movement of chromosomes during mitosis remains a challenging area of active research.

The ultimate goal of spindle assembly is the formation of bivalent attachment for every pair of sister chromatids. Initial kinetochore attachment along the length of a single microtubule is followed by the rapid transport of the sister chromatid pair towards the spindle pole (Rieder and Alexander 1990). In animal cells the high density of microtubules at the spindle pole results in the (+) end attachment of 20-30 additional microtubules to the kinetochore (Brinkley and Cartwright 1971; McEwen et al. 1997), and also pushes the chromatid pair out towards the opposite pole (Rieder et al. 1986; Theurkauf and Hawley 1992). The unattached kinetochore is automatically presented in the correct orientation for attachment to microtubules from the opposite pole because the tight adhesion of sister chromatids by the cohesin complex ensures that kinetochores face in opposite directions (Guacci et al. 1997; Michaelis et al. 1997; Nicklas 1997). The time required to make bivalent attachment for every pair of sister chromatids in mammalian

cells varies between approximately one and several hours because it is dependent on a series of stochastic events (Hyman and Karsenti 1996; Rieder et al. 1994). This variability necessitates a mechanism to ensure that anaphase initiation does not occur prior to the completion of spindle assembly. This is accomplished by a cell cycle checkpoint that links anaphase initiation to the completion of spindle assembly.

B. Cell Cycle Checkpoints

Faithful transmission of genetic information requires correct temporal ordering of key cell cycle events. For example, it is crucial that DNA replication is completed prior to chromosome segregation, and that segregation is completed before cells perform cytokinesis. Furthermore, maintaining the integrity of the genome requires that DNA damage is corrected prior to the initiation of replication and segregation. To ensure that these events proceed in the proper order, cells use cell cycle checkpoints to delay downstream events until upstream events have been completed. These regulatory pathways monitor the status of replication, DNA repair, and spindle assembly, and inhibit downstream cell cycle transitions until they have been completed (Hoyt et al. 1991; Li and Murray 1991; Weinert and Hartwell 1988).

The original paradigm for cell cycle checkpoints was provided by recognition that *S. cerevisiae rad9* mutation relieved the dependence of mitosis on the completion of DNA repair. Whereas wildtype cells exposed to low doses of X-ray irradiation arrest in G2, thus allowing time to repair the DNA damage before continuing the cell cycle, *rad9* cells fail to arrest and proceed to mitosis (Weinert and Hartwell 1988). Failure to arrest the cell cycle and repair damaged DNA results in increased lethality in the irradiated

cells. However, if irradiated *rad9* cells are also treated with nocodazole to delay chromosome segregation, cells are able to repair the damage and maintain high viability, indicating that a primary function of Rad9p is to induce an arrest that allows sufficient time for DNA repair. Interestingly, the *rad9* mutation does not negatively impact growth or viability in cells not exposed to DNA damaging reagents, although it does increase the rate of chromosome loss (Weinert and Hartwell 1988). These results suggest that the DNA damage checkpoint is not essential under normal conditions, but that it becomes critical under circumstances of severe DNA damage. These findings suggested a model of cell cycle checkpoints as non-essential backup systems that monitored normal cell processes and induced cell cycle arrest only in the relatively rare event of a problem (Hartwell and Weinert 1989; Weinert and Hartwell 1988).

The past 13 years have seen further elucidation of the pathways activated by DNA damage and incomplete replication, and the identification and characterization of a checkpoint pathway linking the initiation of anaphase to spindle assembly (Hoyt et al. 1991; Li and Murray 1991; Zhou and Elledge 2000). Research on these checkpoints suggests modification of the original model on two points. The first is that cell cycle arrest appears to be only one aspect of the multi-faceted responses of cells to the lesions that activate checkpoints. For example, DNA damage induces not only cell cycle arrest, but also the activation of repair pathways and apoptosis (Cortez et al. 1999; Lowe et al. 1993; Xu and Baltimore 1996). These responses to DNA damage utilize common pathways with the arrest pathway, and much work remains in understanding how these responses are related. The second point is that despite the demonstration that cell cycle checkpoints are non-essential in *S. cerevisiae*, genetic studies demonstrate that many

checkpoint genes are essential for viability in metazoans (Basu et al. 1999; Brown and Baltimore 2000; Kitagawa and Rose 1999; Liu et al. 2000). Although it is not yet clear which aspect of checkpoint responses are required for viability, several studies indicate that checkpoint-induced cell cycle arrest is not merely a rarely-utilized backup system, but rather is essential to correctly order events in normal cell cycles (Basu et al. 1998; Gorbsky et al. 1998; Kitagawa and Rose 1999) (see Section C.4). With these two modifications, the checkpoint model remains useful in cell cycle research, and current work focuses on identifying additional players, elucidating pathways, and investigating the consequences of loss of checkpoint control.

C. The Spindle Assembly Checkpoint

C.1 Players of the Spindle Assembly Checkpoint

Cells must complete spindle assembly prior to anaphase initiation to avoid permanent alterations to the genomes of both daughter cells and their future progeny. Successful ordering of these events in *S. cerevisiae* is evident by the high accuracy of chromosome segregation: less than one missegregation event occurs per 10^5 cell divisions (Hartwell et al. 1982). Early cytological studies in plant, insect, and animal cells demonstrated that anaphase initiates only after all chromosomes make bivalent attachment to spindle microtubules (Bajer and Mole-Bajer 1956; Nicklas 1967; Zirkle 1970). Furthermore, inhibition of spindle assembly with drugs that disrupt microtubule dynamics (such as taxol, benomyl, and nocodazole) induces pre-anaphase mitotic arrest in both yeast and animal cells (Fuchs and Johnson 1978; Jacobs et al. 1988; Zieve et al. 1980). These observations suggested the existence of a spindle assembly checkpoint that

ensures accurate chromosome segregation by preventing the initiation of anaphase until all chromosomes have made bivalent attachment to the mitotic spindle (McIntosh 1991).

A molecular understanding of the linkage between spindle assembly and anaphase began with genetic screens in *S. cerevisiae* designed to identify mutants that continue cell division at concentrations of benomyl sufficient to induce mitotic arrest in wildtype cells (Hoyt et al. 1991; Li and Murray 1991). Mutants identified in these screens died after a limited number of cell divisions in the presence of benomyl, and were named *mad1*, *2*, and *3* (mitotic arrest defective) and *bub1*, *2*, and *3* (budding uninhibited by benomyl); Bub2p was subsequently shown to be involved in a separate pathway that regulates mitotic exit rather than anaphase initiation (Alexandru et al. 1999; Fraschini et al. 1999; Li 1999). Failure to arrest in response to microtubule disruption suggested that *mad* and *bub* cells lack the capacity to respond to defects in spindle assembly. This interpretation has been supported by their failure to arrest in response to other methods of inhibiting spindle assembly, including the mutation of microtubule and kinetochore proteins and the mutation of centromeric DNA (Guenette et al. 1995; Pangilinan and Spencer 1996; Spencer and Hieter 1992; Strunnikov et al. 1995; Wang and Burke 1995). Although all *MAD* and *BUB* genes are non-essential in the absence of exogenously-induced spindle damage, *mad* cells exhibit an approximately 10-fold increase in chromosome loss under normal growth conditions (with another 1,000-fold increase when treated with benomyl) (Li and Murray 1991). The spindle assembly checkpoint of *S. cerevisiae* thus appears consistent with the originally proposed checkpoint model in that it serves as a backup system to prevent chromosome loss in the event of rare problems, but it is not required for accurate segregation in most mitoses (Hartwell and Weinert 1989).

Several genes involved in the spindle checkpoint have been discovered in addition to those identified in the original genetic screens. *MPS1* is essential for spindle pole duplication, but is also required for mitotic arrest in response to spindle disruption (Weiss and Winey 1996; Winey et al. 1991). The protein phosphatase 2A subunit Cdc55p maintains mitotic arrest in checkpoint-activated cells by preventing inhibitory phosphorylation of the cell cycle regulator Cdc28p. *S. cerevisiae cdc55* mutants are unable to prevent this phosphorylation, and cells with incomplete spindles are able to escape mitotic arrest via inactivation of Cdc28p mitotic activity (Minshull et al. 1996; Wang and Burke 1997). Whether Mps1p and the Mad and Bub proteins that activate mitotic arrest in response to spindle damage also regulate Cdc55p activity has not been examined. Additionally, studies with *Xenopus laevis* egg extracts and human tissue culture cells have demonstrated activation of the MAP kinases ERK2 and p38 upon nocodazole-induced arrest. In *Xenopus* extracts, addition of p38 (along with its activating partner MKK6) induces mitotic arrest, whereas inhibition of p38 or ERK2 inhibits nocodazole-induced mitotic arrest. (Minshull et al. 1994; Takenaka et al. 1997; Takenaka et al. 1998). Although these observations suggest the involvement of MAP kinases in the spindle checkpoint, how they function and whether they interact with the known checkpoint proteins is not yet known.

Recent studies suggest a subset of the bacculoviral inhibitor-of apoptosis (IAP) repeat proteins (BIRPs) may also function in the spindle checkpoint. Although evidence exists that eukaryotic IAP homologs inhibit apoptosis, research has also focused on their role in mitosis (Hay et al. 1995; Li et al. 1998; Speliotes et al. 2000; Uren et al. 1999). *bir1* mutation increases chromosome loss in *S. cerevisiae*, and results in a cut phenotype

in *S. pombe* (Uren et al. 1999; Yoon and Carbon 1999). Dominant negative and antisense expression of Survivin, the human homolog of *BIR1*, causes an increase in ploidy, and *C. elegans* embryos subject to BIR-1 RNA inhibition exhibit failure to complete chromosome segregation (Li et al. 1999; Speliotes et al. 2000). Consistent with a role in chromosome segregation, many BIRPs have been shown to localize to spindle microtubules and chromosomes, and *S. cerevisiae* Bir1p has been proposed to interact with the kinetochore protein Ndc10p (Li et al. 1998; Speliotes et al. 2000; Yoon and Carbon 1999). However, additional defects in these cells suggest BIRP function in a number of other mitotic processes. For example, RNA inhibition of BIR-1 in *C. elegans* causes defects in chromosome condensation and cytokinesis, and disruption of Survivin expression in human cells results in multipolar spindles (Fraser et al. 1999; Li et al. 1999; Speliotes et al. 2000). Thus, BIRPs may have no direct involvement in the spindle checkpoint, and segregation defects may arise not from premature anaphase initiation, but rather from the difficulty of segregating uncondensed chromosomes, or segregating chromosomes in cells with cytokinesis defects in the previous cycle. However, the status of the spindle checkpoint has not been directly tested in any of these mutants and it remains possible that the segregation defects result in part from failure to respond to defects in spindle assembly.

Identification of metazoan homologs to the yeast *MAD*, *BUB,* and *MPS1* genes demonstrates broad conservation of the spindle checkpoint pathway. Genetic disruption of *MAD2* and *BUB3* in mice, *mdf-1* (*mad1*) in *C. elegans*, and *bub1* in *Drosophila* abrogates mitotic arrest in response to drug-induced spindle damage (Basu et al. 1999; Dobles et al. 2000; Kalitsis et al. 2000; Kitagawa and Rose 1999). Although no genetic

studies have been performed with the metazoan homologs of *MPS1* (*Esk/TTK*) or *MAD3* (*BubR1*), injection of anti-BubR1 antibodies into HeLa cells reduces the incidence of mitotic arrest in response to nocodazole treatment (Chan et al. 1999). Checkpoint analysis in the past five years has thus benefited from the advantages of working with both yeast and higher eukaryotes. The ease of genetic experimentation in *S. cerevisiae* allows for the rapid analysis of checkpoint mutations *in vivo*, whereas the large size of chromosomes and spindles in metazoans allows direct observation of spindle assembly and chromosome dynamics, and has lead to an understanding of the cell biology of the checkpoint that would be impossible to achieve by analysis of yeast cells alone (Chen et al. 1999; Howell et al. 2000; Hwang et al. 1998; Martinez-Exposito et al. 1999).

C.2 The Input and Output of the Spindle Assembly Checkpoint Signaling Pathway

A pathway linking anaphase initiation to spindle assembly must have three components: a sensor for spindle assembly, a signal transmission system, and an output onto the cell cycle machinery that induces cell cycle arrest. Understanding of the pathway between sensor and output remains preliminary, but there is now a basic understanding of how cells detect problems with spindle assembly and how they induce mitotic arrest. This section will describe the evidence for microtubule-kinetochore attachment as the event monitored by the spindle checkpoint, and describe the cell cycle activity upon which cells impinge to achieve mitotic arrest. How the checkpoint pathway signals the status of kinetochore attachment to the cell cycle machinery will be described in the section that follows.

Several lines of evidence suggest that the checkpoint monitors the status of spindle assembly by sensing whether or not sister kinetochores have achieved bivalent attachment. The first type of evidence supporting this model comes from studies demonstrating mitotic arrest in response to treatments and mutations that directly disrupt kinetochores. Injection of antibodies against the kinetochore proteins CENP-A, B and C interferes with kinetochore morphogenesis and induces mitotic arrest in HeLa cells (Bernat et al. 1990; Tomkiel et al. 1994). In *S. cerevisiae*, mutation of centromeric DNA or the kinetochore proteins Ctf13p and Cep3p results in mitotic arrest (Pangilinan and Spencer 1996; Spencer and Hieter 1992; Strunnikov et al. 1995; Wang and Burke 1995). Furthermore, arrest in response to mutations in centromeric DNA and *Ctf13* is dependent on *MAD* and *BUB* genes (Pangilinan and Spencer 1996; Wang and Burke 1995), demonstrating that the arrest is mediated by the spindle checkpoint.

A second line of evidence comes from careful cytological observation of mitosis in cultured PtK_1 cells (Rieder et al. 1994). In 126 cells observed, the total time required for spindle assembly (from nuclear envelope breakdown to anaphase initiation) ranged from 23 minutes to over three hours. However, for all cells, anaphase initiated an average of 23 minutes (with a standard error mean of +/-1 minute) after bivalent attachment was achieved for the final sister chromatid pair. This temporal relationship between anaphase initiation and microtubule attachment to the last kinetochore, despite the three hour range in total time required for mitosis, suggests anaphase initiation is regulated specifically by the status of microtubule-kinetochore attachment. Additionally, in cells arrested with just one kinetochore unattached to microtubules, ablation of the unattached kinetochore with a laser releases the anaphase inhibition (Rieder et al. 1995). These results provide strong

evidence that the spindle checkpoint monitors the status of microtubule-kinetochore attachment, and that unattached kinetochores generate a signal negatively regulating anaphase.

Finally, the localization of checkpoint proteins specifically to unattached kinetochores in mammalian tissue culture cells and *Xenopus* egg extracts is consistent with the idea that the spindle checkpoint monitors microtubule-kinetochore attachment. All the Mad and Bub proteins, as well as the MAP kinase ERK2, localize to kinetochores during prophase (prior to the attachment of any microtubules) and when spindle assembly is prevented with high doses of drugs that prevent microtubule polymerization (Chen et al. 1996; Jablonski et al. 1998; Jin et al. 1998; Martinez-Exposito et al. 1999; Shapiro et al. 1998; Taylor and McKeon 1997; Zecevic et al. 1998). In prometaphase, when some kinetochores have attached to microtubules, both Mad2 and Bub3 localizes strongly only to those kinetochores that remain unattached (Martinez-Exposito et al. 1999; Waters et al. 1998). Monovalently attached sister chromatids also exhibit Mad2 and Bub3 staining only on the unattached kinetochore, demonstrating that checkpoint protein recruitment is dependent specifically on the lack of microtubule-kinetochore attachment.

Despite the clear importance of kinetochores in signaling incomplete spindle assembly, it still is not known what molecular events the checkpoint monitors. One possibility is that the checkpoint monitors the tension imposed on bivalently attached sister kinetochores by opposing microtubule-dependent pulling forces. Support for the idea that tension plays a role in checkpoint signaling derives from classic experiments in which a praying mantid spermatocyte arrested in meiosis with an unattached kinetochore could be induced to reenter the cell cycle by imposing tension on the maloriented

chromosome with a micro-needle (Li and Nicklas 1995). Consistent with this model, bivalent attachment of microtubules to sister chromatids induces significant stretching of kinetochores in both yeast and mammalian cells (He et al. 2000; Martinez-Exposito et al. 1999; Waters et al. 1998). These observations raise the question of how cells could recognize the difference between stretched and unstretched kinetochores. Reactivity of the 3F3/2 antibody specifically against kinetochores not under tension suggests an answer by demonstrating a molecular difference between attached and unattached kinetochores (Gorbsky and Ricketts 1993; Nicklas et al. 1995; Waters et al. 1998). Although the protein recognized by 3F3/2 remains unknown, the antibody was originally identified in a screen against phosphorylated mitotic proteins, and kinetochore staining requires treatment with the phosphatase inhibitor microcystin (Gorbsky and Ricketts 1993; Nicklas et al. 1995). These observations suggest unattached kinetochores possess a phospho-epitope that is lost soon after tension is imposed by bivalent attachment.

A second possibility is that the checkpoint monitors microtubule-kinetochore attachment by sensing whether or not microtubule-binding sites on a kinetochore are fully occupied. This model is suggested by studies demonstrating that in HeLa and PtK_1 cells, Mad2 and Bub3 kinetochore localization is dependent directly on microtubule binding rather than on the tension resulting from bivalent attachment (Martinez-Exposito et al. 1999; Waters et al. 1998). Separation of attachment and tension can be achieved by treating metaphase cells with very low doses of the microtubule-stabilizing drug taxol, thus releasing the tension on bivalently attached chromosomes by inhibiting microtubule dynamics. In PtK_1 metaphase cells, nocodazole treatment that depolymerizes microtubules results in re-recruitment of Mad2, but taxol treatment that eliminates

tension while allowing maintenance of microtubule attachment does not. Likewise, taxol-treated metaphase HeLa cells fail to regain the Bub3 staining characteristic of unattached kinetochores not under tension. The relatively low Mad2 and Bub3 kinetochore staining in taxol-arrested cells suggests that lack of tension is insufficient for full recruitment of checkpoint proteins. Furthermore, an inverse correlation has been observed between the number of bound microtubules and the level of Bub3 staining at kinetochores in HeLa cells (Martinez-Exposito et al. 1999). These results suggest that microtubule binding, rather than the tension on kinetochores created by bivalent microtubule attachment, may play the key role in regulating recruitment of checkpoint proteins to kinetochores.

Results from analysis of MAD2 in maize cells suggest a resolution to these different models of how cells detect bivalent attachment. Whereas MAD2 kinetochore localization in mitosis is dependent on microtubule binding, localization in meiosis is dependent on the state of tension on kinetochores (Yu et al. 1999). These results suggest the difference observed between praying mantid spermatocytes and mammalian cells reflects differences between meiotic and somatic cells. It has been suggested that the different meiotic and somatic cell requirements for attachment and tension are due to differences in chromosome geometry (Nicklas 1997). The sister kinetochores of mitotic chromosomes face in opposite directions and lie buried deep within the surrounding chromatin, and thus are accessible to microtubules over only a relatively narrow range of angles. Once one kinetochore has made microtubule attachment, this geometry makes it difficult for the opposite kinetochore to bind microtubules from the same pole. Thus, making anaphase initiation dependent merely on microtubule attachment to all kinetochores will ensure accurate segregation in most cases. In contrast, kinetochores of

homologous meiotic chromosomes are both more exposed and farther apart from each other, and thus more easily accessible to microtubules from the same pole. In these cells, making anaphase initiation dependent on kinetochore tension is required to ensure bivalent attachment (Nicklas 1997). However, it remains possible that both microtubule binding and kinetochore tension contribute to regulation of checkpoint activation in both types of cells.

Activation of the spindle checkpoint induces mitotic arrest by inhibiting the Anaphase Promoting Complex (APC). The APC is an E3 ubiquination complex that regulates both anaphase initiation and mitotic exit. These distinct roles for APC are regulated by two associated proteins: Cdc20p promotes anaphase initiation and Cdh1p promotes mitotic exit (Visintin et al. 1997). Cdc20-APC targets Pds1p/Securin for ubiquination and degradation, releasing the Esp1p/Separin protease to cleave the cohesin protein Scc1p, thus allowing sister chromatid separation and anaphase to occur (Cohen-Fix et al. 1996; Uhlmann et al. 1999; Uhlmann et al. 2000; Visintin et al. 1997). Regulation of Cdc20-APC activity by the spindle checkpoint was suggested by two-hybrid screens revealing interaction between Mad2p and Cdc20p in *S. cerevisiae* and *S. pombe* (Hwang et al. 1998; Kim et al. 1998), and by co-immunoprecipitation of both proteins with the APC in mammalian cells (Fang et al. 1998; Li et al. 1997; Wassmann and Benezra 1998). Support for this hypothesis was provided by demonstration that *cdc20* mutations that disrupt Mad2p-Cdc20p co-immunoprecipitation from yeast cells also prevent mitotic arrest in response to anti-microtubule drugs (Hwang et al. 1998; Kim et al. 1998). Furthermore, APC-dependent ubiquination in *Xenopus* egg extracts can be inhibited with bacterially expressed human Mad2 (Fang et al. 1998). In addition to the

clear role for Mad2 in spindle checkpoint-dependent APC inhibition, two-hybrid screening with yeast Cdc20p has revealed interactions with Mad1p and Mad3p (Hwang et al. 1998). Also, immunoprecipitation of BubR1 from HeLa cells co-precipitates the APC subunits Cdc16, Cdc27, and APC7 (Chan et al. 1999). These interactions suggest checkpoint proteins in addition to Mad2 may directly contribute to the regulation of APC-dependent ubiquination. Recognition of the molecular link between checkpoint proteins and regulation of anaphase initiation provides a broad outline of the checkpoint pathway: kinetochores unattached to microtubules signal incomplete spindle assembly by recruiting checkpoint proteins that then establish a signaling pathway culminating in the inhibition of Cdc20-APC activity (Amon 1999).

Current models suggest that checkpoint activation induces conformational and oligomeric changes in Mad2 that activates it for inhibiting Cdc20-APC. Sizing chromatography of bacterially expressed human Mad2 or cell extracts from *S. cerevisiae* demonstrates that Mad2 exists both as a monomer and oligomer (Chen et al. 1999; Fang et al. 1998). Although monomeric human Mad2 binds Cdc20 (Luo et al. 2000), only the oligomeric form inhibits APC-dependent ubiquination in *Xenopus* egg extracts and induces mitotic arrest when injected into 2-cell *Xenopus* embryos (Fang et al. 1998). Interestingly, the monomeric Mad2 can be converted into the oligomeric form by gentle denaturation and refolding, suggesting that the two states result from differences in protein conformation (Fang et al. 1998). NMR analysis of the hMad2-Cdc20 interaction demonstrates a global change in Mad2 conformation upon binding, and in particular that binding induces a restructuring of the carboxyl-terminal flexible tail (Luo et al. 2000). Deletion of this tail in either human Mad2 or *S. cerevisiae* Mad2p abrogates human

Cdc20 and *S. cerevisiae* Mad1 binding, raising the possibility that Mad1 induces similar conformational changes and that Mad1 plays a role in restructuring or modulating Mad2 to activate it for Cdc20-APC inhibition (Chen et al. 1999; Luo et al. 2000). The study of interactions among these three proteins is an aspect of my research described in Chapter 4.

C.3 The Spindle Assembly Checkpoint Signaling Pathway

The first step in the checkpoint pathway is detecting whether kinetochores have formed bivalent attachment, and thus current research focuses on how checkpoint proteins interact with kinetochores and how they detect microtubule-kinetochore attachment. All the Mad and Bub proteins have been shown to localize to kinetochores in cultured mammalian cells at the onset of nuclear envelope breakdown, and to remain until bivalent attachment is made (Chen et al. 1996; Jablonski et al. 1998; Jin et al. 1998; Li and Benezra 1996; Martinez-Exposito et al. 1999; Taylor and McKeon 1997). Mad2 localization requires Mad1 in *Xenopus*, and Bub1 and BubR1 mutants that lack the Bub3-binding domain fail to localize to kinetochores in HeLa cells, but until recently it was unclear how checkpoint proteins interact with any other components of the kinetochore (Chen et al. 1998; Taylor et al. 1998). Recent experiments with nocodazole-treated *Xenopus* egg extracts demonstrate that immunodepletion of the microtubule motor protein CENP-E prevents mitotic arrest and Mad1 and Mad2 recruitment to kinetochores (Abrieu et al. 2000). Furthermore, CENP-E interaction with BubR1 has been shown in a two-hybrid screen and by co-immunoprecipitation from HeLa cells (Chan et al. 1998). Because CENP-E is a microtubule motor and directly interacts with microtubules (Liao et

al. 1994; Yen et al. 1992), these results suggest a mechanism by which the status of kinetochore-microtubule attachment could be conveyed to checkpoint proteins. CENP-E on an unattached kinetochore may recruit Mad1 and Mad2 (either directly or through interaction with BubR1), and changes in CENP-E conformation upon microtubule binding may then induce release of checkpoint proteins from the kinetochore (Abrieu et al. 2000). It should be noted, however, that this remains a speculative model and much work remains before we understand the molecular nature of how the checkpoint monitors kinetochore-microtubule attachment.

Checkpoint signaling clearly involves phosphorylation of at least some of the proteins involved. Mps1p, Bub1p, and BubR1 all possess a Hanks kinase motif, and exhibit kinase activity when immunoprecipitated from cells (Chan et al. 1999; Chan et al. 1998; Lauze et al. 1995; Roberts et al. 1994). The kinase activity of BubR1 precipitated from HeLa cells is increased dramatically by nocodazole treatment, indicating upregulation in checkpoint-activated cells (Chan et al. 1999). Both Mad1p and Bub3p are phospho-proteins, and the phosphorylation of Mad1p increases in *S. cerevisiae* cells arrested with spindle defects (Hardwick and Murray 1995; Roberts et al. 1994). Although human Bub1 phosphorylates Mad1 *in vitro* (Seeley et al. 1999), several experiments in *S. cerevisiae* suggest that Mps1p is the endogenous kinase for Mad1p: Mps1p precipitated from yeast phosphorylates Mad1p *in vitro*, Mad1p is not phosphorylated in *mps1* yeast cells, and *MPS1* overexpression results in Mad1p hyperphosphorylation (Hardwick et al. 1996). Analysis of Mad1p phosphorylation and checkpoint activation in response to *MPS1* overexpression has been used to dissect the order of checkpoint signaling events in *S. cerevisiae*. In the absence of spindle damage, *MPS1* overexpression induces mitotic

arrest dependent on all the *MAD* and *BUB* genes, although the Mad1p phosphorylation in response to *MPS1* overexpression is not dependent on any other *MAD* or *BUB* genes (Hardwick et al. 1996). These results have lead to a oft-cited model for checkpoint signaling in which Mps1p phosphorylation of Mad1p is a key event that is upstream of the other Mad and Bub activities (Figure 1-2).

A problem with this model is suggested by evidence that most of the proteins involved in the checkpoint exist in multi-protein complexes, making the epistasis data difficult to interpret. Sizing chromatography of *S. cerevisiae* and HeLa cell extracts has shown that Mad1p, Mad2p, and BubR1 all exist in complexes in excess of 500kD (Chan et al. 1999; Chen et al. 1999). Co-precipitation experiments in *S. cerevisiae* have demonstrated interaction of Mad1p with Mad2p, Bub1p, and Bub3p; Mad3p with Mad2p and Bub3p; and Bub1p with Bub3p (Brady and Hardwick 2000; Chen et al. 1999; Hardwick et al. 2000; Roberts et al. 1994). Furthermore, two-hybrid screens and co-precipitation experiments have revealed Cdc20p interactions with all the Mad proteins (Hwang et al. 1998), as well as BubR1 interaction with the APC (Chan et al. 1999). The presence of checkpoint proteins at both the input and output of the pathway (unattached kinetochores and Cdc20-APC) suggests checkpoint signaling cannot be fully explained by a simple linear pathway in which each protein activates a downstream component. Thus, it appears that the manner by which the checkpoint pathway transmits information from kinetochores to Cdc20-APC will turn out to be much more complex than current models suggest.

Current research addresses not only how checkpoint proteins interact to signal the status of spindle assembly, but also how the activated proteins physically translocate

Figure 1-2. The spindle assembly checkpoint signaling pathway. Kinetochores unattached to microtubules inhibit anaphase initiation by signaling through Mps1p/Esk and the Mad and Bub proteins. Activation of the checkpoint induces hyper-phosphorylation of Mad1, possibly via the protein kinases Mps1p/Esk, Bub1, or Bub1R. APC^{CDC20}-dependent degradation of Pds1p/Securin and anaphase initiation is inhibited by Mad2 and possibly by other checkpoint proteins.

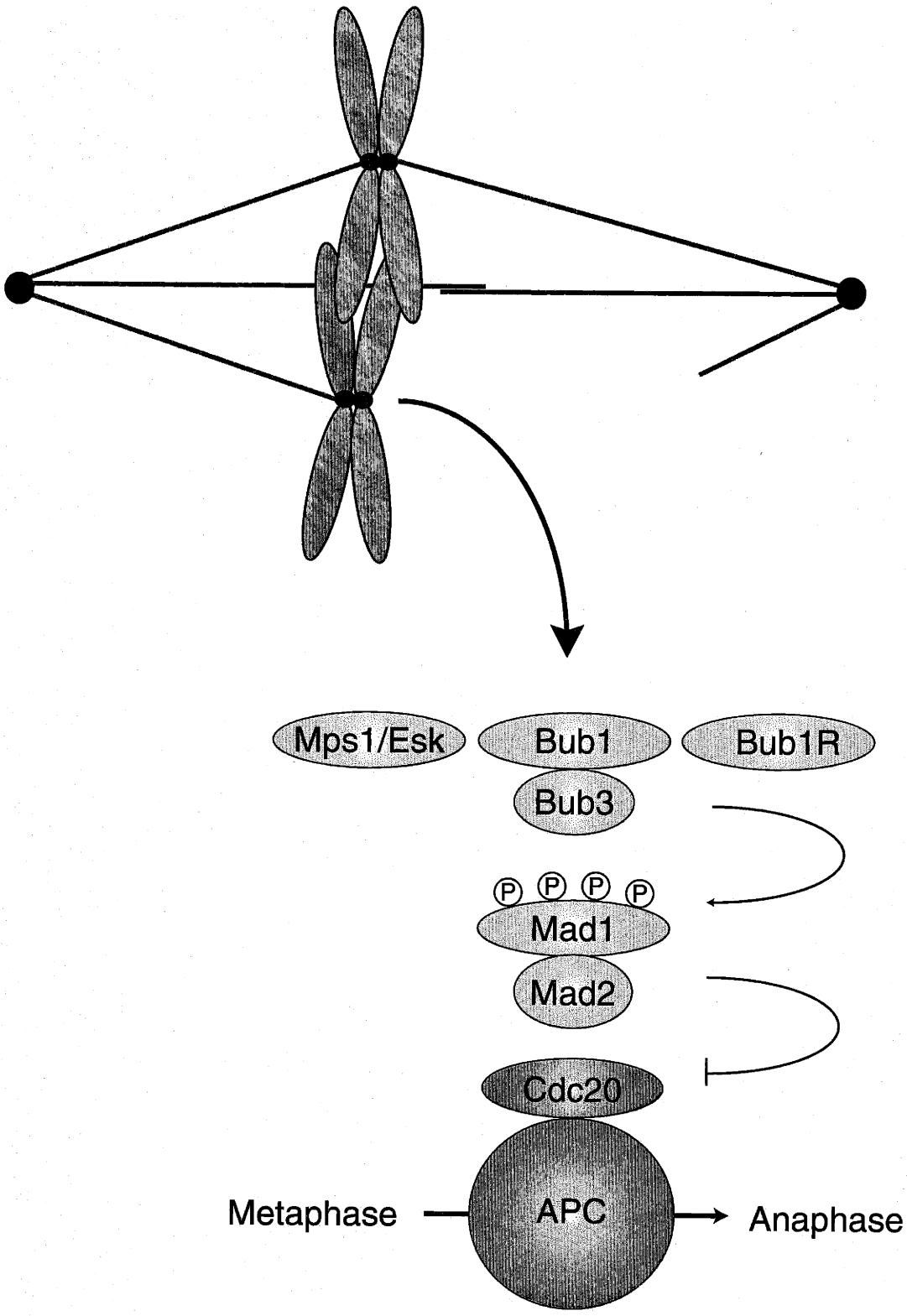
Mps1/Esk
Bub1
Bub1R
Bub3
P
P
P
P
Mad1
Mad2
Cdc20
Metaphase
APC
Anaphase

from kinetochores to the APC. Immunofluorescence localization has shown APC localizes to kinetochores, spindle poles, and along spindle microtubules during mitosis (Jorgensen et al. 1998; Tugendreich et al. 1995). It appears that the checkpoint-dependent signal inhibiting anaphase does not extend beyond this region of APC localization, because experiments with fused cells having two spindles show unattached kinetochores in one spindle do not inhibit anaphase in the other spindle (Rieder et al. 1997). An explanation for this restriction comes from experiments showing that Mad2 transiently associates with unattached kinetochores and then travels along microtubules to spindle poles, where it turns over with a half-life similar to that at kinetochores (23 seconds vs. 24-28 seconds) (Howell et al. 2000). This translocation provides a mechanism to continually signal the status of kinetochore attachment to the APC on spindle microtubules and at the poles, and the ~25 second turnover allows rapid inactivation of APC inhibition once all attachments are made and signaling is silenced (Howell et al. 2000).

The physiological relevance of Mad2 translocation from kinetochores to spindle poles remains to be addressed, but recent results demonstrate that the spindle checkpoint is abrogated by disruption of proteins that recruit motor proteins to kinetochores. Zeste White 10 (Zw10) and Rough deal (Rod) localize to kinetochores during prometaphase where they recruit dynein that then travels along microtubules to spindle poles (Chan et al. 2000; Starr et al. 1998; Williams et al. 1996). Genetic disruption of Zw10 and Rod in *Drosophila* results in failure to arrest in response to spindle disruption induced by the anti-microtubule drug colchicine or by mutation of the spindle pole protein *asp* (Basto et al. 2000). Similarly, HeLa cells microinjected with antibodies against Zw10 and Rod fail

to arrest in response to nocodazole treatment (Chan et al. 2000). Importantly, neither the genetic disruption nor the antibody injection interferes with kinetochore localization of Bub1 and Bub3 in *Drosophila*, or Mad1, Mad2, BubR1, and CENP-E in HeLa cells, suggesting the defect does not arise from displacement of checkpoint proteins from kinetochores. These results suggest a very speculative model in which Zw10 and Rod-recruited microtubule motors transport checkpoint proteins from kinetochores to spindle poles to signal the status of spindle assembly to the APC (Shah and Cleveland 2000). It will be interesting to determine whether other checkpoint proteins travel along with Mad2, and whether Mad2-microtubule translocation is dependent on Zw10, Rod, and other known checkpoint proteins.

C.4 Essential Nature of the Spindle Assembly Checkpoint

The classical view of checkpoints is that they are non-essential and are activated only in response to occasional problems (Hartwell and Weinert 1989). This view is consistent with the finding that spindle checkpoint genes are dispensable for normal growth in *S. cerevisiae* and become essential only when microtubule function is impaired by mutation or drug treatment (Hoyt et al. 1991; Li and Murray 1991). However, experiments in *S. pombe* have demonstrated that Bub1p is required for accurate chromosome segregation (Bernard et al. 1998). Furthermore, all checkpoint gene mutations to date in metazoans have resulted in embryonic lethality and a very high rate of chromosome missegregation (Basu et al. 1999; Dobles et al. 2000; Kalitsis et al. 2000; Kitagawa and Rose 1999). It is not known why chromosome missegregation is lethal in higher eukaryotes and not in *S. pombe*, but a very likely explanation is that only higher

eukaryote cells undergo apoptosis in response to stress. Nevertheless, in both simple and complex eukaryotes it appears that the spindle checkpoint is important for ensuring the accuracy of chromosome segregation under normal growth conditions and is not simply a rarely utilized fail-safe system.

In cells with spindle checkpoint gene mutations, chromosome loss and cell death are thought to occur because anaphase begins before all chromosomes have attached to the spindle. In higher eukaryotes it has not yet been possible to use mutants to test whether checkpoint disruption causes early mitotic exit because the mutations are lethal. However, the timing of mitosis has been examined in tissue culture cells injected with anti-Mad2 antibodies and in cells expressing dominant negative fragments of Bub1. In both cases, the duration of mitosis is shorter and chromosome missegregation is increased (Gorbsky et al. 1998; Taylor and McKeon 1997). Careful analysis of the time between the final chromosome-microtubule attachment and the onset of anaphase in PtK_1 cells suggests the existence of two controls over the duration of mitosis: an intrinsic timing control (presumably dependent on the Cdc2-driven cell cycle engine) and an additional control imposed by the spindle checkpoint. The first control appears to provide sufficient time for most chromosomes to attach to microtubules, but without the second control there exists a high probability that some chromosomes will remain unattached when anaphase starts and will not be properly segregated (Gorbsky et al. 1998; Rieder et al. 1994).

D. Consequences of Chromosome Missegregation in Metazoans

Both cancer and developmental abnormalities in humans are associated with aneuploidy (Carr 1971; Cotran et al. 1999; Maximilian et al. 1980; Mitleman et al. 1994). Several recent results suggest that these changes in chromosome number are caused at least in part by spindle checkpoint defects (Cahill et al. 1998; Lee et al. 1999; Lengauer et al. 1997). Understanding the role of aneuploidy and checkpoint failure in both tumorigenesis and developmental defects will require knowledge of the cellular consequences of changes in chromosome number, and whether these consequences arise from the event of missegregation, the resulting aneuploidy, or both. This section first describes the evidence linking aneuploidy and checkpoint defects to cancer and developmental abnormalities, and then describes what is known about the cellular consequences of chromosome missegregation.

D.1 Organismic Consequences of Chromosome Missegregation

A clear causal link has been established between aneuploidy and developmental abnormality. The majority of spontaneous human abortions exhibit abnormal chromosome number, and almost every deviation from euploidy is lethal (Boue et al. 1975; Carr 1971). The few viable aneuploid states result in severe abnormalities, including Down Syndrome, the leading known cause of mental retardation (Cotran et al. 1999). 95% of Down Syndrome cases are caused by chromosome 21 trisomy, approximately 90% of which result from maternal meiotic missegregation (Licznerski and Lindsten 1972; Sherman et al. 1991). Interestingly, *mad2* mutation in *S. cerevisiae* increases missegregation of a single chromosome by ten-fold in meiosis I, suggesting that

the spindle checkpoint may be very important in preventing the missegregation associated with human developmental abnormalities (Shonn et al. 2000).

It has long been observed that the vast majority of tumors are aneuploid, and that the degree of aneuploidy correlates with disease progression (Mitleman et al. 1994; Rabinovitch et al. 1989; Reid et al. 1992). The potential for aneuploidy to play a causative role in tumorigenesis is demonstrated by the high incidence of leukemia in individuals with Down Syndrome (Cotran et al. 1999). Ploidy changes are a form of genetic instability, and thus have the potential to accelerate the accumulation of mutations required for tumorigenesis. (Lengauer et al. 1998; Nowell 1986). The best characterized role for genetic instability in cancer is that of DNA mismatch repair defects in hereditary nonpolyposis colorectal cancer (HNPCC). Mutation of *MSH2*, *MLH1*, or other mismatch repair enzymes results in failure to correct mismatched DNA bases, and thus the accumulation of mutations throughout the genome (Jiricny and Nystrom-Lahti 2000; Parsons et al. 1995). Individuals with inherited mutations in these genes develop colorectal cancer, demonstrating a clear causative link between genetic instability and tumorigenesis (Bronner et al. 1994; Nicolaides et al. 1994; Papadopoulos et al. 1994; Peltomaki and de la Chapelle 1997). However, despite the strong link between mismatch repair defects and colorectal cancer, only about 15% of colorectal tumors have mismatch repair defects. Cells from the majority of colorectal tumors without mismatch repair defects exhibit aneuploidy, raising the possibility that chromosome missegregation may be a common form of genetic instability contributing to tumorigenesis (Kinzler and Vogelstein 1996).

A role for chromosome missegregation as a causative factor in tumorigenesis is supported by the observation of spindle checkpoint failure and missegregation in tumor cells. Analysis of four human colorectal cancer cell lines demonstrated nocodazole insensitivity and missegregation rates as high as one chromosome per 100 cell divisions (Lengauer et al. 1997). Further evidence comes from examination of thymic lymphomas in mice with a truncation of *Brca2*, a tumor suppressor gene implicated in DNA repair (Connor et al. 1997; Sharan et al. 1997; Wooster et al. 1995). In all four lymphomas examined from *Brca2* mutant mice, a mutation was also found in either *Bub1* or *BubR1* (Lee et al. 1999). Additionally, cells from these lymphomas failed to arrest when treated with nocodazole. Consistent with these observations, our finding that $Mad2^{+/-}$ mice develop a high incidence of lung tumors suggests a causative link between spindle checkpoint defects and cancer (see Chapter 3). However, despite the widely reported finding of two *Bub1* mutations in human colorectal tumors (Cahill et al. 1998), additional screens in human tumors of the lung, breast, and digestive tract have revealed very few mutations in any spindle checkpoint gene (Imai et al. 1999; Myrie et al. 2000; Nomoto et al. 1999; Takahashi et al. 1999). Thus, the aneuploidy commonly observed in human tumors appears not to be caused by mutation of known spindle checkpoint genes.

D.2 Cellular Consequences of Chromosome Missegregation

At least three possible cellular level consequences of chromosome missegregation could contribute to organismic defects: change in gene dosage, DNA damage, and apoptosis. Loss or gain of a whole chromosome changes the copy number of approximately one thousand genes (Consortium 2001). It is difficult to predict the

consequences of these changes, but a dramatic effect would be expected if a cell with only one functional copy of a given gene were to lose that wildtype copy. If, for example, an individual were heterozygous for *p53*, missegregation of the chromosome carrying the wildtype copy would result in *p53* nullizygosity, and thus increase the risk of tumorigenesis (Donehower et al. 1992; Jacks et al. 1994).

A second possible consequence of segregation error is that DNA is damaged when unsegregated chromosomes are trapped by a closing cytokinetic furrow. The most direct evidence that chromosome missegregation leads to DNA damage is that genetic disruption of *Drosophila bub1* results in extensive chromosome breakage (Basu et al. 1999). A second connection is that treating primary mouse fibroblasts with nocodazole causes the cells to arrest transiently in mitosis, and to then slip out of mitosis and enter a prolonged G1-like arrest. The G1-like arrest and the subsequent apoptosis are p53-dependent, consistent with a DNA damage response (Lanni and Jacks 1998). The possibility that chromosome missegregation causes DNA damage suggests a self-reinforcing loop in which double stranded DNA breaks generated by physical shearing of chromosomes cause inappropriate recombination and large scale rearrangements. Chromosome rearrangements not only have well-characterized roles in cancer (Mitleman et al. 1994), but also could in turn produce acentric and dicentric chromosomes that cannot bind correctly to the mitotic spindle and therefore suffer additional physical damage (Figure 1-3).

A third possibility is that missegregation and aneuploidy induces apoptosis. The earliest evidence for this idea was provided by cell culture studies demonstrating apoptosis in response to treatment with anti-microtubule drugs (Duncan and Heddle

Figure 1-3. Model relating DNA damage and chromosome missegregation. Double-stranded DNA breaks (a) can result in improper recombination that creates both dicentric and acentric chromosomes (b). Acentric chromosomes lack kinetochores for microtubule attachment, and dicentric chromosomes may attach so that the same sister chromatid becomes attached to microtubules from opposite spindle poles (c). Shearing of DNA can occur during anaphase when each dicentric chromosomes is pulled in opposite directions by microtubules (d), and during cytokinesis when the unsegregated acentric chromosomes can be caught in the cytokinetic furrow (e). The resulting double stranded breaks create sites for further possible incorrect recombination.

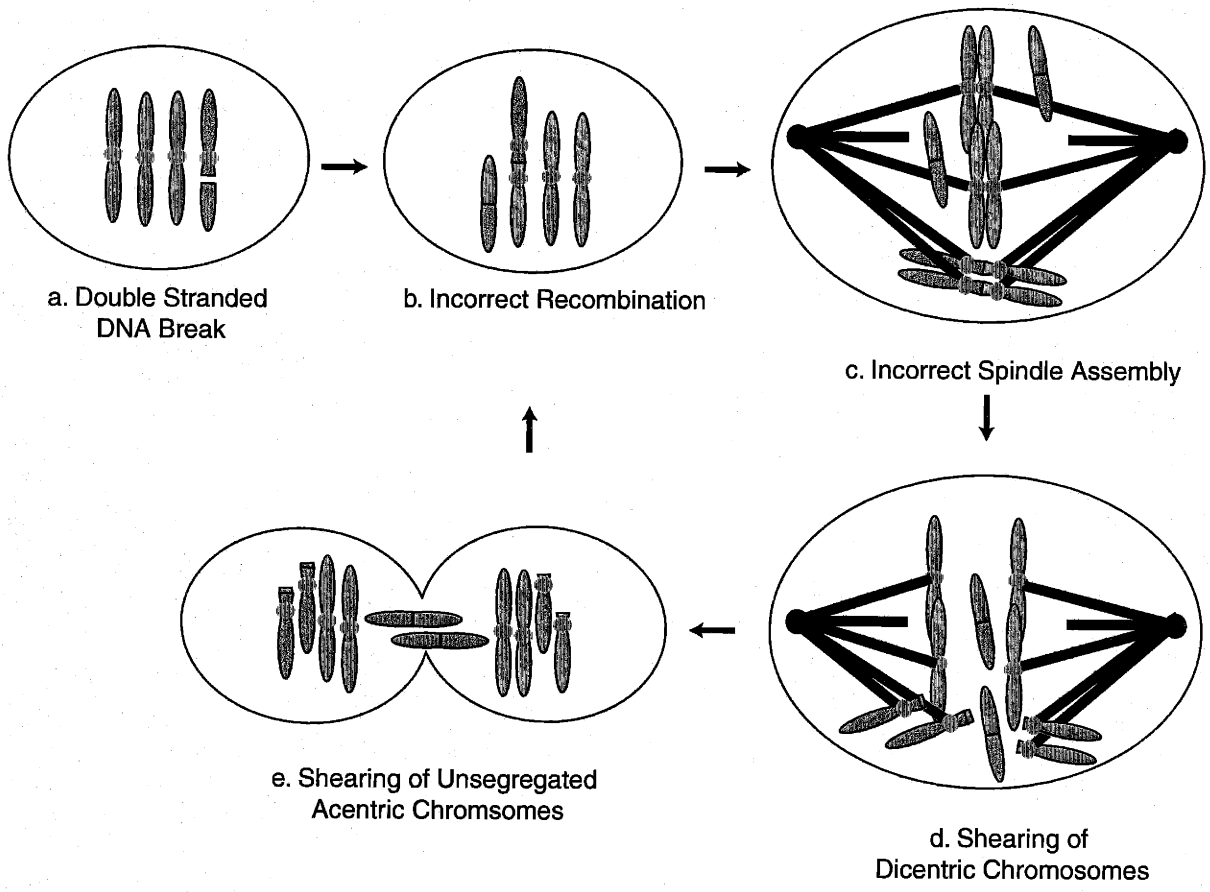
a. Double Stranded DNA Break
b. Incorrect Recombination
c. Incorrect Spindle Assembly
d. Shearing of Dicentric Chromosomes
e. Shearing of Unsegregated Acentric Chromsomes

1984; Gupta 1985; Woods et al. 1995). Although the molecular link between segregation problems and apoptosis is not understood, possible trigger events include prolonged mitotic arrest, DNA damage, and the resulting aneuploidy. It is not known whether or not the spindle checkpoint is involved in this apoptosis. Expression of a dominant negative Bub1 fragment decreases apoptosis in nocodazole-treated HeLa cells, suggesting checkpoint function is required for apoptosis in response to segregation errors (Taylor and McKeon 1997). However, Bub1-mutant *Drosophila* embryos and *Mad2*-null mouse embryos experience high rates of chromosome missegregation and undergo extensive apoptosis, suggesting the opposite interpretation (Basu et al. 1999; Dobles et al. 2000). This issue remains unresolved, but one interesting possibility is that the tumor-derived HeLa cells contain mutations that allow escape from missegregation-induced apoptosis. Finally, it is important to note that aneuploidy is not necessarily lethal, as cell lines, tumor cells, and some normal somatic cells *in vivo* survive changes in chromosome number (Galloway and Buckton 1978; Lengauer et al. 1997; Smith et al. 1996). However, I believe apoptosis to be a general mechanism for preventing the propagation of aneuploidy, and that the abnormalities and disease associated with aneuploidy involve a complex interplay of segregation error, DNA damage, and suppression of apoptotic pathways.

References

Abrieu, A., Kahana, J. A., Wood, K. W., and Cleveland, D. W. (2000). "CENP-E as an essential component of the mitotic checkpoint in vitro." *Cell*, 102(6), 817-26.

Alexandru, G., Zachariae, W., Schleiffer, A., and Nasmyth, K. (1999). "Sister chromatid separation and chromosome re-duplication are regulated by different mechanisms in response to spindle damage." *Embo J*, 18(10), 2707-21.

Allen, C., and Borisy, G. G. (1974). "Structural polarity and directional growth of microtubules of Chlamydomonas flagella." *J Mol Biol*, 90(2), 381-402.

Amon, A. (1999). "The spindle checkpoint." *Curr Opin Genet Dev*, 9(1), 69-75.

Amos, L., and Klug, A. (1974). "Arrangement of subunits in flagellar microtubules." *J Cell Sci*, 14(3), 523-49.

Andersen, S. S. (1998). "Xenopus interphase and mitotic microtubule-associated proteins differentially suppress microtubule dynamics in vitro." *Cell Motil Cytoskeleton*, 41(3), 202-13.

Bajer, A., and Mole-Bajer, J. (1956). "Cine-micrographic studies on mitosis in endosperm. II. Chromosome, cytoplasmic, and brownian movements." *Chromosoma*, 7, 558-607.

Basto, R., Gomes, R., and Karess, R. E. (2000). "Rough deal and Zw10 are required for the metaphase checkpoint in drosophila." *Nat Cell Biol*, 2(12), 939-43.

Basu, J., Bousbaa, H., Logarinho, E., Li, Z., Williams, B. C., Lopes, C., Sunkel, C. E., and Goldberg, M. L. (1999). "Mutations in the essential spindle checkpoint gene bub1 cause chromosome missegregation and fail to block apoptosis in Drosophila." *J Cell Biol*, 146(1), 13-28.

Basu, J., Logarinho, E., Herrmann, S., Bousbaa, H., Li, Z., Chan, G. K., Yen, T. J., Sunkel, C. E., and Goldberg, M. L. (1998). "Localization of the Drosophila checkpoint control protein Bub3 to the kinetochore requires Bub1 but not Zw10 or Rod." *Chromosoma*, 107(6-7), 376-85.

Belmont, L. D., Hyman, A. A., Sawin, K. E., and Mitchison, T. J. (1990). "Real-time visualization of cell cycle-dependent changes in microtubule dynamics in cytoplasmic extracts." *Cell*, 62(3), 579-89.

Belmont, L. D., and Mitchison, T. J. (1996). "Identification of a protein that interacts with tubulin dimers and increases the catastrophe rate of microtubules." *Cell*, 84(4), 623-31.

Bernard, P., Hardwick, K., and Javerzat, J. P. (1998). "Fission yeast bub1 is a mitotic centromere protein essential for the spindle checkpoint and the preservation of correct ploidy through mitosis." *J Cell Biol*, 143(7), 1775-87.

Bernat, R. L., Borisy, G. G., Rothfield, N. F., and Earnshaw, W. C. (1990). "Injection of anticentromere antibodies in interphase disrupts events required for chromosome movement at mitosis." *J Cell Biol*, 111(4), 1519-33.

Boue, J., Bou, A., and Lazar, P. (1975). "Retrospective and prospective epidemiological studies of 1500 karyotyped spontaneous human abortions." *Teratology*, 12(1), 11-26.

Brady, D. M., and Hardwick, K. G. (2000). "Complex formation between Mad1p, Bub1p and Bub3p is crucial for spindle checkpoint function." *Curr Biol*, 10(11), 675-8.

Brinkley, B. R., and Cartwright, J. (1971). "Ultrastructural analysis of mitotic spindle elongation in mammalian cells in vitro. Direct microtubule counts." *J Cell Biol*, 50(2), 416-31.

Bronner, C. E., Baker, S. M., Morrison, P. T., Warren, G., Smith, L. G., Lescoe, M. K., Kane, M., Earabino, C., Lipford, J., Lindblom, A., and et al. (1994). "Mutation in the DNA mismatch repair gene homologue hMLH1 is associated with hereditary non-polyposis colon cancer." *Nature*, 368(6468), 258-61.

Brown, E. J., and Baltimore, D. (2000). "ATR disruption leads to chromosomal fragmentation and early embryonic lethality." *Genes Dev*, 14(4), 397-402.

Cahill, D. P., Lengauer, C., Yu, J., Riggins, G. J., Willson, J. K., Markowitz, S. D., Kinzler, K. W., and Vogelstein, B. (1998). "Mutations of mitotic checkpoint genes in human cancers." *Nature*, 392(6673), 300-3.

Carr, D. H. (1971). "Chromosomes and Abortion." Advances in Human Genetics, H. Harris and K. Hirschhorn, eds., Plenum, New York.

Chan, G. K., Jablonski, S. A., Starr, D. A., Goldberg, M. L., and Yen, T. J. (2000). "Human Zw10 and ROD are mitotic checkpoint proteins that bind to kinetochores." *Nat Cell Biol*, 2(12), 944-7.

Chan, G. K., Jablonski, S. A., Sudakin, V., Hittle, J. C., and Yen, T. J. (1999). "Human BUBR1 is a mitotic checkpoint kinase that monitors CENP-E functions at kinetochores and binds the cyclosome/APC." *J Cell Biol*, 146(5), 941-54.

Chan, G. K., Schaar, B. T., and Yen, T. J. (1998). "Characterization of the kinetochore binding domain of CENP-E reveals interactions with the kinetochore proteins CENP-F and hBUBR1." *J Cell Biol*, 143(1), 49-63.

Chen, R. H., Brady, D. M., Smith, D., Murray, A. W., and Hardwick, K. G. (1999). "The spindle checkpoint of budding yeast depends on a tight complex between the Mad1 and Mad2 proteins." *Mol Biol Cell*, 10(8), 2607-18.

Chen, R. H., Shevchenko, A., Mann, M., and Murray, A. W. (1998). "Spindle checkpoint protein Xmad1 recruits Xmad2 to unattached kinetochores." *J Cell Biol*, 143(2), 283-95.

Chen, R. H., Waters, J. C., Salmon, E. D., and Murray, A. W. (1996). "Association of spindle assembly checkpoint component XMAD2 with unattached kinetochores." *Science*, 274(5285), 242-6.

Cohen-Fix, O., Peters, J. M., Kirschner, M. W., and Koshland, D. (1996). "Anaphase initiation in Saccharomyces cerevisiae is controlled by the APC-dependent degradation of the anaphase inhibitor Pds1p." *Genes Dev*, 10(24), 3081-93.

Connor, F., Bertwistle, D., Mee, P. J., Ross, G. M., Swift, S., Grigorieva, E., Tybulewicz, V. L., and Ashworth, A. (1997). "Tumorigenesis and a DNA repair defect in mice with a truncating Brca2 mutation." *Nat Genet*, 17(4), 423-30.

Consortium, I. H. G. S. (2001). "Initial sequencing and analysis of the human genome." *Nature*, 409, 860-921.

Cortez, D., Wang, Y., Qin, J., and Elledge, S. J. (1999). "Requirement of ATM-dependent phosphorylation of brca1 in the DNA damage response to double-strand breaks." *Science*, 286(5442), 1162-6.

Cotran, R. S., Kumar, V., and Collins, T. (1999). *Robbins Pathologic Basis of Disease*, W.B. Saunders Company, Philadelphia.

Desai, A., Verma, S., Mitchison, T. J., and Walczak, C. E. (1999). "Kin I kinesins are microtubule-destabilizing enzymes." *Cell*, 96(1), 69-78.

Dobles, M., Liberal, V., Scott, M. L., Benezra, R., and Sorger, P. K. (2000). "Chromosome missegregation and apoptosis in mice lacking the mitotic checkpoint protein Mad2." *Cell*, 101, 635-645.

Donehower, L. A., Harvey, M., Slagle, B. L., McArthur, M. J., Montgomery, C. A., Butel, J. S., and Bradley, A. (1992). "Mice deficient for p53 are developmentally normal but susceptible to spontaneous tumours." *Nature*, 356(6366), 215-21.

Duncan, A. M., and Heddle, J. A. (1984). "The frequency and distribution of apoptosis induced by three non-carcinogenic agents in mouse colonic crypts." *Cancer Lett*, 23(3), 307-11.

Fan, J., Griffiths, A. D., Lockhart, A., Cross, R. A., and Amos, L. A. (1996). "Microtubule minus ends can be labelled with a phage display antibody specific to alpha-tubulin." *J Mol Biol*, 259(3), 325-30.

Fang, G., Yu, H., and Kirschner, M. W. (1998). "The checkpoint protein MAD2 and the mitotic regulator CDC20 form a ternary complex with the anaphase-promoting complex to control anaphase initiation." *Genes Dev*, 12(12), 1871-83.

Fraschini, R., Formenti, E., Lucchini, G., and Piatti, S. (1999). "Budding yeast Bub2 is localized at spindle pole bodies and activates the mitotic checkpoint via a different pathway from Mad2." *J Cell Biol*, 145(5), 979-91.

Fraser, A. G., James, C., Evan, G. I., and Hengartner, M. O. (1999). "Caenorhabditis elegans inhibitor of apoptosis protein (IAP) homologue BIR-1 plays a conserved role in cytokinesis." *Curr Biol*, 9(6), 292-301.

Fuchs, D. A., and Johnson, R. K. (1978). "Cytologic evidence that taxol, an antineoplastic agent from Taxus brevifolia, acts as a mitotic spindle poison." *Cancer Treat Rep*, 62(8), 1219-22.

Galloway, S. M., and Buckton, K. E. (1978). "Aneuploidy and ageing: chromosome studies on a random sample of the population using G-banding." *Cytogenet Cell Genet*, 20(1-6), 78-95.

Gorbsky, G. J., Chen, R. H., and Murray, A. W. (1998). "Microinjection of antibody to Mad2 protein into mammalian cells in mitosis induces premature anaphase." *J Cell Biol*, 141(5), 1193-205.

Gorbsky, G. J., and Ricketts, W. A. (1993). "Differential expression of a phosphoepitope at the kinetochores of moving chromosomes." *J Cell Biol*, 122(6), 1311-21.

Guacci, V., Koshland, D., and Strunnikov, A. (1997). "A direct link between sister chromatid cohesion and chromosome condensation revealed through the analysis of MCD1 in S. cerevisiae." *Cell*, 91(1), 47-57.

Guenette, S., Magendantz, M., and Solomon, F. (1995). "Suppression of a conditional mutation in alpha-tubulin by overexpression of two checkpoint genes." *J Cell Sci*, 108(Pt 3), 1195-204.

Gupta, R. S. (1985). "Species-specific differences in toxicity of antimitotic agents toward cultured mammalian cells." *J Natl Cancer Inst*, 74(1), 159-64.

Hardwick, K. G., Johnston, R. C., Smith, D. L., and Murray, A. W. (2000). "MAD3 encodes a novel component of the spindle checkpoint which interacts with Bub3p, Cdc20p, and Mad2p." *J Cell Biol*, 148(5), 871-82.

Hardwick, K. G., and Murray, A. W. (1995). "Mad1p, a phosphoprotein component of the spindle assembly checkpoint in budding yeast." *J Cell Biol*, 131(3), 709-20.

Hardwick, K. G., Weiss, E., Luca, F. C., Winey, M., and Murray, A. W. (1996). "Activation of the budding yeast spindle assembly checkpoint without mitotic spindle disruption." *Science*, 273(5277), 953-6.

Hartwell, L., Dutcher, S., Wood, J., and Garvik, B. (1982). "The fidelity of mitotic chromosome reproductuion in *S. cerevisiae*." *Rec. Adv. Yeast Mol. Biol.*, 1, 28.

Hartwell, L. H., and Weinert, T. A. (1989). "Checkpoints: controls that ensure the order of cell cycle events." *Science*, 246(4930), 629-34.

Hay, B. A., Wassarman, D. A., and Rubin, G. M. (1995). "Drosophila homologs of baculovirus inhibitor of apoptosis proteins function to block cell death." *Cell*, 83(7), 1253-62.

Hayden, J. H., Bowser, S. S., and Rieder, C. L. (1990). "Kinetochores capture astral microtubules during chromosome attachment to the mitotic spindle: direct visualization in live newt lung cells." *J Cell Biol*, 111(3), 1039-45.

He, X., Asthana, S., and Sorger, P. K. (2000). "Transient sister chromatid separation and elastic deformation of chromosomes during mitosis in budding yeast." *Cell*, 101(7), 763-75.

Holy, T. E., and Leibler, S. (1994). "Dynamic instability of microtubules as an efficient way to search in space." *Proc Natl Acad Sci U S A*, 91(12), 5682-5.

Howell, B., Larsson, N., Gullberg, M., and Cassimeris, L. (1999). "Dissociation of the tubulin-sequestering and microtubule catastrophe-promoting activities of oncoprotein 18/stathmin." *Mol Biol Cell*, 10(1), 105-18.

Howell, B. J., Hoffman, D. B., Fang, G., Murray, A. W., and Salmon, E. D. (2000). "Visualization of Mad2 dynamics at kinetochores, along spindle fibers, and at spindle poles in living cells." *J Cell Biol*, 150(6), 1233-50.

Hoyt, M. A., Totis, L., and Roberts, B. T. (1991). "S. cerevisiae genes required for cell cycle arrest in response to loss of microtubule function." *Cell*, 66(3), 507-17.

Hwang, L. H., Lau, L. F., Smith, D. L., Mistrot, C. A., Hardwick, K. G., Hwang, E. S., Amon, A., and Murray, A. W. (1998). "Budding yeast Cdc20: a target of the spindle checkpoint." *Science*, 279(5353), 1041-4.

Hyman, A. A., and Karsenti, E. (1996). "Morphogenetic properties of microtubules and mitotic spindle assembly." *Cell*, 84(3), 401-10.

Hyman, A. A., and Sorger, P. K. (1995). "Structure and function of kinetochores in budding yeast." *Annu Rev Cell Dev Biol*, 11(26), 471-95.

Imai, Y., Shiratori, Y., Kato, N., Inoue, T., and Omata, M. (1999). "Mutational inactivation of mitotic checkpoint genes, hsMAD2 and hBUB1, is rare in sporadic digestive tract cancers." *Jpn J Cancer Res*, 90(8), 837-40.

Jablonski, S. A., Chan, G. K., Cooke, C. A., Earnshaw, W. C., and Yen, T. J. (1998). "The hBUB1 and hBUBR1 kinases sequentially assemble onto kinetochores during prophase with hBUBR1 concentrating at the kinetochore plates in mitosis." *Chromosoma*, 107(6-7), 386-96.

Jacks, T., Remington, L., Williams, B. O., Schmitt, E. M., Halachmi, S., Bronson, R. T., and Weinberg, R. A. (1994). "Tumor spectrum analysis in p53-mutant mice." *Curr Biol*, 4(1), 1-7.

Jacobs, C. W., Adams, A. E., Szaniszlo, P. J., and Pringle, J. R. (1988). "Functions of microtubules in the Saccharomyces cerevisiae cell cycle." *J Cell Biol*, 107(4), 1409-26.

Jin, D. Y., Spencer, F., and Jeang, K. T. (1998). "Human T cell leukemia virus type 1 oncoprotein Tax targets the human mitotic checkpoint protein MAD1." *Cell*, 93(1), 81-91.

Jiricny, J., and Nystrom-Lahti, M. (2000). "Mismatch repair defects in cancer." *Curr Opin Genet Dev*, 10(2), 157-61.

Jorgensen, P. M., Brundell, E., Starborg, M., and Hoog, C. (1998). "A subunit of the anaphase-promoting complex is a centromere-associated protein in mammalian cells." *Mol Cell Biol*, 18(1), 468-76.

Kalitsis, P., Earle, E., Fowler, K. J., and Choo, K. H. (2000). "Bub3 gene disruption in mice reveals essential mitotic spindle checkpoint function during early embryogenesis." *Genes Dev*, 14(18), 2277-82.

Kim, S. H., Lin, D. P., Matsumoto, S., Kitazono, A., and Matsumoto, T. (1998). "Fission yeast Slp1: an effector of the Mad2-dependent spindle checkpoint." *Science*, 279(5353), 1045-7.

King, J. M., Hays, T. S., and Nicklas, R. B. (2000). "Dynein is a transient kinetochore component whose binding is regulated by microtubule attachment, not tension." *J Cell Biol*, 151(4), 739-48.

Kinzler, K. W., and Vogelstein, B. (1996). "Lessons from hereditary colorectal cancer." *Cell*, 87(2), 159-70.

Kitagawa, R., and Rose, A. M. (1999). "Components of the spindle-assembly checkpoint are essential in Caenorhabditis elegans." *Nat Cell Biolog*, 1(8), 514-521.

Lanni, J. S., and Jacks, T. (1998). "Characterization of the p53-dependent postmitotic checkpoint following spindle disruption." *Mol Cell Biol*, 18(2), 1055-64.

Lauze, E., Stoelcker, B., Luca, F. C., Weiss, E., Schutz, A. R., and Winey, M. (1995). "Yeast spindle pole body duplication gene MPS1 encodes an essential dual specificity protein kinase." *Embo J*, 14(8), 1655-63.

Lee, H., Trainer, A. H., Friedman, L. S., Thistlethwaite, F. C., Evans, M. J., Ponder, B. A., and Venkitaraman, A. R. (1999). "Mitotic checkpoint inactivation fosters transformation in cells lacking the breast cancer susceptibility gene, Brca2." *Mol Cell*, 4(1), 1-10.

Lengauer, C., Kinzler, K. W., and Vogelstein, B. (1997). "Genetic instability in colorectal cancers." *Nature*, 386(6625), 623-7.

Lengauer, C., Kinzler, K. W., and Vogelstein, B. (1998). "Genetic instabilities in human cancers." *Nature*, 396(6712), 643-9.

Li, F., Ackermann, E. J., Bennett, C. F., Rothermel, A. L., Plescia, J., Tognin, S., Villa, A., Marchisio, P. C., and Altieri, D. C. (1999). "Pleiotropic cell-division defects and apoptosis induced by interference with survivin function." *Nat Cell Biol*, 1(8), 461-6.

Li, F., Ambrosini, G., Chu, E. Y., Plescia, J., Tognin, S., Marchisio, P. C., and Altieri, D. C. (1998). "Control of apoptosis and mitotic spindle checkpoint by survivin." *Nature*, 396(6711), 580-4.

Li, R. (1999). "Bifurcation of the mitotic checkpoint pathway in budding yeast." *Proc Natl Acad Sci U S A*, 96(9), 4989-94.

Li, R., and Murray, A. W. (1991). "Feedback control of mitosis in budding yeast." *Cell*, 66(3), 519-31.

Li, X., and Nicklas, R. B. (1995). "Mitotic forces control a cell-cycle checkpoint." *Nature*, 373(6515), 630-2.

Li, Y., and Benezra, R. (1996). "Identification of a human mitotic checkpoint gene: hsMAD2." *Science*, 274(5285), 246-8.

Li, Y., Gorbea, C., Mahaffey, D., Rechsteiner, M., and Benezra, R. (1997). "MAD2 associates with the cyclosome/anaphase-promoting complex and inhibits its activity." *Proc Natl Acad Sci U S A*, 94(23), 12431-6.

Liao, H., Li, G., and Yen, T. J. (1994). "Mitotic regulation of microtubule cross-linking activity of CENP-E kinetochore protein." *Science*, 265(5170), 394-8.

Licznerski, G., and Lindsten, J. (1972). "Trisomy 21 in man due to maternal non-disjunction during the first meiotic division." *Hereditas*, 70(1), 153-4.

Liu, Q., Guntuku, S., Cui, X. S., Matsuoka, S., Cortez, D., Tamai, K., Luo, G., Carattini-Rivera, S., DeMayo, F., Bradley, A., Donehower, L. A., and Elledge, S. J. (2000). "Chk1 is an essential kinase that is regulated by Atr and required for the G(2)/M DNA damage checkpoint." *Genes Dev*, 14(12), 1448-59.

Lombillo, V. A., Nislow, C., Yen, T. J., Gelfand, V. I., and McIntosh, J. R. (1995). "Antibodies to the kinesin motor domain and CENP-E inhibit microtubule depolymerization-dependent motion of chromosomes in vitro." *J Cell Biol*, 128(1-2), 107-15.

Lowe, S. W., Schmitt, E. M., Smith, S. W., Osborne, B. A., and Jacks, T. (1993). "p53 is required for radiation-induced apoptosis in mouse thymocytes." *Nature*, 362(6423), 847-9.

Luo, X., Fang, G., Coldiron, M., Lin, Y., Yu, H., Kirschner, M. W., and Wagner, G. (2000). "Structure of the Mad2 spindle assembly checkpoint protein and its interaction with Cdc20." *Nat Struct Biol*, 7(3), 224-9.

Martinez-Exposito, M. J., Kaplan, K. B., Copeland, J., and Sorger, P. K. (1999). "Retention of the BUB3 checkpoint protein on lagging chromosomes." *Proc Natl Acad Sci U S A*, 96(15), 8493-8.

Maximilian, C., Duca, D., Pop, T., Toncescu, N., and Ioan, D. (1980). "Down's syndrome. I. Cytogenetics." *Endocrinologie*, 18(4), 273-5.

McDonald, H. B., Stewart, R. J., and Goldstein, L. S. (1990). "The kinesin-like ncd protein of Drosophila is a minus end-directed microtubule motor." *Cell*, 63(6), 1159-65.

McEwen, B. F., Heagle, A. B., Cassels, G. O., Buttle, K. F., and Rieder, C. L. (1997). "Kinetochore fiber maturation in PtK1 cells and its implications for the mechanisms of chromosome congression and anaphase onset." *J Cell Biol*, 137(7), 1567-80.

McIntosh, J. R. (1991). "Structural and mechanical control of mitotic progression." *Cold Spring Harb Symp Quant Biol*, 56, 613-9.

Michaelis, C., Ciosk, R., and Nasmyth, K. (1997). "Cohesins: chromosomal proteins that prevent premature separation of sister chromatids." *Cell*, 91(1), 35-45.

Minshull, J., Straight, A., Rudner, A. D., Dernburg, A. F., Belmont, A., and Murray, A. W. (1996). "Protein phosphatase 2A regulates MPF activity and sister chromatid cohesion in budding yeast." *Curr Biol*, 6(12), 1609-20.

Minshull, J., Sun, H., Tonks, N. K., and Murray, A. W. (1994). "A MAP kinase-dependent spindle assembly checkpoint in Xenopus egg extracts." *Cell*, 79(3), 475-86.

Mitchison, T., Evans, L., Schulze, E., and Kirschner, M. (1986). "Sites of microtubule assembly and disassembly in the mitotic spindle." *Cell*, 45(4), 515-27.

Mitchison, T., and Kirschner, M. (1984). "Dynamic instability of microtubule growth." *Nature*, 312(5991), 237-42.

Mitchison, T. J. (1993). "Localization of an exchangeable GTP binding site at the plus end of microtubules." *Science*, 261(5124), 1044-7.

Mitleman, F., Johansson, B., and Mertens, F. (1994). *Catalog of Chromosome Aberrations in Cancer*, Wiley-Liss, New York.

Myrie, K. A., Percy, M. J., Azim, J. N., Neeley, C. K., and Petty, E. M. (2000). "Mutation and expression analysis of human BUB1 and BUB1B in aneuploid breast cancer cell lines." *Cancer Lett*, 152(2), 193-9.

Nicklas, R. B. (1967). "Chromosome micromanipulation. II. Induced reorientation and the experimental control of segregation in meiosis." *Chromosoma*, 21(1), 17-50.

Nicklas, R. B. (1997). "How cells get the right chromosomes." *Science*, 275(5300), 632-7.

Nicklas, R. B., Ward, S. C., and Gorbsky, G. J. (1995). "Kinetochore chemistry is sensitive to tension and may link mitotic forces to a cell cycle checkpoint." *J Cell Biol*, 130(4), 929-39.

Nicolaides, N. C., Papadopoulos, N., Liu, B., Wei, Y. F., Carter, K. C., Ruben, S. M., Rosen, C. A., Haseltine, W. A., Fleischmann, R. D., Fraser, C. M., and et al. (1994). "Mutations of two PMS homologues in hereditary nonpolyposis colon cancer." *Nature*, 371(6492), 75-80.

Nomoto, S., Haruki, N., Takahashi, T., Masuda, A., Koshikawa, T., Fujii, Y., and Osada, H. (1999). "Search for in vivo somatic mutations in the mitotic checkpoint gene, hMAD1, in human lung cancers." *Oncogene*, 18(50), 7180-3.

Nowell, P. C. (1986). "Mechanisms of Tumor Progression." *Cancer Research*, 46, 2203-2207.

Ookata, K., Hisanaga, S., Bulinski, J. C., Murofushi, H., Aizawa, H., Itoh, T. J., Hotani, H., Okumura, E., Tachibana, K., and Kishimoto, T. (1995). "Cyclin B interaction with microtubule-associated protein 4 (MAP4) targets p34cdc2 kinase to microtubules and is a potential regulator of M-phase microtubule dynamics." *J Cell Biol*, 128(5), 849-62.

Pangilinan, F., and Spencer, F. (1996). "Abnormal kinetochore structure activates the spindle assembly checkpoint in budding yeast." *Mol Biol Cell*, 7(8), 1195-208.

Papadopoulos, N., Nicolaides, N. C., Wei, Y. F., Ruben, S. M., Carter, K. C., Rosen, C. A., Haseltine, W. A., Fleischmann, R. D., Fraser, C. M., Adams, M. D., and et al. (1994). "Mutation of a mutL homolog in hereditary colon cancer." *Science*, 263(5153), 1625-9.

Parsons, R., Li, G. M., Longley, M., Modrich, P., Liu, B., Berk, T., Hamilton, S. R., Kinzler, K. W., and Vogelstein, B. (1995). "Mismatch repair deficiency in phenotypically normal human cells." *Science*, 268(5211), 738-40.

Paschal, B. M., Shpetner, H. S., and Vallee, R. B. (1987). "MAP 1C is a microtubule-activated ATPase which translocates microtubules in vitro and has dynein-like properties." *J Cell Biol*, 105(3), 1273-82.

Paschal, B. M., and Vallee, R. B. (1987). "Retrograde transport by the microtubule-associated protein MAP 1C." *Nature*, 330(6144), 181-3.

Peltomaki, P., and de la Chapelle, A. (1997). "Mutations predisposing to hereditary nonpolyposis colorectal cancer." *Adv Cancer Res*, 71, 93-119.

Pfarr, C. M., Coue, M., Grissom, P. M., Hays, T. S., Porter, M. E., and McIntosh, J. R. (1990). "Cytoplasmic dynein is localized to kinetochores during mitosis." *Nature*, 345(6272), 263-5.

Pryer, N., Walker, R., Skeen, V., Bourns, B., Soboeiro, M., and Salmon, E. (1992). "Brain microtuble-associated proteins modulate microtubule dynamic instability in vitro. Real-time observations using video microscopy." *Journal of Cell Science*, 103, 965-76.

Rabinovitch, P. S., Reid, B. J., Haggitt, R. C., Norwood, T. H., and Rubin, C. E. (1989). "Progression to cancer in Barrett's esophagus is associated with genomic instability." *Lab Invest*, 60(1), 65-71.

Reid, B. J., Blount, P. L., Rubin, C. E., Levine, D. S., Haggitt, R. C., and Rabinovitch, P. S. (1992). "Flow-cytometric and histological progression to malignancy in Barrett's esophagus: prospective endoscopic surveillance of a cohort." *Gastroenterology*, 102(4 Pt 1), 1212-9.

Rieder, C. L., and Alexander, S. P. (1990). "Kinetochores are transported poleward along a single astral microtubule during chromosome attachment to the spindle in newt lung cells." *J Cell Biol*, 110(1), 81-95.

Rieder, C. L., Cole, R. W., Khodjakov, A., and Sluder, G. (1995). "The checkpoint delaying anaphase in response to chromosome monoorientation is mediated by an inhibitory signal produced by unattached kinetochores." *J Cell Biol*, 130(4), 941-8.

Rieder, C. L., Davison, E. A., Jensen, L. C., Cassimeris, L., and Salmon, E. D. (1986). "Oscillatory movements of monooriented chromosomes and their position relative to the spindle pole result from the ejection properties of the aster and half-spindle." *J Cell Biol*, 103(2), 581-91.

Rieder, C. L., Khodjakov, A., Paliulis, L. V., Fortier, T. M., Cole, R. W., and Sluder, G. (1997). "Mitosis in vertebrate somatic cells with two spindles: implications for the metaphase/anaphase transition checkpoint and cleavage." *Proc Natl Acad Sci U S A*, 94(10), 5107-12.

Rieder, C. L., Schultz, A., Cole, R., and Sluder, G. (1994). "Anaphase onset in vertebrate somatic cells is controlled by a checkpoint that monitors sister kinetochore attachment to the spindle." *J Cell Biol*, 127(5), 1301-10.

Roberts, B. T., Farr, K. A., and Hoyt, M. A. (1994). "The Saccharomyces cerevisiae checkpoint gene BUB1 encodes a novel protein kinase." *Mol Cell Biol*, 14(12), 8282-91.

Schaar, B. T., Chan, G. K., Maddox, P., Salmon, E. D., and Yen, T. J. (1997). "CENP-E function at kinetochores is essential for chromosome alignment." *J Cell Biol*, 139(6), 1373-82.

Scholey, J., Heuser, J., Yang, J., and Goldstein, L. (1989). "Identification of globular mechanochemical heads of kinesin." *Nature*, 338, 355-357.

Schulze, E., and Kirschner, M. (1986). "Microtubule dynamics in interphase cells." *J Cell Biol*, 102(3), 1020-31.

Seeley, T. W., Wang, L., and Zhen, J. Y. (1999). "Phosphorylation of human MAD1 by the BUB1 kinase in vitro." *Biochem Biophys Res Commun*, 257(2), 589-95.

Shah, J. V., and Cleveland, D. W. (2000). "Waiting for Anaphase: Mad2 and the Spindle Assembly Checkpoint." *Cell*, 103(7), 997-1000.

Shapiro, P. S., Vaisberg, E., Hunt, A. J., Tolwinski, N. S., Whalen, A. M., McIntosh, J. R., and Ahn, N. G. (1998). "Activation of the MKK/ERK pathway during somatic cell mitosis: direct interactions of active ERK with kinetochores and regulation of the mitotic 3F3/2 phosphoantigen." *J Cell Biol*, 142(6), 1533-45.

Sharan, S. K., Morimatsu, M., Albrecht, U., Lim, D. S., Regel, E., Dinh, C., Sands, A., Eichele, G., Hasty, P., and Bradley, A. (1997). "Embryonic lethality and radiation hypersensitivity mediated by Rad51 in mice lacking Brca2." *Nature*, 386(6627), 804-10.

Sharp, D. J., Rogers, G. C., and Scholey, J. M. (2000). "Cytoplasmic dynein is required for poleward chromosome movement during mitosis in Drosophila embryos." *Nat Cell Biol*, 2(12), 922-30.

Sherman, S. L., Takaesu, N., Freeman, S. B., Grantham, M., Phillips, C., Blackston, R. D., Jacobs, P. A., Cockwell, A. E., Freeman, V., Uchida, I., and et al. (1991). "Trisomy 21: association between reduced recombination and nondisjunction." *Am J Hum Genet*, 49(3), 608-20.

Shonn, M. A., McCarroll, R., and Murray, A. W. (2000). "Requirement of the spindle checkpoint for proper chromosome segregation in budding yeast meiosis." *Science*, 289(5477), 300-3.

Smith, A. L., Hung, J., Walker, L., Rogers, T. E., Vuitch, F., Lee, E., and Gazdar, A. F. (1996). "Extensive areas of aneuploidy are present in the respiratory epithelium of lung cancer patients." *Br J Cancer*, 73(2), 203-9.

Speliotes, E. K., Uren, A., Vaux, D., and Horvitz, H. R. (2000). "The survivin-like C. elegans BIR-1 protein acts with the Aurora-like kinase AIR-2 to affect chromosomes and the spindle midzone." *Mol Cell*, 6(2), 211-23.

Spencer, F., and Hieter, P. (1992). "Centromere DNA mutations induce a mitotic delay in Saccharomyces cerevisiae." *Proc Natl Acad Sci U S A*, 89(19), 8908-12.

Starr, D. A., Williams, B. C., Hays, T. S., and Goldberg, M. L. (1998). "ZW10 helps recruit dynactin and dynein to the kinetochore." *J Cell Biol*, 142(3), 763-74.

Steuer, E. R., Wordeman, L., Schroer, T. A., and Sheetz, M. P. (1990). "Localization of cytoplasmic dynein to mitotic spindles and kinetochores." *Nature*, 345(6272), 266-8.

Strunnikov, A. V., Kingsbury, J., and Koshland, D. (1995). "CEP3 encodes a centromere protein of Saccharomyces cerevisiae." *J Cell Biol*, 128(5), 749-60.

Takahashi, T., Haruki, N., Nomoto, S., Masuda, A., Saji, S., and Osada, H. (1999). "Identification of frequent impairment of the mitotic checkpoint and molecular analysis of the mitotic checkpoint genes, hsMAD2 and p55CDC, in human lung cancers." *Oncogene*, 18(30), 4295-300.

Takenaka, K., Gotoh, Y., and Nishida, E. (1997). "MAP kinase is required for the spindle assembly checkpoint but is dispensable for the normal M phase entry and exit in Xenopus egg cell cycle extracts." *J Cell Biol*, 136(5), 1091-7.

Takenaka, K., Moriguchi, T., and Nishida, E. (1998). "Activation of the protein kinase p38 in the spindle assembly checkpoint and mitotic arrest." *Science*, 280(5363), 599-602.

Taylor, S. S., Ha, E., and McKeon, F. (1998). "The human homologue of Bub3 is required for kinetochore localization of Bub1 and a Mad3/Bub1-related protein kinase." *J Cell Biol*, 142(1), 1-11.

Taylor, S. S., and McKeon, F. (1997). "Kinetochore localization of murine Bub1 is required for normal mitotic timing and checkpoint response to spindle damage." *Cell*, 89(5), 727-35.

Theurkauf, W. E., and Hawley, R. S. (1992). "Meiotic spindle assembly in Drosophila females: behavior of nonexchange chromosomes and the effects of mutations in the nod kinesin-like protein." *J Cell Biol*, 116(5), 1167-80.

Tomkiel, J., Cooke, C. A., Saitoh, H., Bernat, R. L., and Earnshaw, W. C. (1994). "CENP-C is required for maintaining proper kinetochore size and for a timely transition to anaphase." *J Cell Biol*, 125(3), 531-45.

Tournebize, R., Popov, A., Kinoshita, K., Ashford, A. J., Rybina, S., Pozniakovsky, A., Mayer, T. U., Walczak, C. E., Karsenti, E., and Hyman, A. A. (2000). "Control of microtubule dynamics by the antagonistic activities of XMAP215 and XKCM1 in Xenopus egg extracts." *Nat Cell Biol*, 2(1), 13-19.

Tugendreich, S., Tomkiel, J., Earnshaw, W., and Hieter, P. (1995). "CDC27Hs colocalizes with CDC16Hs to the centrosome and mitotic spindle and is essential for the metaphase to anaphase transition." *Cell*, 81(2), 261-8.

Uhlmann, F., Lottspeich, F., and Nasmyth, K. (1999). "Sister-chromatid separation at anaphase onset is promoted by cleavage of the cohesin subunit Scc1." *Nature*, 400(6739), 37-42.

Uhlmann, F., Wernic, D., Poupart, M. A., Koonin, E. V., and Nasmyth, K. (2000). "Cleavage of cohesin by the CD clan protease separin triggers anaphase in yeast." *Cell*, 103(3), 375-86.

Uren, A. G., Beilharz, T., O'Connell, M. J., Bugg, S. J., van Driel, R., Vaux, D. L., and Lithgow, T. (1999). "Role for yeast inhibitor of apoptosis (IAP)-like proteins in cell division." *Proc Natl Acad Sci U S A*, 96(18), 10170-5.

Vaisberg, E. A., Koonce, M. P., and McIntosh, J. R. (1993). "Cytoplasmic dynein plays a role in mammalian mitotic spindle formation." *J Cell Biol*, 123(4), 849-58.

Vale, R. D., Reese, T. S., and Sheetz, M. P. (1985a). "Identification of a novel force-generating protein, kinesin, involved in microtubule-based motility." *Cell*, 42(1), 39-50.

Vale, R. D., Schnapp, B. J., Mitchison, T., Steuer, E., Reese, T. S., and Sheetz, M. P. (1985b). "Different axoplasmic proteins generate movement in opposite directions along microtubules in vitro." *Cell*, 43(3 Pt 2), 623-32.

Verde, F., Dogterom, M., Stelzer, E., Karsenti, E., and Leibler, S. (1992). "Control of microtubule dynamics and length by cyclin A- and cyclin B-dependent kinases in Xenopus egg extracts." *J Cell Biol*, 118(5), 1097-108.

Visintin, R., Prinz, S., and Amon, A. (1997). "CDC20 and CDH1: a family of substrate-specific activators of APC- dependent proteolysis." *Science*, 278(5337), 460-3.

Walczak, C. E., Mitchison, T. J., and Desai, A. (1996). "XKCM1: a Xenopus kinesin-related protein that regulates microtubule dynamics during mitotic spindle assembly." *Cell*, 84(1), 37-47.

Wang, Y., and Burke, D. J. (1995). "Checkpoint genes required to delay cell division in response to nocodazole respond to impaired kinetochore function in the yeast Saccharomyces cerevisiae." *Mol Cell Biol*, 15(12), 6838-44.

Wang, Y., and Burke, D. J. (1997). "Cdc55p, the B-type regulatory subunit of protein phosphatase 2A, has multiple functions in mitosis and is required for the kinetochore/spindle checkpoint in Saccharomyces cerevisiae." *Mol Cell Biol*, 17(2), 620-6.

Wassmann, K., and Benezra, R. (1998). "Mad2 transiently associates with an APC/p55Cdc complex during mitosis." *Proc Natl Acad Sci U S A*, 95(19), 11193-8.

Waters, J. C., Chen, R. H., Murray, A. W., and Salmon, E. D. (1998). "Localization of Mad2 to kinetochores depends on microtubule attachment, not tension." *J Cell Biol*, 141(5), 1181-91.

Weinert, T. A., and Hartwell, L. H. (1988). "The RAD9 gene controls the cell cycle response to DNA damage in Saccharomyces cerevisiae." *Science*, 241(4863), 317-22.

Weisenberg, R. C., and Deery, W. J. (1976). "Role of nucleotide hydrolysis in microtubule assembly." *Nature*, 263(5580), 792-3.

Weiss, E., and Winey, M. (1996). "The Saccharomyces cerevisiae spindle pole body duplication gene MPS1 is part of a mitotic checkpoint." *J Cell Biol*, 132(1-2), 111-23.

Williams, B. C., Gatti, M., and Goldberg, M. L. (1996). "Bipolar spindle attachments affect redistributions of ZW10, a Drosophila centromere/kinetochore component required for accurate chromosome segregation." *J Cell Biol*, 134(5), 1127-40.

Winey, M., Goetsch, L., Baum, P., and Byers, B. (1991). "MPS1 and MPS2: novel yeast genes defining distinct steps of spindle pole body duplication." *J Cell Biol*, 114(4), 745-54.

Woods, C., Zhu, J., McQueney., P.A., Bollag, D., Lazarides, E. (1995). "Taxol-induced mitotic block triggers rapid onset of a p53-independent apoptotic pathway." *Molecular Medicine*, 1, 506-526.

Wooster, R., Bignell, G., Lancaster, J., Swift, S., Seal, S., Mangion, J., Collins, N., Gregory, S., Gumbs, C., and Micklem, G. (1995). "Identification of the breast cancer susceptibility gene BRCA2." *Nature*, 378(6559), 789-92.

Xu, Y., and Baltimore, D. (1996). "Dual roles of ATM in the cellular response to radiation and in cell growth control." *Genes Dev*, 10(19), 2401-10.

Yao, X., Abrieu, A., Zheng, Y., Sullivan, K. F., and Cleveland, D. W. (2000). "CENP-E forms a link between attachment of spindle microtubules to kinetochores and the mitotic checkpoint." *Nat Cell Biol*, 2(8), 484-91.

Yen, T. J., Li, G., Schaar, B. T., Szilak, I., and Cleveland, D. W. (1992). "CENP-E is a putative kinetochore motor that accumulates just before mitosis." *Nature*, 359(6395), 536-9.

Yoon, H. J., and Carbon, J. (1999). "Participation of Bir1p, a member of the inhibitor of apoptosis family, in yeast chromosome segregation events." *Proc Natl Acad Sci U S A*, 96(23), 13208-13.

Yu, H. G., Muszynski, M. G., and Kelly Dawe, R. (1999). "The maize homologue of the cell cycle checkpoint protein MAD2 reveals kinetochore substructure and contrasting mitotic and meiotic localization patterns." *J Cell Biol*, 145(3), 425-35.

Zecevic, M., Catling, A. D., Eblen, S. T., Renzi, L., Hittle, J. C., Yen, T. J., Gorbsky, G. J., and Weber, M. J. (1998). "Active MAP kinase in mitosis: localization at kinetochores and association with the motor protein CENP-E." *J Cell Biol*, 142(6), 1547-58.

Zhou, B. B., and Elledge, S. J. (2000). "The DNA damage response: putting checkpoints in perspective." *Nature*, 408(6811), 433-9.

Zieve, G. W., Turnbull, D., Mullins, J. M., and McIntosh, J. R. (1980). "Production of large numbers of mitotic mammalian cells by use of the reversible microtubule inhibitor nocodazole. Nocodazole accumulated mitotic cells." *Exp Cell Res*, 126(2), 397-405.

Zirkle, R. E. (1970). "Ultraviolet-microbeam irradiation of newt-cell cytoplasm: spindle destruction, false anaphase, and delay of true anaphase." *Radiat Res*, 41(3), 516-37.

The following chapter is adapted, with permission, from Dobles et al., 2000. This work was done in collaboration with Martin Scott, Vasco Liberal, and Robert Benezra. Martin Scott provided training for creating the gene-targeted Mad2 mouse, and Vasco Liberal performed the analysis shown in Figures 2-4 and 2-6, and Table 2-1b. *Mad2c*, described in Figure 1, was cloned by Regina Kirchwegger in the lab of Robert Benezra.

Dobles, M., Liberal, V., Scott, M.L., Benezra, R., Sorger, P.K. (2000) Chromosome missegregation and apoptosis in mice lacking the mitotic checkpoint protein Mad2. Cell 101: 635-645.

Chapter 2: Chromosome missegregation and apoptosis in mice lacking the mitotic checkpoint protein Mad2

Abstract

The initiation of chromosome segregation at anaphase is linked by the spindle assembly checkpoint to the completion of chromosome-microtubule attachment during metaphase. To determine the function of the mitotic checkpoint protein Mad2 during normal cell division and when mitosis goes awry, we have knocked out *Mad2* in mice. We find that E5.5 embryonic cells lacking *Mad2*, like *mad2* yeast, grow normally but are unable to arrest in response to spindle disruption. At E6.5, the cells of the epiblast begin rapid cell division and the absence of a checkpoint results in widespread chromosome mis-segregation and apoptosis. In contrast, the post-mitotic trophoblast giant cells survive without *Mad2*. Thus, the spindle assembly checkpoint is required for accurate chromosome segregation in mitotic mouse cells, and for embryonic viability, even in the absence of spindle damage.

Introduction

During mitosis, chromosomes are segregated with high fidelity. In *S. cerevisiae*, for example, the frequency of chromosome non-disjunction is only about 1×10^{-5} per cell division (Hartwell et al., 1982). This remarkable fidelity depends both on the intrinsic accuracy of the segregation machinery and on the operation of the spindle assembly checkpoint. The spindle checkpoint is a highly conserved signal transduction pathway that links the initiation of anaphase to spindle assembly and the completion of chromosome-microtubule attachment (Hoyt et al., 1991; Li and Murray, 1991; Li and Benezra, 1996; Taylor and McKeon, 1997). The presence of even a single misaligned or unattached chromosome is sufficient to activate the checkpoint, inhibit the Anaphase

Promoting Complex (APC), and arrest a cell at the metaphase to anaphase transition (Hwang et al., 1998; Kim et al., 1998; Li and Nicklas, 1995; Li et al., 1997; Rieder et al., 1994). Arrest caused by an unattached chromosome is overcome by laser ablation of the kinetochore, the structure that mediates chromosome-microtubule attachment (Rieder et al., 1995). Thus, the signal for checkpoint-dependent arrest arises from, or is transduced through, kinetochores. Genes involved in the spindle assembly checkpoint were first identified in the yeast *S. cerevisiae* and include the mitotic arrest defective genes *MAD1-3* (Li and Murray, 1991) and the budding uninhibited by benzimidazole genes *BUB1-3* (Hoyt et al., 1991). Mad1-3p, Bub1p and Bub3p are proteins that link anaphase to the completion of spindle assembly (Alexandru et al., 1999; Hardwick et al., 1996) but Bub2p appears to be part of a second pathway that acts later in the cell cycle to link spindle assembly to mitotic exit and cytokinesis (Alexandru et al., 1999; Clute and Pines, 1999; Fraschini et al., 1999; Li, 1999). All six of these genes are dispensable for normal growth, apparently because mitosis in *S. cerevisiae* lasts long enough for all chromosomes to attach to the spindle before anaphase begins, even in the absence of a checkpoint. The addition of anti-microtubule drugs to yeast cells lacking any single *MAD* or *BUB* gene causes the cells to proceed through mitosis without having established chromosome-microtubule attachments. This causes extensive chromosome loss and cell death (Hoyt et al., 1991; Li and Murray, 1991).

Homologues of the yeast checkpoint genes have been cloned from animal cells (Chan et al., 1998; Jin et al., 1998; Li and Benezra, 1996; Taylor et al., 1998; Taylor and McKeon, 1997). Genetic analysis of these genes has just begun, but *C. elegans mad1* (Kitagawa and Rose, 1999) and *Drosophila bub1* (Basu et al., 1999) are essential genes

whose mutation causes aberrant chromosome segregation. It is not yet known why spindle checkpoint genes are dispensable in budding and fission yeast but essential in worms and flies. One important difference between yeast and metazoans is that only the later undergo apoptosis, an event that can be induced by chromosome damage (Jordan et al., 1996; Lanni and Jacks, 1998; Woods et al., 1995). The expression of a dominant negative fragment of *BUB1* in human cells reduces nocodazole-dependent apoptosis (Taylor and McKeon, 1997), arguing that there is a specific connection between the spindle checkpoint and programmed cell death. One possibility is that apoptosis is triggered after a cell has experienced a prolonged mitotic arrest, thereby reducing the chance that the cell can escape the checkpoint and become aneuploid (Lanni and Jacks, 1998).

Biochemical, genetic and cell biological experiments suggest that Mad and Bub proteins function as components of two closely linked pathways (Alexandru et al., 1999; Hardwick et al., 1996; Li, 1999). In animal cells, several Mad and Bub proteins localize to kinetochores unattached to microtubules, consistent with the observation that kinetochores are involved in generating the checkpoint signal (Chan et al., 1998; Jin et al., 1998; Li and Benezra, 1996; Martinez-Exposito et al., 1999; Taylor and McKeon, 1997). The recruitment of Mad2 to kinetochores involves an interaction with Mad1 (Chen et al., 1999; Chen et al., 1998; Jin et al., 1998). Mad2 also binds to Cdc20 (Fang et al., 1998; Hwang et al., 1998; Kim et al., 1998; Li et al., 1997; Wassmann and Benezra, 1998), an essential activator of the APC (Shirayama et al., 1998; Visintin et al., 1997), preventing APC activation and stopping cell division at the metaphase to anaphase transition (Fang et al., 1998; Hwang et al., 1998; Kim et al., 1998; Wassmann and

Benezra, 1998). Many molecular details remain to be worked out, but a reasonable model is that the activation of checkpoint kinases such as Bub1 promotes the formation of Mad2p-Cdc20p-APC complexes, thereby inhibiting APC and preventing the degradation of proteins such as Pds1p (a regulator of sister chromatid cohesion) whose degradation is necessary for progression to anaphase (Alexandru et al., 1999; Cohen-Fix et al., 1996; Yamamoto et al., 1996). However, alternative pathways have also been proposed (Chan et al., 1999; Hardwick et al., 2000).

To explore the function of the spindle assembly checkpoint in chromosome segregation, apoptosis and genomic stability in mammalian cells, we have undertaken a genetic analysis of the murine *Mad2* checkpoint gene. We find that *Mad2* is essential and that *Mad2*$^{-/-}$ embryos die *in utero* about 6.5-7.5 days after conception (E6.5-7.5). However, homozygous knockout embryos appear normal both in utero and in culture until embryonic day 5.5. *Mad2* E5.5 cells are unable to arrest in mitosis in response to drug-induced spindle disruption, showing that they lack a functional spindle assembly checkpoint. The absence of this checkpoint allows *Mad2*-null cells to divide even when unattached chromosomes are present. This causes chromosomes to be missegregated and results in apoptotic cell death.

Results

Disrupting the murine *Mad2* gene

To isolate *Mad2* genomic DNA from mice, we probed strain 129Sv libraries with ^{32}P-labelled rat or human *Mad2* cDNA (Li and Benezra, 1996). Restriction analysis and subsequent sequencing revealed four distinct *Mad2* genes (Figure 2-1a). Although

Mad2a-c have the potential to encode full-length Mad2 *(Mad2d* lacks an initiating methionine), only *Mad2a* contains introns within the putative coding region. Two experiments were performed to test the idea that *Mad2a* is the only functional gene, (i) a murine embryonic cDNA library was probed with DNA sequences conserved among *Mad2a-c* and (ii) RT-PCR was performed on RNA from adult tissues. Sequencing of the *Mad2*-encoding cDNAs and RT- generated products showed that all *Mad2* mRNA was derived from the *Mad2a* gene. We conclude that *Mad2a* is the functional *Mad2* locus and that *Mad2b-d* are pseudogenes. However, we cannot rule out completely the possibility that *Mad2b* and *c* are expressed in some tissues. To disrupt *Mad2a* in ES cells, gene targeting was used to replace the entire *Mad2* coding region with a PGK-neomycin resistance cassette (Figure 2-2a). Cells from two independent 129Sv-derived ES lines were injected into C57 BL/6 blastocysts, and the resulting chimeras were backcrossed to BL/6 wildtype animals to generate lines 40 and 42. The structure of the disrupted *Mad2* locus was confirmed by Southern blotting and by PCR (Figure 2-2b and c).

Mad2 is essential for the growth of mitotic but not post-mitotic embryonic cells

No homozygous null animals were observed in a total of 296 live births from $Mad2^{+/-}$ heterozygous intercrosses using either of the two founder lines (Table 2-1). Wild-type (WT) and heterozygous mice were born at the expected frequencies and appeared normal and healthy. Subtle differences in morbidity rates between age-matched colonies of $Mad2^{+/+}$ and $Mad2^{+/-}$ animals have been observed and histological analysis of some $Mad2^{+/-}$ animals reveals abnormalities of the spleen (increased germinal center formation) and a possible increase in tumor incidence. However, further analysis is required to

determine the significance of these findings. We conclude that *Mad2* is an essential gene in mice and that *Mad2*$^{+/-}$ animals are largely normal.

To determine when *Mad2*$^{-/-}$ embryos die, we analyzed embryos from heterozygous intercrosses at various points of gestation. At E9.5 – 13.5, none of 23 embryos examined were *Mad*2-null. However, homozygous null embryos could be recovered during the blastocyst stage of development and then grown in culture (at E3.5, too early to establish fibroblast lines; Table 2-1). After 24-48 hours in culture, the spherical blastocysts flatten onto the culture dish and form a multi-component structure in which the inner cell mass (ICM) grows as a mound on top of the extra-embryonic (but embryonically derived) trophoblast cells (Fig 3). When *Mad*2-null and WT embryos were cultured *in vitro*, they were observed to grow at similar rates through E5.5. However, the ICM of *Mad*2-null embryos stopped proliferating after E6.5 and the cells began to die. Virtually no *Mad2*$^{-/-}$ ICM cells persisted to E8.5 (Figure 2-3). In contrast, *Mad2*$^{-/-}$ trophoblast giant cells remained attached to the culture dish and continued to grow in size though E8.5 (the end of the experiment; Figure 2-3). The analysis of *Mad*2-null trophoblast cells by phase contrast microscopy and BrdU labeling demonstrated that they were alive and undergoing DNA replication at E8.5 (data not shown), well past the point at which highly mitotic ICM cells die. Trophoblast giant cells are derived from cells that become mitotically inactive at about E4.5 and undergo repeated rounds of S-phase, generating a polyploid nucleus and a large cytoplasm (Rugh, 1990). We hypothesize that the survival of *Mad2*$^{-/-}$ trophoblast giant cells reflects a requirement for Mad2 specifically during mitosis.

Apoptosis in *Mad2*-null embryos

When the gross morphologies of hematoxylin and eosin (H&E) stained embryos from *Mad2*$^{+/-}$ intercrosses were compared, no clear differences were seen at E5.5. By E6.5-7.5 presumptive *Mad2* $^{-/-}$ embryos were considerably smaller than control littermates and were very disorganized (Figure 2-4; Table 2-1). To investigate the cause of death in *Mad2*$^{-/-}$ embryos, we performed TUNEL on embryonic tissue sections. Embryos from WT animals appeared normal, with only a few apoptotic cells near the center of the embryo (Figure 2-4; Table 2-1). About one-quarter of the embryos arising from heterozygous intercrosses exhibited a high incidence of TUNEL staining (Figure 2-4; Table 2-1). Not all embryos from *Mad2*$^{+/-}$ intercrosses could be genotyped (see Figure 2-4 legend for details) but those Mad2$^{-/-}$ embryos whose genotype could be determined had an abnormal gross morphology and were TUNEL positive. We conclude from these data that Mad2-null embryos undergo programmed cell death at E6.5 – 7.5. Despite the apparent restriction of the *Mad2*-null phenotype to day E6.5 and later, nullizygous embryos were recovered from heterozygous intercrosses at less than the Mendelian frequency of 25% ($p<0.05$, for embryos with unambiguous genotyping). It seems unlikely that this is due to defects in gamete production, because *Mad2*$^{+/-}$ x WT crosses, in which the *Mad2*$^{+/-}$ parent was either the male or the female, yielded 50% *Mad2*$^{+/-}$ offspring (data not shown). Three measures of the frequency of *Mad2*$^{-/-}$ embryos among the progeny of *Mad2*$^{+/-}$ intercrosses (Table 2-1) imply that 30-50% of *Mad2*-null embryos die before implantation. We conclude that loss of *Mad2* causes some embryos to die prior to implantation (see discussion), and the majority to undergo apoptotic death at about E6.5-7.5.

Mad2 is required for mitotic arrest in response to spindle disruption

Is Mad2 required for the mitotic checkpoint in mice as it is in yeast? The observation that *Mad*2-null blastocysts grow normally in culture until E5.5 makes it possible to investigate this critical question. We treated cultured E5.5 embryos from heterozygous intercrosses with 2.5μM nocodazole for 6 hours to disrupt spindle microtubules, disaggregated the embryos with trypsin, and then fixed cells onto coverslips for DAPI staining (Figure 2-5a-d). The mitotic index of each embryo was determined by counting the fraction of cells with condensed chromosomes. A portion of the cells from each disaggregated embryo was reserved for genotyping by PCR. Whereas approximately 25% of the cells from *Mad* $^{+/+}$ and *Mad2*$^{+/-}$ embryos contained condensed chromosomes, only 2% of the cells from *Mad2*$^{-/-}$ embryos were mitotic after nocodazole treatment. Thus, cells from *Mad*2-null embryos do not arrest in mitosis in response to spindle disruption.

A potential caveat to the spindle depolymerization experiment is that *Mad*2-null cells may fail to accumulate in mitosis simply because they are not actively cycling during the period of nocodazole treatment. To eliminate this possibility, we measured the fraction of cells in S-phase by labeling with BrdU and the fraction in mitosis by staining for phosphorylated-Histone H3 (Mahadevan et al., 1991). If *Mad*2-null cells proceed through the cell cycle during nocodazole treatment they should have a similar (or higher) S-phase index than WT cells. Embryos were grown on chambered microscope slides to E5.5, treated with 2.5μM nocodazole for 6 hours and with BrdU during the final 3 hours, digested with collagenase (to remove the basal lamina and promote antibody access to the ICM), and then fixed and stained (Figure 2-5). WT and heterozygous embryos treated

with nocodazole showed a large increase in the number of phospho-Histone H3 positive cells as compared to untreated embryos (Figure 2-5f and g). In contrast, no increase in the number phospho-Histone H3 positive cells was observed in nocodazole-treated *Mad*2-null embryos (Figure 2-5h). This confirms data obtained with disaggregated cells (Figure 2-5a-d). Significantly, the fraction of BrdU-positive cells was similar in WT and *Mad*2-null embryos (about 50%) indicating that similar numbers of cells were actively synthesizing DNA. Thus, *Mad*2-null cells are passing through the cell cycle at E5.5 even though they fail to arrest in response to nocodazole treatment. We conclude that the disruption of *Mad2* in mice inactivates the mitotic spindle assembly checkpoint just as it does in yeast (He et al., 1997; Li and Murray, 1991). In yeast, *MAD2* deletion causes an alteration in the regulation rather than the mechanics of mitosis. We have been unable to investigate this in detail in early mouse embryos but we do see evidence of correct spindle assembly and aligned chromosomes in *Mad2*$^{-/-}$ cells even past E5.5 (Figure 2-6). Thus, the mechanics of chromosome segregation appear to be more or less normal.

Chromosome missegregation in *Mad*2-null cells

Why do *Mad*2-null mouse cells die *in utero* and in culture at E6.5 - 7.5? One possibility is that the loss of checkpoint function results in a gross failure of chromosome segregation so that one daughter cell ends up with little or no DNA and dies. This type of missegregation is observed in yeast mutants such as *ndc10* and *esp1* (Goh and Kilmartin, 1993; McGrew et al., 1992). An alternate possibility is that there are subtle defects in mitosis and that the missegregation of one or a small number of chromosomes induces cell death. To investigate the occurrence of chromosome missegregation in mice, E6.5 -

7.5 embryos from intercrosses of WT and *Mad2*$^{+/-}$ animals were sectioned *in utero*, chromosomes were stained with Hoechst 33342 and the sections examined by laser confocal microscopy (Figure 2-6). In WT embryos, the total number of mitotic cells more than doubled between E6.5 and E7.5 (Figure 2-6a, dark bars). In virtually all anaphase cells mitosis appeared normal (>97% of mitotic cells) with chromosomes in two distinct groups clustered around the spindle poles. In contrast, in histologically abnormal embryos from heterozygous intercrosses (presumptive *Mad*2-nulls; see above) mitosis appeared to have gone awry (Figure 2-6a and b, light bars). By E6.5 the total number of mitotic cells was markedly reduced and remained relatively unchanged through E7.5. Strikingly, about 25% of mitotic cells in abnormal embryos contained one or more chromosomes that were separated from the bulk of the pole-proximal DNA (Figure 2-6c and d). The high incidence of these lagging chromosomes suggests that anaphase is proceeding in *Mad*2-null cells in the absence of complete chromosome-microtubule attachment. This type of missegregation is consistent with the failure of *Mad*2-null cells to arrest in response to spindle damage induced by microtubule depolymerization (Figure 2-5). Even though mutant embryos contain a high proportion of cells with lagging chromosomes, it is important to note that at least until E6.5, mitotic spindles still assemble and the bulk of the DNA is evenly divided between daughter cells (Figure 2-6e and f). We have observed no difference between the spindles of WT and *Mad*2-null cells, nor have we observed cells with obviously subgenomic complements of DNA, in contrast to what is seen in budding yeast that carry mutations in essential kinetochore proteins (Goh and Kilmartin, 1993). We conclude from these observations that cells in which the Mad2-dependent checkpoint is abolished (as evidenced by *in vitro* challenges with

nocodazole) are capable of assembling largely normal spindles and of correctly segregating the bulk of their DNA.

Figure 2-1. Structure of *Mad2* genes in mice

(a) Organization of the *Mad2* cDNA and of four distinct genomic loci. Regions homologous to the coding sequence of the cDNA are indicated (black boxes) as are the 5' and 3' UTR's (white boxes) and a potential alternatively spliced final coding region (hatched box). "Met" indicates the initiating methionine and "*" indicates the stop codon. *Mad2d* lacks an initiating methionine. **(b)** Mad2 protein sequences determined from conceptual translations of the mouse genomic loci *Mad2a*-c, rat (*rMad2*), human (*hMad2*) and yeast (*yMAD2*) cDNAs. Gray boxes indicate conserved changes and black boxes indicate differences relative to mMad2a. Mouse Mad2a is 40% identical in protein sequence to yeast Mad2p and 95% identical to human Mad2. Mad2a' denotes the protein that could be produced by splicing exon IV to exon VI, skipping exon V. This alternative splicing has not been observed to occur in isolated cDNA's. The sequences of mMad2b and c are shown only where they differ from that of mMad2a. The arrow marks the primer used to sequence polymorphic regions of cDNA clones. Complete sequences of MAD2a-d have been deposited in Genebank, accession numbers AF261919-261921, and AF259902.

a. Murine Mad2 loci

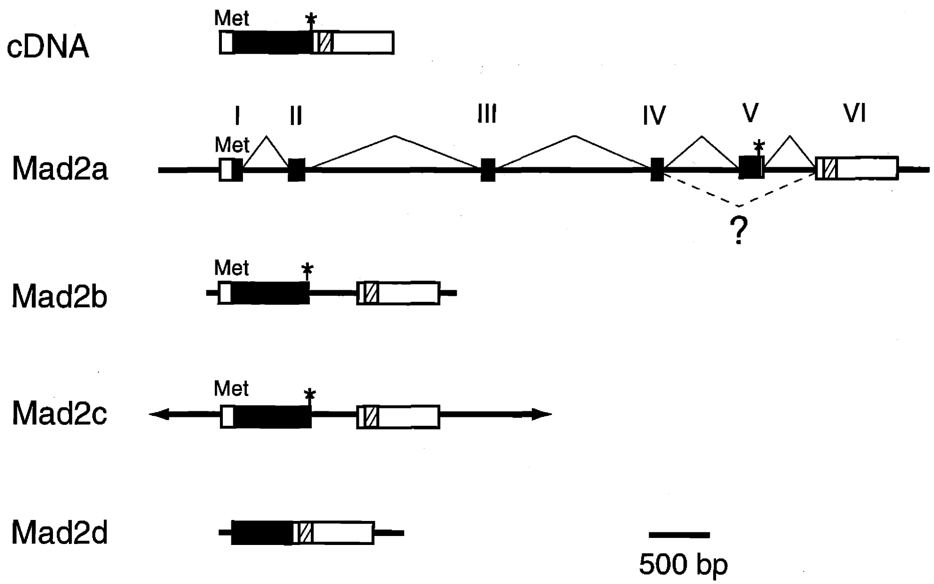

b. Mad2 Gene sequences

```
          ┌b
mMad2  ──┤c           Q   DQ                                                                                                       R
          │a       MAQ QLAREQGITLRGSAEIVAEFFSFGINSILYQRGIYPSETFTRVQKYGLTLLTTTDPELIKYLNNVVEQLKEWLYKCSVQKLVVVISNIESGEVLERWQFDIECDKTAKEEGVRREK
mMad      └a'      MAQ QLAREQGITLRGSAEIVAEFFSFGINSILYQRGIYPSETFTRVQKYGLTLLTTTDPELIKYLNNVVEQLKEWLYKCSVQKLVVVISNIESGEVLERWQFDIECDKTAKEEGVRREK
rMad2              MAQ QLARDQGITLRGSAEIVAGFFSFGINSILYQRGIYPSETFTRVQKYGLTLLVTTDPELIKYLNNVVEQLKEWLYKCSVQKLVVVISNIESGEVLERWQFDIECDKTAKEEGVRREK
hMad2              MAL QLSREQGITLRGSAEIVAEFFSFGINSILYQRGIYPSETFTRVQKYGLTLLVTTDLELIKYLNNVVEQLKDWLYKCSVQKLVVVISNIESGEVLERWQFDIECDKTAKDDSAPREK
ymad2                  MSQSISLKGSTRTVTEFFEYSINSILYQRGVYPAEDFVTVKKYDLTLLKTHDDELKDYIRKILLQVHRWLLGGKCNQLVLCIVDKDEGEVVERWSFNVQ HISGNSNGQDDVV

          ┌b 120                                                    A
mMad2  ──┤c 121                    ┌──→                             A
          │a 120  SQKAIQDEIRSVIRQITATVTFLPLLEVS   CSFDLLIYTDKDLVVPEKWEESGPQFITNCEEVRLRSFTTTIHKVNSMVAYKTPVND*
mMad      └a'120  SQKAIQDEIRSVIRQITATVTFLPLLEVS   CSFGLLIYTDKDLVVPETREESGPQFITSSEEIRLH*
rMad2        120  SQKAIQDEIRSVIRQITATVTFLPLLEVS   CSFDLLIYTDKDLVVPEKWEESGPQFITNSEEVRLRSFTTTIHKVNSMVAYKTPVSD*
hMad2        120  SQKAIQDEIRSVIRQITATVTFLPLLEVS   CSFDLLIYTDKDLVVPEKWEESGPQFITNSEEVRLRSFTTTIHKVNSMVAYKIPVND*
ymad2        113  DLNTTQSQIRALIRQITSSVTFLPELTKEGGYTFTVLAYTDADAKVPLEWADSNSKEIPDGEVVQFKTFSTNDHKVGAQVSYKY*
```

Figure 2-2. Disrupting the *Mad2a* locus in ES cells

(a) Structure of the WT *Mad2a* locus, the targeting vector and the disrupted locus. The PGK-neomycin resistance cassette (hatched box) replaces *Mad2a* coding sequences (dark boxes) from the initiating methionine to the stop codon (*). White boxes indicate 5' and 3' UTRs of the *Mad2* locus, and the gray box indicates a PGK-Thymidine Kinase cassette used for negative selection of ES cells. The restriction fragments used in the analysis of WT and targeted *Mad2a* loci are shown by arrows "a", "b", "a'" and "b'" and locations of Southern probes by "p1" and "p2". PCR-A, -B and -C indicate the PCR products used for genotyping (see Experimental Procedures for details). Diagnostic restriction sites are indicated as follows Ps -- PstI; Kp -- KpnI; Sc -- SacI; H3-- HindIII; Xb – XbaI, but additional sites for these enzymes are also present. **(b)** Confirmation of *Mad2a* disruption in ES cells by Southern blotting following KpnI (Kp; probe p1) or PstI (Ps; p2) digestion. The origin of various bands is indicated with reference to the schematic (part a). **(c)** PCR genotyping of embryos grown in culture. Separate PCR reactions were performed to amplify the WT *Mad2* allele (PCR-B, see part a) and the disrupted allele (PCR-C), and the samples then combined and analyzed on ethidium bromide-stained agarose gels. "M" indicates molecular weight markers.

a.

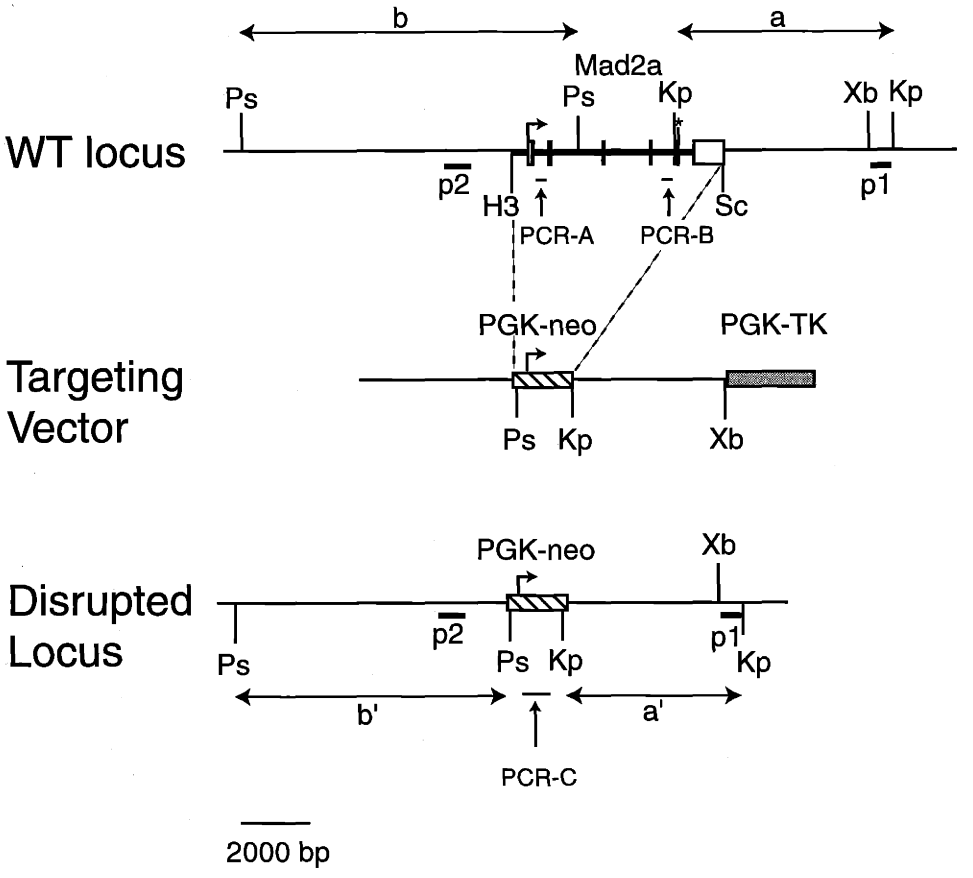
b
a
Mad2a
Ps
Ps
Kp
Xb Kp
WT locus
p2
H3
PCR-A
PCR-B
Sc
p1
PGK-neo
PGK-TK
Targeting Vector
Ps Kp
Xb
PGK-neo
Xb
Disrupted Locus
p2
p1
Ps
Ps Kp
Kp
b'
a'
PCR-C
2000 bp

b.

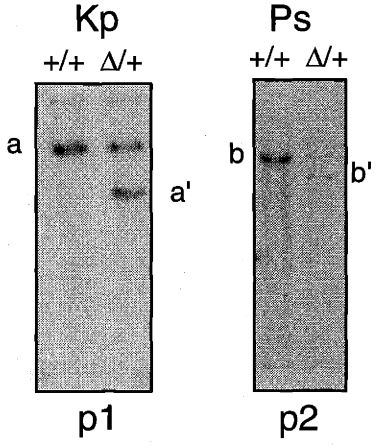
Kp
+/+ Δ/+
a
a'
p1
Ps
+/+ Δ/+
b
b'
p2

c.

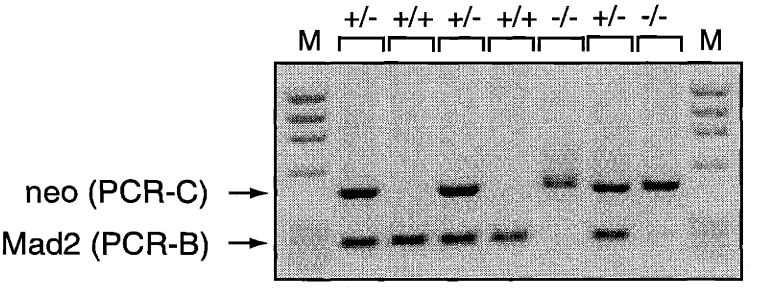
+/- +/+ +/- +/+ -/- +/- -/-
M
M
neo (PCR-C)
Mad2 (PCR-B)

Figure 2-3. Growth of WT and *Mad2*$^{-/-}$ embryos in culture

Embryos grown in culture. E3.5 blastocysts from *Mad2* heterozygous intercrosses were cultured *in vitro* for 48 hours and then photographed using phase contrast microscopy. Arrows point to the inner cell mass (ICM) and to the trophoblast giant cells (GC). Photos were taken at E5.5, and then every 24 hours until E8.5. Genotypes were determined by PCR. Embryos exhibiting more extensive loss of ICM cells were common, but these embryos generally failed to yield PCR bands in the genotyping assay.

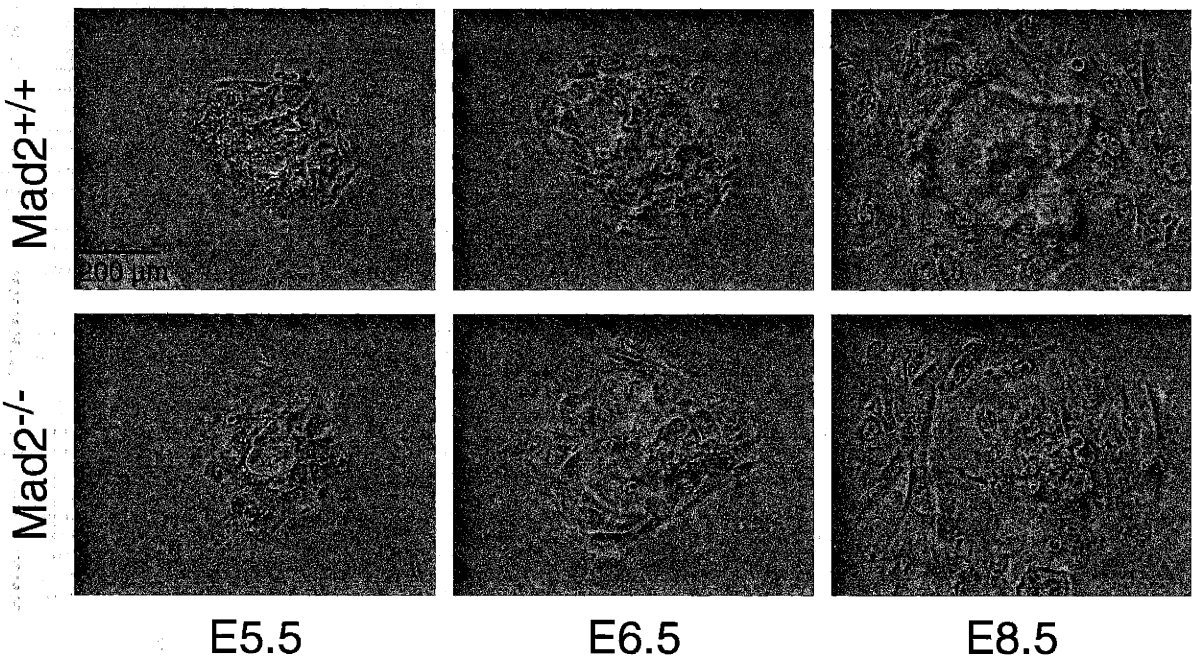
Mad2+/+
Mad2-/-
200 μm
E5.5
E6.5
E8.5

Figure 2-4. Analysis of apoptosis in *Mad2*$^{-/-}$ embryos *in utero*

TUNEL staining of transversely sectioned E7.0 embryos *in utero* at low (a and c) and high (b and d) magnifications. Arrows point to TUNEL-positive apoptotic cells. The genotyping of embryonic sections was performed on samples collected by laser capture microscopy and was often complicated by the contamination of embryonic tissue by maternal tissue. We therefore relied on morphological methods to genotype the majority of embryos. However, the mutant embryos shown in this figure were unambiguously genotyped by PCR. WT embryos were derived from WT intercrosses (and therefore did not require genotyping). H&E analysis showed that embryos unambiguously genotyped as homozygous *Mad*2-nulls were small and abnormal in gross morphology as compared to WT controls, and displayed evidence of aberrant mitosis (Figure 2-6). Both of these phenotypes were seen in only about a fifth of the embryos from *Mad2*$^{+/-}$ intercrosses, and never in wild-type crosses, linking them to the *Mad*2-null genotype (Table 2-1). We therefore classified as presumptive *Mad*2-nulls all those embryos that were small and exhibited abnormal histology.

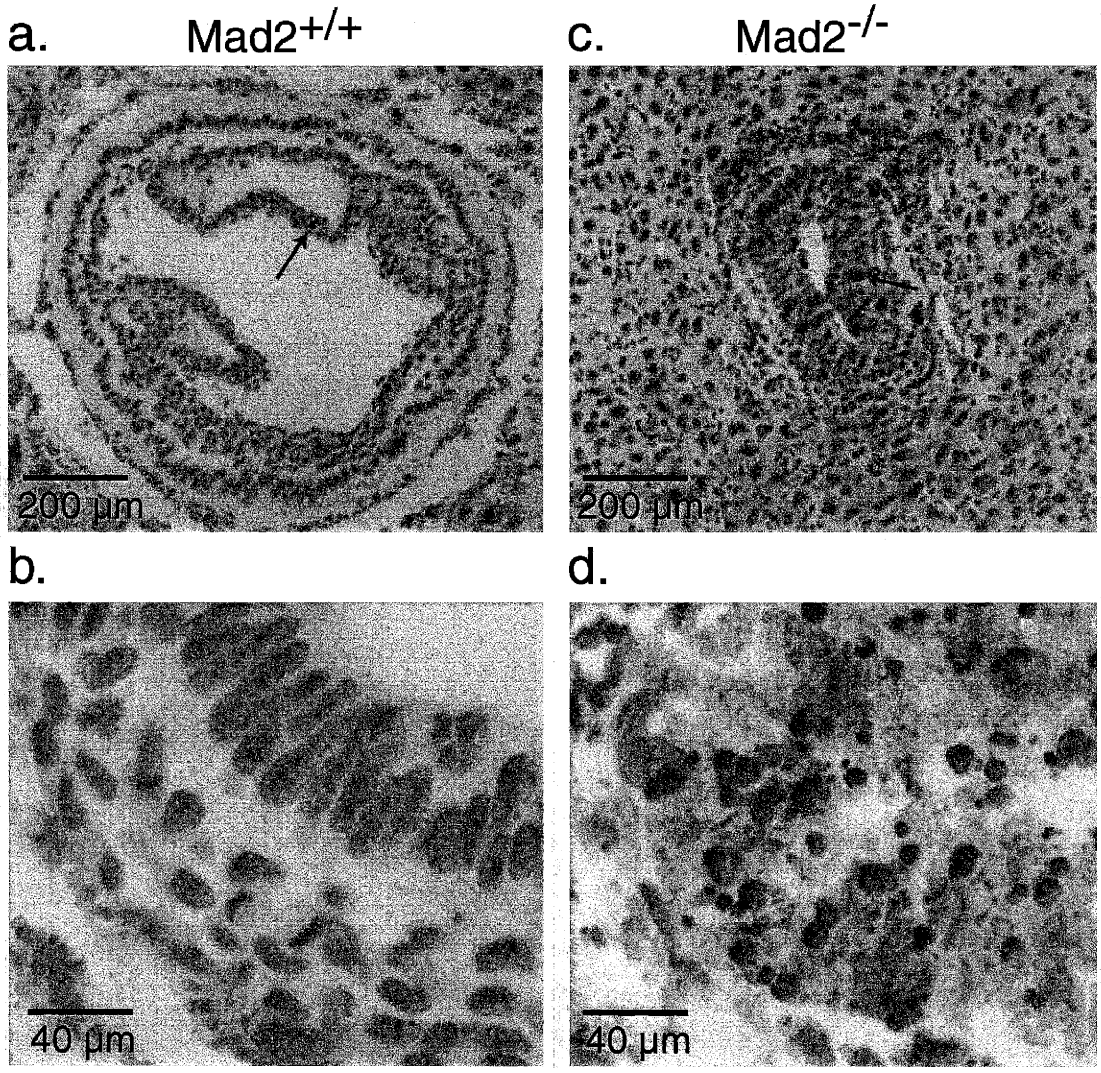
a.
Mad2+/+
c.
Mad2-/-
200 µm
200 µm
b.
d.
40 µm
40 µm

Figure 2-5. Analysis of checkpoint response in cultured *Mad2*$^{-/-}$ embryos

(a) Experimental outline. Blastocysts harvested at E3.5 from intercrosses of *Mad2*$^{+/-}$ mice were cultured *in vitro* to E5.5, treated with 2.5μM nocodazole for 6 hr. and analyzed for mitotic arrest. **(b-d)** Quantitative analysis of mitotic arrest in disaggregated embryos. **(b)** Mitotic index for embryos of various genotypes. "n" indicates number of embryos analyzed. Error bars represent one standard deviation. The total number of DAPI-stained cells per embryo ranged from 17 to 113, with no statistically significant differences between genotypes. The mitotic index was determined by counting cells with condensed (c) and non-condensed chromosomes (d). **(e-h)** Analysis of S-phase and mitotic index in whole-mounts. **(e)** Experimental outline. Blastocysts harvested at E3.5 from intercrosses of *Mad2*$^{+/-}$ mice were cultured *in vitro* to E5.5, treated with 2.5μM nocodazole for 6 hr. and 10μM BrdU for 3hr., and then briefly digested with collagenase to promote antibody access to the inner cell mass. After imaging, embryos were genotyped by PCR. **(f-h)** Embryos were processed for indirect immunofluorescence using anti-BrdU (red) and anti-phospho-Histone-H3 (yellow) antibodies. Each embryo is shown both with DAPI staining to show all cells, and without DAPI to make BrdU and anti-phosopho-Histone-H3 signals more obvious. Nocodazole-treated *Mad2*$^{+/-}$ embryo is representative of both *Mad2*$^{+/-}$ and WT embryos, as no difference was observed in the incidence of mitotic arrest between heterozygous and WT embryos.

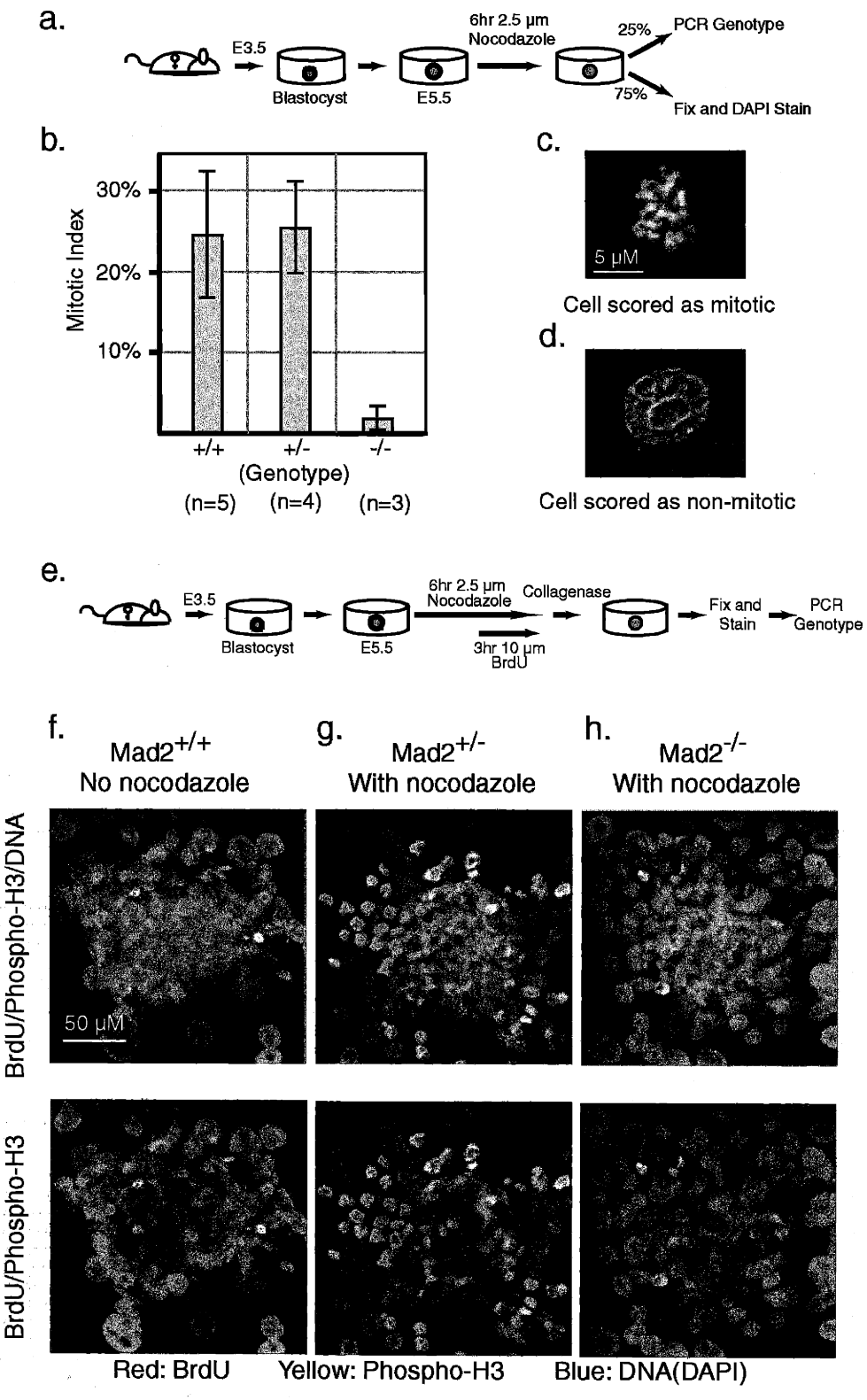
a.
E3.5
Blastocyst
E5.5
6hr 2.5 µm Nocodazole
25%
PCR Genotype
75%
Fix and DAPI Stain
b.
Mitotic Index
30%
20%
10%
+/+
+/-
-/-
(Genotype)
(n=5)
(n=4)
(n=3)
c.
5 µM
Cell scored as mitotic
d.
Cell scored as non-mitotic
e.
E3.5
Blastocyst
E5.5
6hr 2.5 µm Nocodazole
Collagenase
3hr 10 µm BrdU
Fix and Stain
PCR Genotype
f.
Mad2+/+
No nocodazole
g.
Mad2+/-
With nocodazole
h.
Mad2-/-
With nocodazole
BrdU/Phospho-H3/DNA
50 µM
BrdU/Phospho-H3
Red: BrdU
Yellow: Phospho-H3
Blue: DNA(DAPI)

Figure 2-6. Analysis of chromosome missegregation in *Mad2*$^{-/-}$ cells

Analysis of chromosome segregation *in utero* in E6.5-7.5 embryos. Embryos were fixed, embedded, sectioned, stained with Hoechst 33342, and examined by confocal microscopy. Abnormal embryos, with a presumptive *Mad2*$^{-/-}$ genotype, were distinguished from presumptive WT and *Mad2*$^{+/-}$ embryos by overall size and morphology in H&E stained sections (Figure 2-4 legend). Each data point is derived from an analysis of at least three embryos. **(a)** Comparison of the total number of mitotic cells in abnormal and normal embryos. Cells were scored as mitotic based on chromosome condensation. Error bars represent one standard deviation. **(b)** Quantitative analysis of chromosome missegregation. The fraction of mitotic cells in anaphase that exhibited a defect in segregation, such as a lagging chromosome (see c and d) is shown. **(c-f)** Spindle morphologies in cells from presumptive *Mad2*-null embryos at E6.5. A significant fraction of anaphase cells contained one or more chromosomes clearly separated from the bulk of DNA clustered at the poles (c and d). These lagging chromosomes DNA are indicated by arrows. Other cells had apparently normal spindle morphologies (e and f).

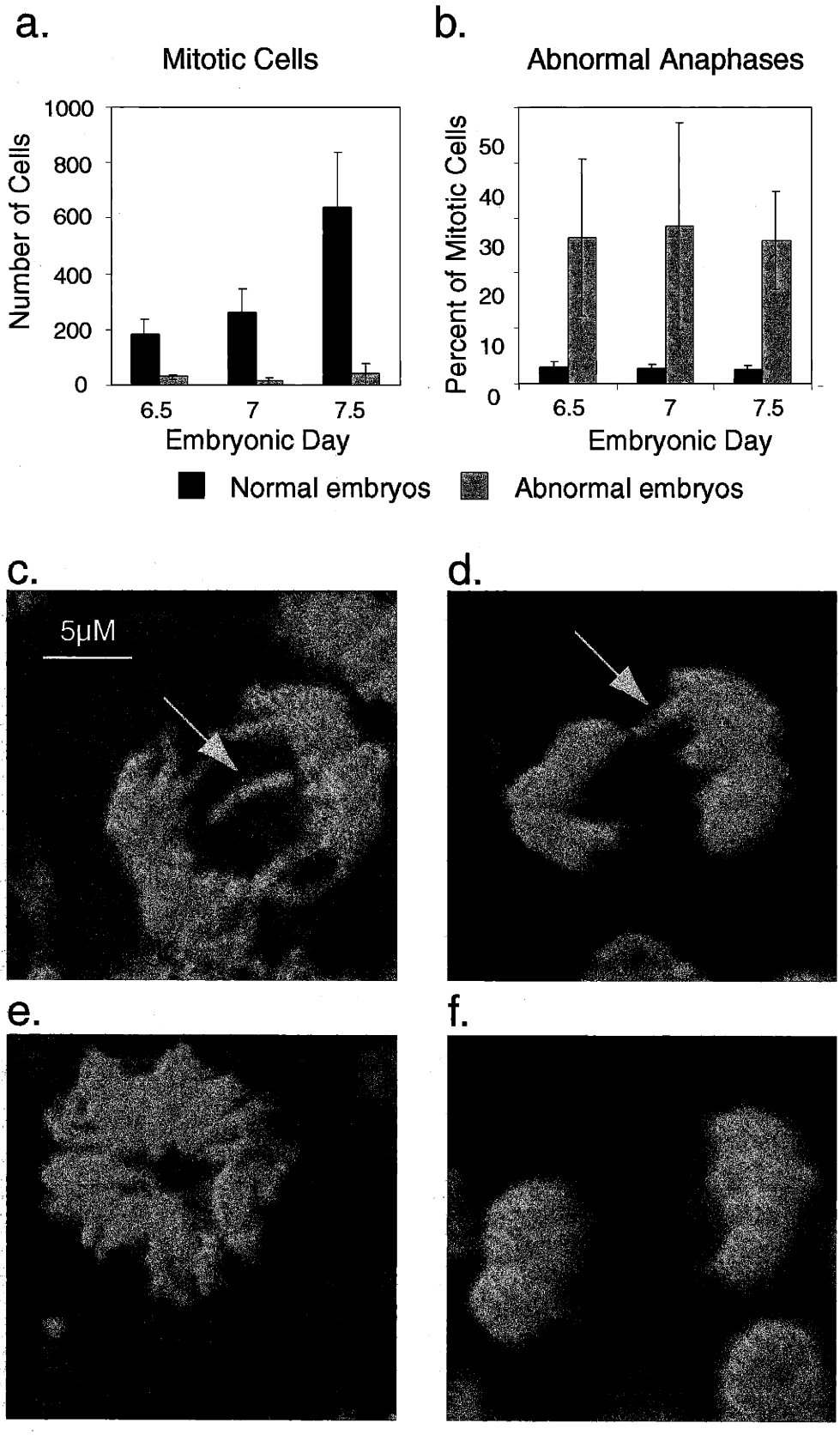
a.
Mitotic Cells
Number of Cells
1000
800
600
400
200
0
6.5
7
7.5
Embryonic Day
b.
Abnormal Anaphases
Percent of Mitotic Cells
50
40
30
20
10
0
6.5
7
7.5
Embryonic Day
Normal embryos
Abnormal embryos
c.
5μM
d.
e.
f.

Table 2-1. Viability Analysis of *Mad2*$^{+/-}$ Mice and Embryos

A. Genotypes of Live Births and Embryos from *Mad2*$^{+/-}$ Intercrosses

	Genotype				
	Mad2$^{+/+}$	*Mad2*$^{+/-}$	*Mad2*$^{-/-}$	ND[a]	Total
Live Births, Line 40	12	23	0		35
Live Births, Line 42	84	177	0		261
Embryos, E9.5-13.5[b]	5	18	0		23
Blastocysts, E3.5[b]	20	31	7	9	67
Blastocysts grown in culture[b,c]					
Healthy at E8.5	5	11	0	0	16
ICM atrophied by E8.5	1	0	3	2	6

B. Histological Analysis of Embryos *In Utero*

		Number of Embryos			
Cross	Age	Total	Abnormal (A)	Resorbed (R)	Total A+R
Mad2$^{+/-}$ X *Mad2*$^{+/-}$	E6.0-6.5	32	4	2	19%
Mad2$^{+/-}$ X *Mad2*$^{+/-}$	E6.5-7.5	73	8	5	18%
Mad $^{+/+}$ X *Mad2*$^{+/+}$	E6.5-7.5	37	0	0	0%

Mice and E9.5-13.5 embryos were genotyped either by Southern blotting Kpn I digested DNA (Figure 2-2) or by PCR of fragments PCR-A and C (see Figure 2-2). E3.5-8.5 embryos were genotyped by amplification of regions PCR-B and C (see Figure 2-2). All embryos harvested at E3.5 were grown in culture to at least E5.5 before recovering DNA for genotyping.

For histological analysis embryos were fixed, sectioned, H&E stained, and scored as normal or abnormal based on size and general morphology. (Examples shown in Figure 2-4.) Empty decidua were scored as "Resorbed". Embryos from wildtype crosses were also examined as controls.

TUNEL analysis was performed on 13 of the E6.5-7.5 embryos from *Mad2*$^{+/-}$ intercrosses, and on 16 embryos from WT crosses. 3 embryos from *Mad2*$^{+/-}$ intercrosses, and none from WT crosses, were TUNEL positive (Figure 2-4).

[a] Not determined – genotyping was ambiguous.

[b] Derived from heterozygous intercrosses of Line 42.

[c] This represents typical data from one set of experiments. In related experiments, a total of 303 embryos were grown in culture. By E8.5, ICM cells atrophied in 5% (n = 95) of embryos from *Mad2*$^{+/-}$ x *Mad2*$^{+/+}$ crosses as compared to 17% (n=208) from *Mad2*$^{+/-}$ intercrosses.

Discussion

We have shown that *Mad2*$^{-/-}$ embryonic mouse cells at E5.5, like *mad2* yeast, assemble spindles and undergo mitosis but do not arrest in response to microtubule depolymerization. The most striking difference between *Mad2* in higher and lower eucaryotes is that *Mad2* is essential in mouse cells after E6.5 but is dispensable for normal cell division in yeast (He et al., 1997; Li and Murray, 1991). *In utero*, *Mad2*-null mouse embryos undergo programmed cell death after the initiation of gastrulation (E6.5), a particularly active period of cell division characterized by very short cell cycles (as short as 4-6 hours for some cell types) (Hogan et al., 1994; Snow, 1977). In culture, the death of *Mad2*$^{-/-}$ cells is restricted to the rapidly dividing cells of the inner cell mass. The post-mitotic and highly polyploid trophoblast giant cells survive, arguing that Mad2 is required selectively in cells undergoing mitosis. Although we have found that *Mad2*$^{-/-}$ animals derived from either of two independent lines are inviable, a number of animal studies remain to be done. One issue requiring further investigation is that fewer *Mad2*$^{-/-}$ embryos are recoverable, even at the earliest times after conception, than one would expect. It is possible that this reflects some probability of catastrophic chromosome missegregation prior to E3.5, the time at which embryos are harvested. Alternatively, *Mad2*$^{-/-}$ embryos may have a partially penetrant early embryonic defect unrelated to mitosis. Also requiring follow-up is preliminary histology that shows atypical germinal center morphology in the spleens of *Mad2*$^{+/-}$ animals. We are currently looking for cell cycle defects and tumors in highly proliferative hematopoetic lineages.

Mouse Mad2 is required for checkpoint-dependent arrest

The observation that Mad2 binds to Mad1 (Chen et al., 1999; Chen et al., 1998; Jin et al., 1998) and to Cdc20-APC (Fang et al., 1998; Hwang et al., 1998; Kim et al., 1998; Li et al., 1997; Wassmann and Benezra, 1998) in both animal cells and yeast implies that Mad2 is part of a signaling pathway conserved among higher and lower eucaryotes. However, the presence in animal cells of multiple Mad2-like proteins (Li and Benezra, 1996) and the discovery that Mad2 may bind to proteins as diverse as the insulin receptor (O'Neill et al., 1997) and metalloprotease disintegrins (Nelson et al., 1999) makes it essential to obtain genetic data about Mad2 function. By manipulating E5.5 embryonic cells in culture, we have examined the effect of deleting *Mad2* on the cell cycle arrest induced by disrupting microtubules of the mitotic spindle. We find that that the mitotic index of *Mad2*$^{-/-}$ embryonic cells is virtually identical before and after treatment with nocodazole. In contrast, the mitotic index of wild-type embryonic cells rises nearly 10-fold in response to a 6 hour nocodazole treatment. Thus, spindle damage provokes a cell cycle arrest in wild-type embryonic cells, but not in *Mad2*$^{-/-}$ cells. We conclude that Mad2 is required for the spindle assembly checkpoint in mouse cells as it is in yeast (He et al., 1997; Li and Murray, 1991). These data are consistent with previously reported injection/electroporation experiments performed with PtK_1 (Gorbsky et al., 1998) and HeLa cells (Li and Benezra, 1996) in which anti-Mad2 antibodies abolish nocodazole-induced mitotic arrest and cause premature mitotic exit.

Mad2-null cells have high rates of chromosome loss

In this paper we provide genetic evidence in mammalian cells that the spindle assembly checkpoint is required for accurate chromosome segregation in the absence of spindle damage. The deletion of mouse *Mad2* appears to cause the rate of chromosome mis-segregation to rise dramatically. In many cases, we see evidence that one chromosome is left behind at the metaphase plate when the majority of chromosomes have moved to the poles. However, spindles do form and the great majority of chromosomes are correctly aligned and properly segregated. It seems very likely that the high proportion of lagging chromosomes reflects a failure of *Mad2*$^{-/-}$ cells to delay anaphase until all chromosomes have achieved proper bivalent attachment to spindle microtubules. We conclude that the checkpoint is not necessary for spindle assembly *per se*, but is required to provide sufficient time for the completion of the stochastic process of chromosome capture. This conclusion is consistent with anti-Mad2 microinjection experiments in HeLa cells (Gorbsky et al., 1998), and with the finding that the expression of a dominant negative fragment of mouse *Bub1* shortens the average time that a cell spends in mitosis (Taylor and McKeon, 1997). Technical difficulties prevent us from scoring chromosome missegregation prior to E5.5 but there is no evidence that early *Mad2*$^{-/-}$ embryos have reduced rates of growth or altered S-phase and mitotic indexes. Thus, the rate of chromosome missegregation appears to rise dramatically at E6.5. Why does mis-segregation only become apparent this late in development? One possibility is that in mice, as in *Xenopus*, the checkpoint does not function (and is not required) in the very early embryonic cell cycles (Chen et al., 1996). A second possibility is that maternal transcripts provide sufficient Mad2 for early divisions but that the maternal store is

eventually exhausted. However, several studies have shown that the vast majority of RNA in E3.5 and later embryos arises from zygotic transcription and that maternal mRNAs are largely gone (Bachvarova and De Leon, 1980; Nothias et al., 1995). Exhaustion of maternal *Mad2* mRNA therefore seems an unlikely explanation for the late onset of a phenotype. A final possibility is that the checkpoint only becomes critical at about the time of gastrulation, when embryos enter a period of rapid cell division (Hogan et al., 1994; Snow, 1977). We favor this final explanation because it links changes in cell cycle timing to an increased reliance on checkpoint-imposed mitotic delay.

Death in *Mad2*-null cells

What is the cause of apoptosis in *Mad2*-null cells? While we cannot exclude the possibility that cell death is unrelated to the function of Mad2 in mitosis, the most attractive possibility is that missegregated chromosomes themselves trigger programmed cell death. Apoptosis occurs across the entire embryo at E6.5-7.5, the point in development at which the cell cycle is reduced to as few as 4-6 hours (Hogan et al., 1994; Snow, 1977), making correct chromosome segregation more dependent on the spindle assembly checkpoint. We propose that cells lacking Mad2 at E6.5 exit mitosis early, causing DNA damage that induces apoptosis, perhaps via p53 (Basu et al., 1998; Lanni and Jacks, 1998). We are currently testing this idea by determining whether the disruption of p53 increases the survival of *Mad2*$^{-/-}$ embryos. The finding that Mad2-deletion promotes apoptosis contrasts with an earlier observation that apoptosis induced by treating HeLa cells with nocodazole is reduced by the over-expression of dominant negative fragments of *Bub1* (Taylor and McKeon, 1997). Whether this reflects a

difference between Mad2 and Bub1 or between embryonic cells and a transformed cell line is not known.

Mitotic checkpoints in yeast and metazoans

The remarkable fidelity of chromosome segregation is dependent in part on the operation of mitotic checkpoints (Hoyt et al., 1991; Li and Murray, 1991; Li and Nicklas, 1995). In the classical view (Hartwell and Weinert, 1989), checkpoints are nonessential and their inactivation only has an effect on those few cells in which mitosis goes awry. However, genetic analysis of *Mad2* in mouse, *bub1* in *Drosophila* (Basu et al., 1999) and *mad1* in *C. elegans* (Kitagawa and Rose, 1999) indicates that mitotic checkpoint genes are essential for cell viability in higher eucaryotes. This might appear to represent a fundamental difference between higher and lower eucaryotes, but real-time observations of mitosis in PtK_1 cells suggest a unifying model (Gorbsky et al., 1998; Rieder et al., 1994). The duration of mitosis in PtK_1 cells (from nuclear envelope breakdown to the initiation of anaphase) varies from about 30 minutes to over 3 hours. Regardless of the total time required for mitosis, anaphase starts almost exactly 23 minutes after the final chromosome makes proper attachment to the microtubules of the mitotic spindle (Rieder et al., 1994). In cells microinjected with anti-Mad2 antibodies, anaphase starts an average of 15 minutes after nuclear envelope breakdown, regardless of the status of spindle assembly (Gorbsky et al., 1998). Thus, the duration of mitosis in PtK1 cells appears to depend on both intrinsic timing (which accounts for the first about 15 minutes of mitosis) and on checkpoint-imposed delays (which provide whatever additional time is required to complete spindle assembly). We can easily imagine that differences in the intrinsic rate of

cell-cycle progression or the rate chromosome-microtubule capture could alter the importance of checkpoint-imposed delays, even in the absence of exogenous spindle damage. Thus, the absolute requirement for the checkpoint in higher eucaryotes, but not in budding yeast, might reflect a faster intrinsic clock and slower rate of chromosome-microtubule attachment and the presence of cell death pathways that are sensitive to chromosome damage. The observation that the deletion of *S. pombe Bub1* causes widespread chromosome missegregation demonstrates that checkpoints are required for accurate mitosis under normal growth conditions, but that fission yeast can tolerate high rates of chromosome loss (Bernard et al., 1998).

Mitotic checkpoints, apoptosis and tumorigenesis

The connection between checkpoints, aneuploidy and cancer has several intriguing facets. In addition to the long-standing observation that the vast majority of tumor cells are aneuploid (Hartwell and Kastan, 1994; Kinzler and Vogelstein, 1996; Mitelman, 1971), it has recently been shown that cells from human colorectal cancers have a continuous high rate of chromosome loss and gain (giving rise to a chromosome instability or CIN phenotype; (Lengauer et al., 1997). Some human lung and colorectal cancers have also been shown to harbor mutations in the spindle assembly checkpoint genes *Bub1* and *Mad1* (Cahill et al., 1998; Nomoto et al., 1999). Checkpoint lesions that increase the rate of chromosome missegregation have the potential to be tumor promoting by acting as mutators that cause wildtype tumor suppressor alleles to be lost and recessive mutations to be uncovered. However, if chromosome missegregation triggers cell death, as suggested by the findings in this paper, it may be necessary for cells to acquire anti-

apoptotic mutations to exhibit a CIN phenotype. If so, we might expect chromosome instability to occur not during the earliest stages of tumorigenisis, but rather at later stages when anti-apoptotic oncogenic lesions have already accumulated. Using various recombinant mouse strains it should be possible to test this idea.

Materials and Methods

Cloning and Sequence Analysis of Murine *Mad2*

Mouse *Mad2* genomic DNA was isolated from a 129Sv/Ev/Brd genomic library (Stratagene 946308) using bp5-102 of rat *Mad2* cDNA (dbEST ID 294792). Sequencing three of the 19 clones yielded *Mad2a*, *b*, and *d* (Figure 2-1). A separate screen yielded *Mad2c* (Figure 2-1). To determine which locus contributes to *Mad2* mRNA, rat *Mad2* cDNA was used to probe a mouse E10.5 cDNA library (Novagene). 23 of 28 clones contained cDNAs encoded by *Mad2a*; 2 of these contained an alternative 3' noncoding UTR; 5 cDNAs encoded either truncated *Mad2* genes or genes unrelated to *Mad2*.

Generating *Mad2*$^{+/-}$ Mice

The *Mad2* targeting construct was generated by first filling in the overhanging bases of the 4.6kb SacI-XbaI fragment immediately downstream of *Mad2* exon VI and cloning into the blunted EcoRI site of pPNT (obtained as a kind gift of Tyler Jacks). The 5' sequence was provided by a 4.6kb NotI-HindIII fragment in which the HindIII site is 622bp upstream of the initiating methionine codon and the NotI site is provided by the polylinker of the phage vector. The NotI-HindIII fragment was cloned into pBlueScriptII,

and a NotI-XhoI fragment transferred from this construct to the pPNT plasmid containing the 3' Mad2 sequence (Figure 2-2a).

Gene targeting of *Mad2* in 129/SvPas-derived D3 embryonic stem cells (Gossler et al., 1986) was carried out using positive-negative selection (Capecchi, 1989). Chimeric mice were created by injecting two independently derived *Mad2a*-targeted ES cell lines into C57BL/6 blastocysts generated by superovulation. Chimeras were crossed to BL/6 WT animals to generate founder lines.

Growth and Analysis of Mouse Embryos in Culture

Embryo culture. E3.5 blastocysts from natural matings were harvested into 96-well plates or gelatinized chambered microscopy slides (Nalge Nunc International 177445). Acidic Tyrode solution was used to remove the zona pellucida of blastocysts grown on slides (Hogan et al., 1994). Embryos were cultured in ES cell media lacking LIF with 15% fetal bovine serum for a total of 2-5 days and examined by phase contrast microscopy prior to genotyping by PCR.

Whole Mounts. Blastocysts harvested at E3.5 were grown in culture on chambered microscope slides to E5.5, digested with 0.04% collagenase 3 (Worthington) for 20 min at 37°C to remove the basal lamina, and fixed for 10 min with 4% paraformaldehyde (EM Science). Cells were permeabilized with 0.5% Triton X-100 for 10 min, the DNA denatured and the embryos blocked (Leonhardt et al., 1992) and reacted with anti-BrdU antibodies (Becton Dickinson, 1:3.5 dilution) and anti-phospho-Histone H3 antibodies (Upstate BioTechnology, 1:400 dilution) for 1 hr at 37°C, followed by 45 min with anti-rabbit or anti-mouse secondary antibodies (Jackson ImmunoResearch). Embryos were

viewed and photographed on a Zeiss-DeltaVision deconvolution microscope (Applied Precision), and then genotyped by PCR.

Disaggregated Embryonic Cells. E3.5 blastocysts grown to E5.5-6.5 in 96-well round bottom plates were washed twice with 200µl PBS, digested 8-10 min with 35µl 0.25% Trypsin at 37°C, and the trypsin inactivated and cells dissagregated with 100µl media. Samples were transferred to 0.2ml thinwall PCR tubes on ice (already containing 65µl media), and cells pelleted by a 5min centrifugation in a swinging bucket rotor. Cells were washed in 200µl PBS, resuspended in 200µl PBS, and one-third removed for PCR genotyping. (See below for genotyping of non-paraformaldehyde fixed embryos.) The remaining cells were pelleted and resuspended in 200µl 3.7% paraformaldehyde for 20 min at room temperature. After centrifugation and removal of most of the supernatant, cells were resupended in the 10-15µl remaining in the tube and mounted onto a coverslip pretreated with Histogrip (Zymed). After thorough drying, coverslips were briefly rinsed twice in PBS, stained with 1µg/ml DAPI for 10 min, rinsed twice in PBS, and mounted onto slides with PPD. The mitotic index for each embryo was measured by determining the fraction of cells with condensed DNA as shown in Figure 2-5.

In utero analysis

Chromosome Staining and Histology. E5.5-E7.5 embryos were prepared from timed matings of *Mad2* heterozygous mice. The uterus was surgically removed and decidua separated, rinsed twice in PBS, fixed 12-24 hr with 4% Paraformaldehyde (Electron Microscopy Sciences 15710) in PBS at 4°C, rinsed twice in PBS, and stored in 70% EtOH at 4°C. Embryos were embedded in paraffin blocks, cut in 8µm sections, and

dried overnight on a 42°C slide warmer. Sections were then deparaffinized (3X10 min washes in Histoclear), rehydrated (2X10 min in EtOH, 5 min in 95% EtOH, 5 min in 70% EtOH, 3 min in H_2O), mounted in 1ng/ml Hoechst in Fluorescence Mounting medium (1mg/ml p-phenylenedamine, 0.1X PBS, 80% glycerol) and analyzed by fluorescence microscopy (Axiophot2 - Zeiss).

After Hoechst analysis, slides were washed 5 min in PBS, 5 min in 70% EtOH, and 5 min in PBS. Sections were then stained with hematoxylin and eosin (1.5 min. in Gill's hematoxylin (Fisher CS400-1D), washed in tap water until clear, 2 min in Scott's water (Fisher Scientific) to differentiate, 2 min in tap water, 5 min in 85% EtOH, 5 sec in eosin (SIGMA)), dehydrated (3X5 min in 95% EtOH, 2X10 min in 100% EtOH, 3X10 min in histoclear solution) and mounted in Permount (Fisher Scientific).

TUNEL Staining. Embryo sections were prepared, dewaxed and rehydrated as described for the *in utero* analysis, incubated 15 min in 20µg/ml of Proteinase K in dH_20 and washed 5 min in PBS. Sections were then fixed 10 min in 4% paraformaldeyde and washed 5X3 min in PBS. Endogenous peroxidase was quenched in 0.1% H_2O_2 in PBS for 15 min. Slides were washed 5 min in dH_2O, 5 min in TdT buffer (30mM Tris [pH 7.2], 140mM sodium cacodylate, 1mM cobalt choride) and incubated 1hr at 37° C in TdT-biotin-dUTP mix (30 units TdT, 5µM biotin-dUTP in TdT buffer) using a humid chamber. Reactions were stopped in 2xSSC for 15 min, tissues blocked 10 min in 2% BSA in PBS and incubated 1hr with ABC Vectastain reagent (Vector laboratories, Burlingame CA). Slides were washed 3X5 min in PBS, 2.5 min in PBS with 0.5% Triton X-100, stained with DAB (3,3'-diaminobenzidine) and counterstained with Gill's Hematoxylin. Finally, sections were dehydrated (5 min in 70% EtOH, 5 min in 95%

EtOH, 2X10 min in 100% EtOH, 3X10 min in Histoclear solution) and mounted in Permount. Following microscopic examination, embryos were genotyped by PCR analysis of laser captured embryonic tissue (see below).

Mad2 PCR Genotyping

Mice. DNA was prepared from tails by overnight digestion at 55°C with 1mg/ml Proteinase K (Worthington) in Tail Digest Buffer (67mM Tris [pH 8.8], 16.6mM Ammonium Sulfate, 6.5mM $MgCl_2$, 0.5% Triton-X 100, 143mM β-mercaptoethanol). An MJ-Research PTC-100 PCR machine was used to amplify *Mad2* and *neo* genes in 25μl PCR reactions with 200μM deoxyribonucleotides, 1μM each primer (MOL 232, 233, 242, 243 – sequences below), and PCR reaction buffer (50mM KCl, 10mM Tris-HCl [pH8.8], 1.5mM $MgCl_2$, 0.1% Triton-X 100). 20μl of a room temperature mix containing all components except Taq were added to 1μl DNA at room temperature, preheated to 95°C for 3min, and then brought to 82°C for addition of Taq (diluted to 4μl on ice). Reactions were subjected to 35 cycles (94°C 1min, 64°C 1.5min, 72°C 1.5min), and then extended at 72°C for 10 min.

MOL 232-233 amplify a 295bp band from intron 1 of *Mad2* (PCR-A in Figure 2-2), and MOL 242-243 amplify a 547bp band from the neomycin gene (PCR-C in Figure 2-2).

MOL 232, Agg CTg AgC Cgg gCC TTA ggA C

MOL233, gTA ACC gTg TAA TAA CgT TTA AgT CTC

MOL242, CgC TgT TCT CCT CTT CCT CAT CTC

MOL243, CCC CTg ATg CTC TTC gTC CAg ATC

Disaggregated embryos. Embryos used for measuring mitotic index by scoring the fraction of cells with condensed chromosomes were trypsinized and washed as described above (Disaggregated embryos section of Growth and Analysis of Mouse Embryos). The cells used for PCR genotyping were washed a total of 3 times in 200µl PBS, and after the final centrifugation all supernatant except 4-5µl was removed, and an equal volume of 2mg/ml Proteinase K in 2X Tail Digest Buffer added. A Stratagene Robocycler Gradient 96 was used for digestion at 60°C for 4hr followed by 30 min at 90°C to inactivate trypsin.

1µM each of MOL236 and 237 were used to amplify *Mad2* (PCR-B in Figure 2-2) from 1µl of DNA in 25µl reactions using 0.625U AmpliTaq (Perkin Elmer) with AmpliTaq Buffer and 200µM deoxyribonucleotides in a Stratagene Robocycler Gradient 96. As with the tail DNA PCR protocol, 20µl of a master mix was mixed into 1µl DNA at room temperature, and this was then preheated to 95°C for 3min, and brought to 75°C for addition of AmpliTaq (diluted to 4µl on ice). Reactions were subjected to 35 cycles (94°C 1 min, 61°C 2 min, 72°C 3 min), and then extended at 72°C for 10 min. *neo* reactions were performed in separate reaction tubes using 1µM each of MOL242 and 243 (sequences below) with identical reaction conditions as those used for *Mad2*, except the annealing step was performed at 63°C.

1µl from each of the *Mad2* and *neo* reactions was used in a second round PCR reaction with nested primers to amplify specific *Mad2* and *neo* PCR products. Both sets of reactions were done with reaction conditions identical to those described above, with the exceptions that the *Mad2* reaction used MOL252 and 255 (sequences below), the *neo*

reaction used MOL257 and 259 (sequences below), and 40 cycles were performed (94°C 1 min, 60°C 2 min, 72°C 2 min) followed by a 5 min extension.

MOL236, ACg TTg gCC AgC TCT Cgg TCT gC

MOL237, Tgg gCC TCA CTA TTg AAC CAC CTC

MOL242, CgC TgT TCT CCT CTT CCT CAT CTC

MOL243 CCC CTg ATg CTC TTC gTC CAg ATC

MOL252 TCA ATA AAg TgA AAg CAC AgC Tg

MOL255 CCA CCT CTT gCT AgA AAg gTA g

MOL257 ggC TgC AgC TAT ggg ATC

MOL259 gAC AAg ACC ggC TTC CAT CC

MOL 236-237: 291bp

MOL 242-243: 547bp

MOL 252-255: 249bp

MOL 257-259: 480bp

Paraformaldehyde-fixed embryos. To harvest whole mount embryos after microscopy, coverslips were removed and embryos washed 3X5 min in PBS, immersed in PBS with 0.5% Triton-X 100, and scraped loose using glass needles (Sutter Instrument Co. BF100-78-10, pulled to the same fineness as used for mouse pronuclei injections). Embryos were washed through 300µl PBS in 0.2ml thinwall PCR tubes by centrifugation for 5 min, and digested overnight at 58°C in a total of 50µl 1mg/ml Proteinase K in Tail Digest Buffer using Proteinase K resuspended from powder the same day. Sectioned embryos were collected from slides using laser capture microscopy or by manually

scraping out embryo cells, and the DNA prepared by digestion as described for whole mount embryos.

DNA was diluted to 200µl TE [pH 8.0], phenol/chloroform extracted, chloroform extracted, EtOH precipitated, washed with 70% EtOH, and resuspended in 7µl TE overnight at 4°C. All of these steps were performed with Low Binding Micro Centrifuge Tubes (Marsh T6050G), to prevent sample loss. *Mad2* and *neo* bands were amplified exactly as described above for disaggregated embryos, using 3µl DNA for each reaction.

References

Alexandru, G., Zachariae, W., Schleiffer, A., and Nasmyth, K. (1999). Sister chromatid separation and chromosome re-duplication are regulated by different mechanisms in response to spindle damage. Embo J *18*, 2707-21.

Bachvarova, R., and De Leon, V. (1980). Polyadenylated RNA of mouse ova and loss of maternal RNA in early development. Dev Biol *74*, 1-8.

Basu, J., Bousbaa, H., Logarinho, E., Li, Z., Williams, B. C., Lopes, C., Sunkel, C. E., and Goldberg, M. L. (1999). Mutations in the essential spindle checkpoint gene bub1 cause chromosome missegregation and fail to block apoptosis in Drosophila. J Cell Biol *146*, 13-28.

Basu, J., Logarinho, E., Herrmann, S., Bousbaa, H., Li, Z., Chan, G. K., Yen, T. J., Sunkel, C. E., and Goldberg, M. L. (1998). Localization of the Drosophila checkpoint control protein Bub3 to the kinetochore requires Bub1 but not Zw10 or Rod. Chromosoma *107*, 376-85.

Bernard, P., Hardwick, K., and Javerzat, J. P. (1998). Fission yeast bub1 is a mitotic centromere protein essential for the spindle checkpoint and the preservation of correct ploidy through mitosis. J Cell Biol *143*, 1775-87.

Cahill, D. P., Lengauer, C., Yu, J., Riggins, G. J., Willson, J. K., Markowitz, S. D., Kinzler, K. W., and Vogelstein, B. (1998). Mutations of mitotic checkpoint genes in human cancers. Nature *392*, 300-3.

Capecchi, M. R. (1989). Altering the genome by homologous recombination. Science *244*, 1288-92. Chan, G. K., Jablonski, S. A., Sudakin, V., Hittle, J. C., and Yen, T. J. (1999). Human BUBR1 is a mitotic checkpoint kinase that monitors CENP-E functions at kinetochores and binds the cyclosome/APC. J Cell Biol *146*, 941-54.

Chan, G. K., Schaar, B. T., and Yen, T. J. (1998). Characterization of the kinetochore binding domain of CENP-E reveals interactions with the kinetochore proteins CENP-F and hBUBR1. J Cell Biol *143*, 49- 63.

Chen, R. H., Brady, D. M., Smith, D., Murray, A. W., and Hardwick, K. G. (1999). The spindle checkpoint of budding yeast depends on a tight complex between the Mad1 and Mad2 proteins. Mol Biol Cell *10*, 2607-18.

Chen, R. H., Shevchenko, A., Mann, M., and Murray, A. W. (1998). Spindle checkpoint protein Xmad1 recruits Xmad2 to unattached kinetochores. J Cell Biol *143*, 283-95.

Chen, R. H., Waters, J. C., Salmon, E. D., and Murray, A. W. (1996). Association of spindle assembly checkpoint component XMAD2 with unattached kinetochores. Science *274*, 242-6.

Clute, P., and Pines, J. (1999). Temporal and spatial control of cyclin B1 destruction in metaphase. Nat Cell Biol 1, 82-7.

Cohen-Fix, O., Peters, J. M., Kirschner, M. W., and Koshland, D. (1996). Anaphase initiation in Saccharomyces cerevisiae is controlled by the APC-dependent degradation of the anaphase inhibitor Pds1p. Genes Dev *10*, 3081-93.

Fang, G., Yu, H., and Kirschner, M. W. (1998). The checkpoint protein MAD2 and the mitotic regulator CDC20 form a ternary complex with the anaphase-promoting complex to control anaphase initiation. Genes Dev *12*, 1871-83.

Fraschini, R., Formenti, E., Lucchini, G., and Piatti, S. (1999). Budding yeast Bub2 is localized at spindle pole bodies and activates the mitotic checkpoint via a different pathway from Mad2. J Cell Biol *145*, 979-91.

Gavrieli, Y., Sherman, Y., and Ben-Sasson, S. A. (1992). Identification of programmed cell death in situ via specific labeling of nuclear DNA fragmentation. J Cell Biol *119*, 493-501.

Goh, P. Y., and Kilmartin, J. V. (1993). NDC10: a gene involved in chromosome segregation in Saccharomyces cerevisiae. J Cell Biol *121*, 503-12.

Gorbsky, G. J., Chen, R. H., and Murray, A. W. (1998). Microinjection of antibody to Mad2 protein into mammalian cells in mitosis induces premature anaphase. J Cell Biol *141*, 1193-205.

Gossler, A., Doetschman, T., Korn, R., Serfling, E., and Kemler, R. (1986). Transgenesis by means of blastocyst-derived embryonic stem cell lines. Proc Natl Acad Sci U S A *83*, 9065-9.

Hardwick, K. G., Johnston, R. C., Smith, D. L., and Murray, A. W. (2000). MAD3 encodes a novel component of the spindle checkpoint which interacts with bub3p, cdc20p, and mad2p. J Cell Biol *148*, 871-82.

Hardwick, K. G., Weiss, E., Luca, F. C., Winey, M., and Murray, A. W. (1996). Activation of the budding yeast spindle assembly checkpoint without mitotic spindle disruption. Science *273*, 953-6.

Hartwell, L., Dutcher, S., Wood, J., and Garvik, B. (1982). The fidelity of mitotic chromosome reproductuion in *S. cerevisiae*. Rec. Adv. Yeast Mol. Biol. 1, 28.

Hartwell, L. H., and Kastan, M. B. (1994). Cell cycle control and cancer. Science *266*, 1821-8. Hartwell, L. H., and Weinert, T. A. (1989). Checkpoints: controls that ensure the order of cell cycle events. Science *246*, 629-34.

He, X., Patterson, T. E., and Sazer, S. (1997). The Schizosaccharomyces pombe spindle checkpoint protein mad2p blocks anaphase and genetically interacts with the anaphase-promoting complex. Proc Natl Acad Sci U S A *94*, 7965-70.

Hogan, B., Beddington, R., Constantini, F., and Lacy, E. (1994). Manipulating the Mouse Embryo, 2nd Edition (New York: Cold Spring Harbor Press).

Hoyt, M. A., Totis, L., and Roberts, B. T. (1991). S. cerevisiae genes required for cell cycle arrest in response to loss of microtubule function. Cell *66*, 507-17.

Hwang, L. H., Lau, L. F., Smith, D. L., Mistrot, C. A., Hardwick, K. G., Hwang, E. S., Amon, A., and Murray, A. W. (1998). Budding yeast Cdc20: a target of the spindle checkpoint. Science *279*, 1041-4.

Jin, D. Y., Spencer, F., and Jeang, K. T. (1998). Human T cell leukemia virus type 1 oncoprotein Tax targets the human mitotic checkpoint protein MAD1. Cell *93*, 81-91.

Jordan, M. A., Wendell, K., Gardiner, S., Derry, W. B., Copp, H., and Wilson, L. (1996). Mitotic block induced in HeLa cells by low concentrations of paclitaxel (Taxol) results in abnormal mitotic exit and apoptotic cell death. Cancer Res *56*, 816-25.

Kim, S. H., Lin, D. P., Matsumoto, S., Kitazono, A., and Matsumoto, T. (1998). Fission yeast Slp1: an effector of the Mad2-dependent spindle checkpoint. Science *279*, 1045-7.

Kinzler, K. W., and Vogelstein, B. (1996). Lessons from hereditary colorectal cancer. Cell *87*, 159-70.

Kitagawa, R., and Rose, A. M. (1999). Components of the spindle-assembly checkpoint are essential in Caenorhabditis elegans. Nat Cell Biolog 1, 514-521.

Lanni, J. S., and Jacks, T. (1998). Characterization of the p53-dependent postmitotic checkpoint following spindle disruption. Mol Cell Biol *18*, 1055-64.

Lengauer, C., Kinzler, K. W., and Vogelstein, B. (1997). Genetic instability in colorectal cancers. Nature *386*, 623-7.

Leonhardt, H., Page, A. W., Weier, H. U., and Bestor, T. H. (1992). A targeting sequence directs DNA methyltransferase to sites of DNA replication in mammalian nuclei. Cell *71*, 865-73.

Li, R. (1999). Bifurcation of the mitotic checkpoint pathway in budding yeast. Proc Natl Acad Sci U S A *96*, 4989-94.

Li, R., and Murray, A. W. (1991). Feedback control of mitosis in budding yeast. Cell *66*, 519-31.

Li, X., and Nicklas, R. B. (1995). Mitotic forces control a cell-cycle checkpoint. Nature *373*, 630-2.

Li, Y., and Benezra, R. (1996). Identification of a human mitotic checkpoint gene: hsMAD2. Science *274*, 246-8.

Li, Y., Gorbea, C., Mahaffey, D., Rechsteiner, M., and Benezra, R. (1997). MAD2 associates with the cyclosome/anaphase-promoting complex and inhibits its activity. Proc Natl Acad Sci U S A *94*, 12431- 6.

Mahadevan, L. C., Willis, A. C., and Barratt, M. J. (1991). Rapid histone H3 phosphorylation in response to growth factors, phorbol esters, okadaic acid, and protein synthesis inhibitors. Cell *65*, 775- 83.

Martinez-Exposito, M. J., Kaplan, K. B., Copeland, J., and Sorger, P. K. (1999). Retention of the BUB3 checkpoint protein on lagging chromosomes. Proc Natl Acad Sci U S A *96*, 8493-8.

McGrew, J. T., Goetsch, L., Byers, B., and Baum, P. (1992). Requirement for ESP1 in the nuclear division of Saccharomyces cerevisiae. Mol Biol Cell 3, 1443-54.

Mitelman, F. (1971). The chromosomes of fifty primary Rous rat sarcomas. Hereditas *69*, 155-86.

Nelson, K. K., Schlondorff, J., and Blobel, C. P. (1999). Evidence for an interaction of the metalloprotease-disintegrin tumour necrosis factor alpha convertase (TACE) with mitotic arrest deficient 2 (MAD2), and of the metalloprotease-disintegrin MDC9 with a novel MAD2- related protein, MAD2beta. Biochem J *343 Pt* 3, 673-80.

Nomoto, S., Haruki, N., Takahashi, T., Masuda, A., Koshikawa, T., Fujii, Y., and Osada, H. (1999).Search for in vivo somatic mutations in the mitotic checkpoint gene, hMAD1, in human lung cancers. Oncogene *18*, 7180-3.

Nothias, J. Y., Majumder, S., Kaneko, K. J., and DePamphilis, M. L. (1995). Regulation of gene expression at the beginning of mammalian development. J Biol Chem *270*, 22077-80.

O'Neill, T. J., Zhu, Y., and Gustafson, T. A. (1997). Interaction of MAD2 with the carboxyl terminus of the insulin receptor but not with the IGFIR. Evidence for release from the insulin receptor after activation. J Biol Chem *272*, 10035-40.

Rieder, C. L., Cole, R. W., Khodjakov, A., and Sluder, G. (1995). The checkpoint delaying anaphase in response to chromosome monoorientation is mediated by an inhibitory signal produced by unattached kinetochores. J Cell Biol *130*, 941-8.

Rieder, C. L., Schultz, A., Cole, R., and Sluder, G. (1994). Anaphase onset in vertebrate somatic cells is controlled by a checkpoint that monitors sister kinetochore attachment to the spindle. J Cell Biol *127*, 1301-10.

Rugh, R. (1990). Normal development of the mouse. In The mouse (London, UK: Oxford Universtiy Press), pp. 44-101.

Shirayama, M., Zachariae, W., Ciosk, R., and Nasmyth, K. (1998). The Polo-like kinase Cdc5p and the WD-repeat protein Cdc20p/fizzy are regulators and substrates of the anaphase promoting complex in Saccharomyces cerevisiae. Embo J *17*, 1336-49.

Snow, M. (1977). Gastrulation in the Mouse: Growth and regionalization of the epiblast. J. Embryol. Exp. Morphol. *42*, 293-303.

Taylor, S. S., Ha, E., and McKeon, F. (1998). The human homologue of Bub3 is required for kinetochore localization of Bub1 and a Mad3/Bub1-related protein kinase. J Cell Biol *142*, 1-11.

Taylor, S. S., and McKeon, F. (1997). Kinetochore localization of murine Bub1 is required for normal mitotic timing and checkpoint response to spindle damage. Cell *89*, 727-35.

Visintin, R., Prinz, S., and Amon, A. (1997). CDC20 and CDH1: a family of substrate-specific activators of APC- dependent proteolysis. Science *278*, 460-3.

Wassmann, K., and Benezra, R. (1998). Mad2 transiently associates with an APC/p55Cdc complex during mitosis. Proc Natl Acad Sci U S A *95*, 11193-8.

Woods, C., J, Z., PA, M., D, B., and E, L. (1995). Taxol-induced mitotic block triggers rapid onset of a p53-independent apoptotic pathway. Molecular Medicine 1, 506-526.

Yamamoto, A., Guacci, V., and Koshland, D. (1996). Pds1p is required for faithful execution of anaphase in the yeast, Saccharomyces cerevisiae. J Cell Biol *133*, 85-97.

The work presented in the following chapter was published in part in Michel et al., 2001. This work was done in collaboration with Vasco Liberal and Robert Benezra, and the analysis culminating in Figure 3-2 was performed largely by Vasco.

Michel, L.S., Liberal, V., Chatterjee, A., Kirchwegger, R., Pasche, B., Gerald, W., Dobles, M., Sorger, P.K., Murty, V.V., Benezra, R. (2001) *MAD2* haplo-insufficiency causes premature anaphase and chromosome instability in mammalian cells. Nature 409: 355-359.

Chapter 3: Lung Cancer in *Mad2*$^{+/-}$ mice

Abstract

The spindle assembly checkpoint ensures accurate chromosome segregation in eukaryotes by preventing anaphase initiation until the completion of mitotic spindle assembly. The mutation of spindle checkpoint genes in metazoans results in high rates of chromosome missegregation. Because chromosome loss and gain is commonly observed in cancer, it has been proposed that spindle checkpoint genes may be tumor suppressors. To investigate this hypothesis, we have performed an aging study with mice heterozygous for the spindle checkpoint gene *Mad2*. Although *Mad2*$^{+/-}$ mice are overtly normal and do not exhibit increased morbidity, they do exhibit a high incidence of lung tumors. These results demonstrate that *Mad2* is a tumor suppressor gene in mice.

Introduction

Cancer is a complex disease requiring multiple genetic changes (Fearon and Vogelstein 1990; Lengauer et al. 1998). Cells with genetic instability, caused by defects in DNA replication, repair, segregation, or the coordination of these activities, accumulate mutations at an accelerated rate and are thus more susceptible to transformation than normal cells (Lengauer et al. 1998; Loeb 1991; Nowell 1976). Many tumors exhibit abnormally high rates of gene amplification, loss or gain of whole chromosomes, or mutation of short tracts of DNA, suggesting genetic instability may be a common mechanism of transformation (Ionov et al. 1993; Lengauer et al. 1997; Tlsty et al. 1989). A clear causative association between genetic instability and cancer has been demonstrated by the role of DNA mismatch repair defects in hereditary nonpolyposis colorectal cancer (HNPCC). Mutation of *MSH2*, *MLH1*, and other mismatch repair genes

results in the failure to correct mismatched DNA bases, and thus the accumulation of mutations throughout the genome (Jiricny and Nystrom-Lahti 2000; Parsons et al. 1995). Individuals with inherited mutations in these genes develop colorectal cancer as well as cancers of the endometrium, ovary, stomach and small intestine (Bronner et al. 1994; Nicolaides et al. 1994; Papadopoulos et al. 1994; Peltomaki and de la Chapelle 1997).

Despite the unambiguous contribution of mismatch repair defects to HNPCC, these defects occur in only about 13% of all colorectal cancers, and in less than 2% of most other tumor types, and thus cannot explain the high mutation rate of most cancers (Lengauer et al. 1998). In contrast, aneuploidy is commonly observed in almost all major forms of human cancer, and therefore chromosome missegregation has long been viewed as a potentially important source of genetic instability (Mitleman et al. 1994; Nowell 1976). The relevance of aneuploidy as a causative factor in tumorigenesis is suggested by the observation that some known carcinogens induce changes in chromosome number without being directly mutagenic to DNA bases (Li et al. 1997). It has also been observed that aneuploidy appears early in tumorigenesis, and increases with disease progression (Rabinovitch et al. 1989; Reid et al. 1992; Smith et al. 1996). Importantly, it has been shown that some colorectal cancer cell lines exhibit as high as one chromosome missegregation event per 100 cell divisions. This indicates that changes in ploidy can arise from an intrinsic and ongoing chromosome segregation defect as opposed to a single catastrophic event (Lengauer et al. 1997).

Chromosome segregation in eukaryotes is performed by a self-assembling bipolar spindle that uses microtubules to distribute chromosomes to daughter cells (Hyman and Karsenti 1996). The spindle assembly checkpoint ensures accurate segregation by sensing

whether or not spindle microtubules have attached to kinetochores, the protein complexes that mediate microtubule-chromosome attachment, and delaying anaphase initiation until all these attachments have been made (Rieder et al. 1995; Rieder et al. 1994). Treatments that interfere with microtubule-kinetochore attachment, including mutation of kinetochore proteins and exposure to anti-microtubule drugs such as nocodazole and taxol, induce a checkpoint-dependent mitotic arrest (Fuchs and Johnson 1978; Strunnikov et al. 1995; Wang and Burke 1995; Zieve et al. 1980). Most of the known checkpoint genes were originally cloned in *S. cerevisiae* and include *MAD1-3*, *BUB1*, *BUB3*, and *MPS1* (Hoyt et al. 1991; Li and Murray 1991; Weiss and Winey 1996). Identification of homologous genes with checkpoint roles in metazoans demonstrates that this pathway is broadly conserved (Chen et al. 1996; Jin et al. 1998; Li and Benezra 1996; Taylor et al. 1998; Taylor and McKeon 1997). Direct observation in metazoans has shown that checkpoint proteins are recruited specifically to kinetochores not attached to microtubules (Martinez-Exposito et al. 1999; Waters et al. 1998; Yu et al. 1999). These proteins function as part of a signaling pathway that culminates in the inhibition of the Anaphase Promoting Complex (APC), thus preventing the ubiquination of Pds1p/Securin and ultimately the initiation of anaphase (Alexandru et al. 1999; Cohen-Fix et al. 1996; Fang et al. 1998). Mad2 plays a key role in this pathway, as it both localizes to unattached kinetochores and directly inhibits ubiquination by binding the APC activator Cdc20 (Fang et al. 1998; Hwang et al. 1998; Kim et al. 1998; Waters et al. 1998).

The *MAD* and *BUB* genes are non-essential in *S. cerevisiae*, apparently because the intrinsic mitotic timing usually allows for the completion of spindle assembly before anaphase initiates (Hoyt et al. 1991; Li and Murray 1991). However, if spindle assembly

is inhibited by the microtubule depolymerizing drug benomyl, cells with mutant *mad* and *bub* genes fail to arrest and exhibit massive chromosome loss and rapid lethality (Hoyt et al. 1991; Li and Murray 1991; Winey et al. 1991). Thus, in *S. cerevisiae*, the checkpoint is not required during most mitoses and only becomes essential when spindle assembly is inhibited. In contrast, genetic disruption of *bub1* in *Drosophila*, *mdf-1* (*mad1*) in *C. elegans*, and *Mad2* or *Bub3* in mice results in early embryonic lethality (Basu et al. 1999; Dobles et al. 2000; Kalitsis et al. 2000; Kitagawa and Rose 1999). All of these mutants exhibit a high incidence of chromosome missegregation, demonstrating that the checkpoint is required to ensure accurate segregation in metazoans, even in the absence of exogenously generated spindle damage.

The role of the spindle checkpoint in preventing aneuploidy raises the possibility that loss of checkpoint function may contribute to tumorigenesis. Three lines of evidence support this hypothesis. First, many tumor-derived cell lines fail to arrest in response to anti-microtubule drugs that disrupt spindle assembly and induce mitotic arrest in normal cells (Cahill et al. 1998; Takahashi et al. 1999; Weitzel and Vandre 2000). Second, several studies have identified spindle checkpoint defects and gene mutations in human tumors, albeit at low frequency (Cahill et al. 1998; Lengauer et al. 1997; Takahashi et al. 1999). Most notably, two colorectal cancer cell lines defective in the spindle checkpoint were found to carry mutations in *Bub1*, and a screen of human lung tumors identified mutations in *Mad1* (Cahill et al. 1998; Nomoto et al. 1999). Finally, analysis of lymphomas in *Brca2*-mutant mice indicated that each lymphoma harbored a mutation in *Bub1* or the related protein *BubR1* (Lee et al. 1999). Although preliminary, these results provide a tentative connection between spindle checkpoint defects and tumorigenesis.

To obtain direct evidence linking loss of spindle checkpoint function to tumorigenesis, we have generated a *Mad2* targeted mutation in mice. *Mad2*-null mice die *in utero* with massive chromosome missegregation (Dobles et al. 2000). We therefore conducted an aging study using heterozygous mice to examine the effects of *Mad2* mutation on longevity and tumorigenesis. Although $Mad2^{+/-}$ mice do not exhibit increased morbidity during the first 19 months, we have observed an increase in tumor incidence, particularly in a rare form of lung cancer. This result provides the strongest evidence to date that spindle checkpoint mutation can play a causative role in tumorigenesis.

Results

Morbidity in $Mad2^{+/-}$ Mice

To examine the role of *Mad2* loss in disease and morbidity, we monitored the health and viability of 64 heterozygous mice and 32 wildtype mice to nineteen months of age (Table 3-1). Consistent with our previous observations, the $Mad2^{+/-}$ mice displayed no overt abnormalities (Dobles et al. 2000). Figure 3-1 shows that 17% of $Mad2^{+/-}$ mice had to be euthanized by nineteen months due to poor health, a statistically insignificant number compared to the wildtype population. Thus, we conclude that loss of one allele of *Mad2* in mice does not cause overt health problems or increased morbidity over the first 19 months.

Tumorigenesis in *Mad2*$^{+/-}$ mice

To examine *Mad2*$^{+/-}$ mice for internal abnormalities and disease symptoms, we first visually inspected all organs in nine heterozygous mice and two wildtype mice euthanized due to poor health, as well as in nine heterozygous and nine wildtype healthy mice aged 19-20 months. As this analysis revealed no gross pathology, we then examined hematoxylin and eosin-stained tissue sections from the heart, brain, liver, spleen, kidneys, lungs, and small intestine. This examination revealed lymphomas in two wildtype and two heterozygous mice. While these lymphomas were the only evidence of tumorigenesis in the wildtype mice, six of the *Mad2*$^{+/-}$ mice also had lung tumors and one additional mouse exhibited signs of a hepatocellular carcinoma (Table 3-2).

To pursue these findings, we examined sections from the lungs of an additional 31 heterozygous and 15 wildtype mice that were healthy when euthanized at 19-20 months. This analysis revealed tumors in the lungs of 9 *Mad2*$^{+/-}$ mice. Additionally, we identified six more tumors by visual inspection of organs during the harvest of lungs. In contrast, no tumors were found in the 18 wildtype mice, either by examination of lung sections or by visual inspection of organs. Consideration of all 49 *Mad2*$^{+/-}$ mice and 26 wildtype mice examined shows that 45% of heterozygotes exhibit tumors by 19-20 months of age, as compared to only 8% of the wildtype mice.

The most striking phenotype in the *Mad2*$^{+/-}$ mice is the high incidence of lung tumors (Table 3-2). 31% of *Mad2*$^{+/-}$ mice developed lung tumors, whereas no lung tumors were found in any wildtype mice. Histological analysis shows that fourteen of the fifteen lung tumors exhibit the fingerlike-projections characteristic of papillary adenocarcinomas (Fig 3-2) (Rehm et al. 1994). Interestingly, even the smallest tumors

exhibited papillary structure (Fig 3-2d), even though these structures normally manifest only in late stages of lung tumorigenesis (Johnson et al. 2001; Rehm et al. 1994; Shimkin 1955). Although lung tumors are not uncommon in older mice, they rarely develop spontaneously in wildtype BL/6 mice by this age (Shimkin 1955). We thus believe their development is directly linked to loss of the *Mad2* allele, and conclude that *Mad2* heterozygosity can contribute to tumorigenesis in mice.

Figure 3-1. Viability of *Mad2*$^{+/-}$ mice. *Mad2* wildtype mice (open circles) and heterozygous mice (black circles) were monitored until nineteen months of age, and those exhibiting poor health euthanized. Each point represents the fraction of mice alive at end of the month. Mice that were found dead or euthanized solely due to fight wounds were not included in the analysis (Table 3-1).

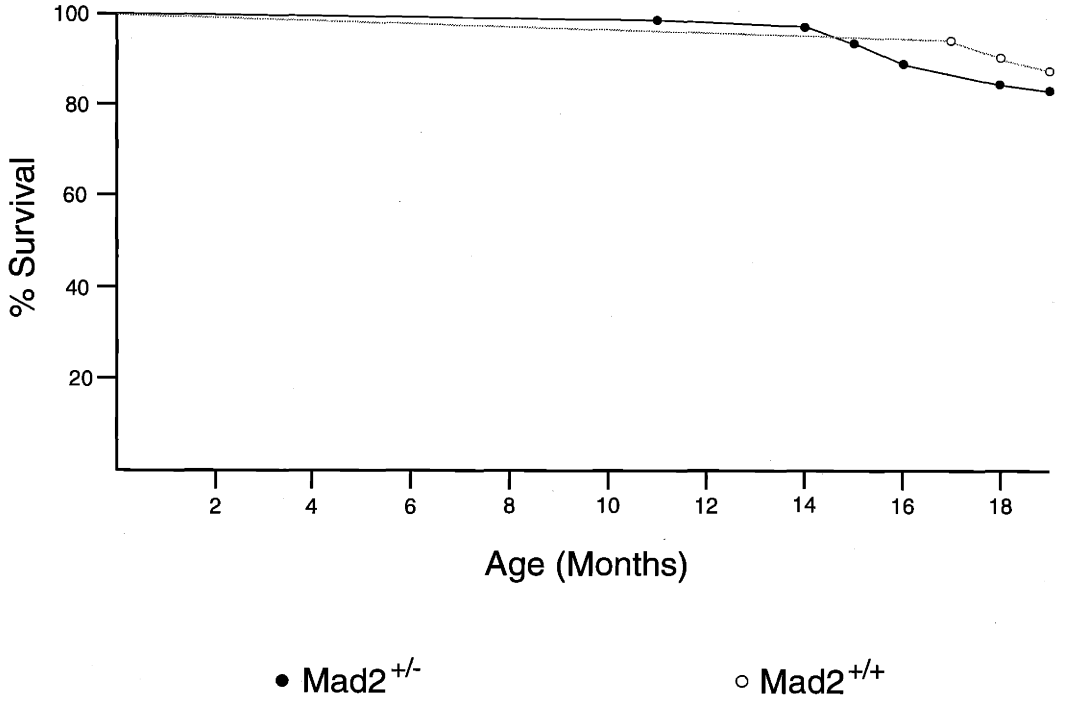
100
80
60
40
20
% Survival
2
4
6
8
10
12
14
16
18
Age (Months)
• Mad2+/-
○ Mad2+/+

Figure 3-2. Histopathology of papillary lung adenocarcinomas in *Mad2*$^{+/-}$ mice. (a-b) Representative tumors at 5X magnification. Most tumors were 1-2mm in diameter, although four were approximately 1cm across and encompassed nearly half the lung. **(c-d)** 5X and 10X magnification images of a small tumor surrounded by normal alveolar tissue (NAT). **(e-f)** Tumors at 20X magnification showing the "finger-like" structures typical of papillary tumors. Arrow indicates interface between tumor and normal alveolar tissue.

a.

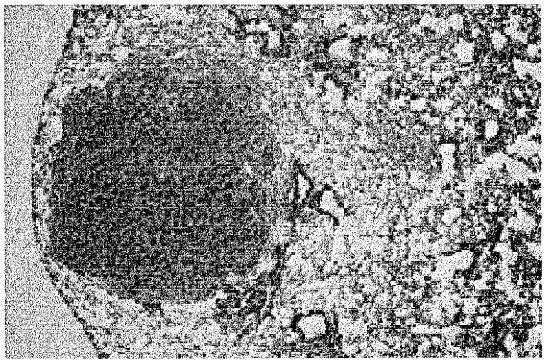

b.

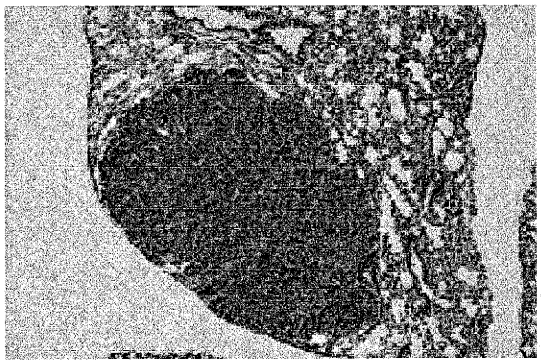

c.

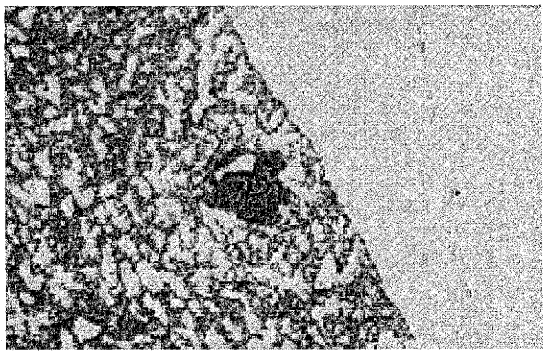

d.

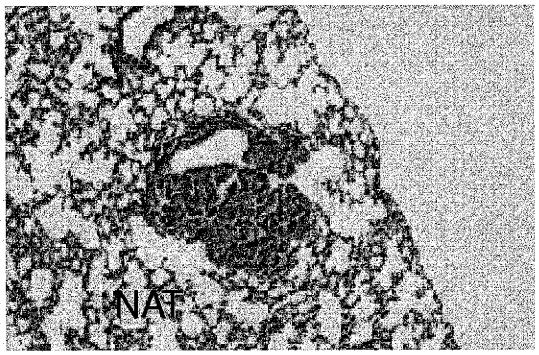

e.

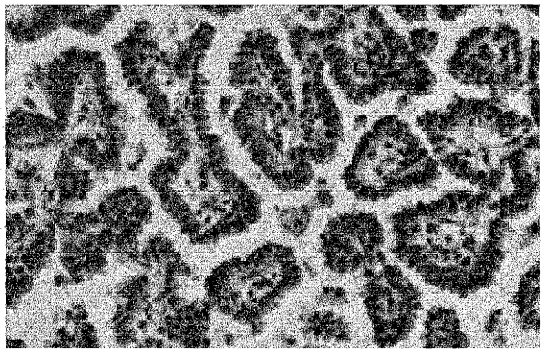

f.

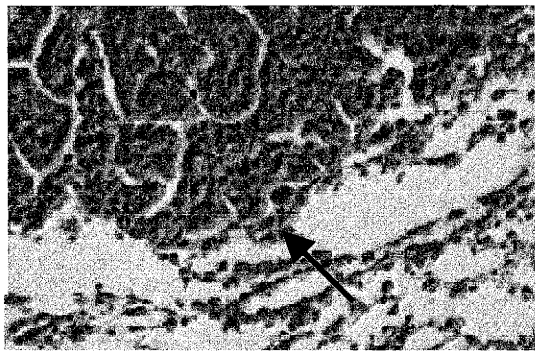

Table 3-1. Mice Analyzed in Morbidity Study

	Genotype		
	Mad2$^{+/-}$	*Mad2*$^{+/+}$	Total
Starting Population	82	41	123
Eliminated from Study:	18	9	27
Found Dead	14	6	20
Fight Wounds	4	3	7
Population Analyzed	64	32	96

Mice that were found dead were eliminated from analysis because it was not possible to determine whether they had died from trivial causes. Mice euthanized solely due to injuries incurred from fighting were also eliminated.

Table 3-2. Tumor Analysis of *Mad2*$^{+/-}$ Mice

	Genotype					
	Mad2$^{+/-}$			*Mad2*$^{+/+}$		
	Euthanized[a]	Healthy[b]	Total	Euthanized[a]	Healthy[b]	Total
Examined	9	40	49[c]	2	24	26[d]
Lung Tumor[e]	1[f]	13	14 (29%)	0	0	0
Lymphoma	2	2	4 (8%)	1	1	2 (8%)
Other Tumor	1[g]	3[h]	4 (8%)	0	0	0
Total Tumors	4	18	22 (45%)	1	1	2 (8%)

Mice from the morbidity study were used for hisotological analysis of tumors as described in text.

a – Euthanized prior to 19 months due to poor health

b – Healthy when sacrificed at 19-20 months

c – 34 males, 15 females

d – 14 males, 12 females

e – Lung papillary adenocarcinoma

f – Euthanized at 18 months

g – Non-carcinoma lung tumor

h – 1 vascular neoplasia, 1 hepatocellular carcinoma, 1 hepatocellular carcinoma or adrenal carcinoma

Discussion

In this study, we have shown that mice lacking one allele of *Mad2* exhibit a dramatically increased incidence of lung tumors, thus establishing the first causal connection between spindle checkpoint gene mutation and cancer. However, consistent with preliminary observation of $Bub3^{+/-}$ mice, $Mad2^{+/-}$ mice are overtly normal and do not exhibit increased morbidity as compared to wildtype controls (Kalitsis et al. 2000). The high viability of $Mad2^{+/-}$ mice is not inconsistent with the high incidence of lung tumors as spontaneously developing papillary lung adenocarcinomas in mice are rarely lethal (Rehm et al. 1994). Although we do not understand why the high rate of tumorigenesis is limited to the lungs, these results are consistent with the frequent spindle checkpoint impairment and less common *Mad1* mutations in human lung tumors (Nomoto et al. 1999; Takahashi et al. 1999).

Although these results demonstrate that mutation of *Mad2* contributes to tumorigenesis, we have not yet shown that the mutation results in checkpoint defects or aneuploidy in the tumor cells. However, cultured $Mad2^{+/-}$ mouse embryonic fibroblasts and $Mad2^{+/-}$ human cells generated by gene targeting both fail to maintain pre-anaphase mitotic arrest when exposed to the anti-microtubule drug colcemid and exhibit increased aneuploidy as compared to control cells (Michel et al. 2001). Furthermore, loss of checkpoint control would provide a mechanism to generate the aneuploidy observed in over 80% of human lung tumors (Bunn et al. 1983; Smith et al. 1996; Volm et al. 1988). We are currently deriving cells from both normal and tumor tissue in $Mad2^{+/-}$ mice to investigate the status of spindle checkpoint function and to look for aneuploidy. To further examine whether the tumor phenotype of $Mad2^{+/-}$ mice is a function of a

checkpoint defect, we plan to disrupt spindle assembly *in vivo* with the anti-microtubule drug taxol (Innocenti et al. 1995; Milas et al. 1995). If tumorigenesis in *Mad2*$^{+/-}$ mice is indeed the result of a spindle checkpoint defect, then taxol-mediated spindle disruption would be expected to exacerbate the tumor phenotype.

An important issue remaining to be resolved is whether tumors in *Mad2*$^{+/-}$ mice have lost expression of the wildtype allele thus making them effectively *Mad2*-null, or whether tumors arise as a consequence of haploinsufficiency. PCR genotyping of tumors indicates the presence of a wildtype *Mad2* allele (data not shown), but this does not rule out the possibility of gene inactivation by small deletions or by methylation (Baylin et al. 1998; Zochbauer-Muller et al. 2001), or that tumors had been infiltrated by non-tumor macrophage cells (Johnson et al. 2001). Checkpoint disruption and aneuploidy in human and mouse *Mad2* heterozygous cells suggest that loss of the wildtype allele may not be required for phenotypic consequences in adult mice (Michel et al. 2000). We plan to resolve this issue by determining if Mad2 protein is expressed in cells derived from the mouse lung tumors.

The results described here provide preliminary evidence linking spindle checkpoint disruption to cancer. We hypothesize that partial loss of checkpoint function in *Mad2* heterozygotes contributes to cancer progression via an increase in chromosome missegregation. The model that tumorigenesis in *Mad2*$^{+/-}$ mice is the result of genetic instability is consistent with the tumor phenotypes of mice with defects in DNA repair and recombination (Donehower et al. 1992; Gao et al. 2000; Jacks et al. 1994). One mechanism by which chromosome missegregation could contribute to tumorigenesis is by direct loss of tumor suppressor genes. This hypothesis can be tested by screening

Mad2$^{+/-}$ tumors for the loss of chromosomes that carry tumor suppressor genes, particularly chromosome 4, which carries p16/p15, a genetic locus commonly lost or inactivated in lung cancer (Herzog et al. 1996; Okamoto et al. 1995; Washimi et al. 1995). Another mechanism is suggested by the presence of broken chromosomes in *Drosophila* embryos with a genetic disruption of *bub1* (Basu et al. 1999). This observation raises the possibility that segregation defects cause DNA damage that can result in the mutation of proto-oncogenes or tumor suppressors. However, if tumorigenesis does indeed arise as a consequence of missegregation or DNA damage, it is not clear how cells escape the apoptosis observed in homozygous checkpoint mutants that exhibit severe segregation problems (Basu et al. 1999; Dobles et al. 2000). Heterozygotes may have less severe problems that do not induce apoptosis, or possibly mutation of pro-apoptotic genes allows survival of cells that missegregate chromosomes. Currently our lab is generating a conditional *Mad2* knockout mouse that we expect to be extremely valuable in investigating the cellular consequences of *Mad2* mutation and the general role of checkpoint defects in tumorigenesis.

Materials and Methods

Breeding and Genotyping

Mad2$^{+/-}$ mice were generated and genotyped by a Southern assay or PCR assay as described in Chapter 2. All mice were F1 or F2 progeny from backcrosses of chimeric *Mad2*$^{+/-}$ males against C57 BL/6 wildtype females, or the progeny of intercrosses between the F1 and F2 mice. Thus, all mice were of BL/6-129/SvPas mixed background.

Tissue Harvest and Histology

Tissues harvested from euthanized mice were washed, fixed, and stored as described for embryos in Chapter 2. Air in lungs was displaced by syringe-injection of 1-2ml Paraformaldehyde solution. Tissues were embedded in paraffin blocks, sectioned, and stained as described for embryos in Chapter 2.

References

Alexandru, G., Zachariae, W., Schleiffer, A., and Nasmyth, K. (1999). "Sister chromatid separation and chromosome re-duplication are regulated by different mechanisms in response to spindle damage." Embo J, 18(10), 2707-21.

Basu, J., Bousbaa, H., Logarinho, E., Li, Z., Williams, B. C., Lopes, C., Sunkel, C. E., and Goldberg, M. L. (1999). "Mutations in the essential spindle checkpoint gene bub1 cause chromosome missegregation and fail to block apoptosis in Drosophila." J Cell Biol, 146(1), 13-28.

Baylin, S. B., Herman, J. G., Graff, J. R., Vertino, P. M., and Issa, J. P. (1998). "Alterations in DNA methylation: a fundamental aspect of neoplasia." Adv Cancer Res, 72, 141-96.

Bronner, C. E., Baker, S. M., Morrison, P. T., Warren, G., Smith, L. G., Lescoe, M. K., Kane, M., Earabino, C., Lipford, J., Lindblom, A., and et al. (1994). "Mutation in the DNA mismatch repair gene homologue hMLH1 is associated with hereditary non-polyposis colon cancer." Nature, 368(6468), 258-61.

Bunn, P. A., Carney, D. N., Gazdar, A. F., Whang-Peng, J., and Matthews, M. J. (1983). "Diagnostic and biological implications of flow cytometric DNA content analysis in lung cancer." Cancer Res, 43(10), 5026-32.

Cahill, D. P., Lengauer, C., Yu, J., Riggins, G. J., Willson, J. K., Markowitz, S. D., Kinzler, K. W., and Vogelstein, B. (1998). "Mutations of mitotic checkpoint genes in human cancers." Nature, 392(6673), 300-3.

Chen, R. H., Waters, J. C., Salmon, E. D., and Murray, A. W. (1996). "Association of spindle assembly checkpoint component XMAD2 with unattached kinetochores." Science, 274(5285), 242-6.

Cohen-Fix, O., Peters, J. M., Kirschner, M. W., and Koshland, D. (1996). "Anaphase initiation in Saccharomyces cerevisiae is controlled by the APC-dependent degradation of the anaphase inhibitor Pds1p." Genes Dev, 10(24), 3081-93.

Dobles, M., Liberal, V., Scott, M. L., Benezra, R., and Sorger, P. K. (2000). "Chromosome missegregation and apoptosis in mice lacking the mitotic checkpoint protein Mad2." Cell, 101, 635-645.

Donehower, L. A., Harvey, M., Slagle, B. L., McArthur, M. J., Montgomery, C. A., Butel, J. S., and Bradley, A. (1992). "Mice deficient for p53 are developmentally normal but susceptible to spontaneous tumours." Nature, 356(6366), 215-21.

Fang, G., Yu, H., and Kirschner, M. W. (1998). "The checkpoint protein MAD2 and the mitotic regulator CDC20 form a ternary complex with the anaphase-promoting complex to control anaphase initiation." Genes Dev, 12(12), 1871-83.

Fearon, E. R., and Vogelstein, B. (1990). "A genetic model for colorectal tumorigenesis." Cell, 61(5), 759-67.

Fuchs, D. A., and Johnson, R. K. (1978). "Cytologic evidence that taxol, an antineoplastic agent from Taxus brevifolia, acts as a mitotic spindle poison." Cancer Treat Rep, 62(8), 1219-22.

Gao, Y., Ferguson, D. O., Xie, W., Manis, J. P., Sekiguchi, J., Frank, K. M., Chaudhuri, J., Horner, J., DePinho, R. A., and Alt, F. W. (2000). "Interplay of p53 and DNA-repair protein XRCC4 in tumorigenesis, genomic stability and development." Nature, 404(6780), 897-900.

Herzog, C. R., Soloff, E. V., McDoniels, A. L., Tyson, F. L., Malkinson, A. M., Haugen-Strano, A., Wiseman, R. W., Anderson, M. W., and You, M. (1996).

"Homozygous codeletion and differential decreased expression of p15INK4b, p16INK4a-alpha and p16INK4a-beta in mouse lung tumor cells." Oncogene, 13(9), 1885-91.

Hoyt, M. A., Totis, L., and Roberts, B. T. (1991). "S. cerevisiae genes required for cell cycle arrest in response to loss of microtubule function." Cell, 66(3), 507-17.

Hwang, L. H., Lau, L. F., Smith, D. L., Mistrot, C. A., Hardwick, K. G., Hwang, E. S., Amon, A., and Murray, A. W. (1998). "Budding yeast Cdc20: a target of the spindle checkpoint." Science, 279(5353), 1041-4.

Hyman, A. A., and Karsenti, E. (1996). "Morphogenetic properties of microtubules and mitotic spindle assembly." Cell, 84(3), 401-10.

Innocenti, F., Danesi, R., Di Paolo, A., Agen, C., Nardini, D., Bocci, G., and Del Tacca, M. (1995). "Plasma and tissue disposition of paclitaxel (taxol) after intraperitoneal administration in mice." Drug Metab Dispos, 23(7), 713-7.

Ionov, Y., Peinado, M. A., Malkhosyan, S., Shibata, D., and Perucho, M. (1993). "Ubiquitous somatic mutations in simple repeated sequences reveal a new mechanism for colonic carcinogenesis." Nature, 363(6429), 558-61.

Jacks, T., Remington, L., Williams, B. O., Schmitt, E. M., Halachmi, S., Bronson, R. T., and Weinberg, R. A. (1994). "Tumor spectrum analysis in p53-mutant mice." Curr Biol, 4(1), 1-7.

Jin, D. Y., Spencer, F., and Jeang, K. T. (1998). "Human T cell leukemia virus type 1 oncoprotein Tax targets the human mitotic checkpoint protein MAD1." Cell, 93(1), 81-91.

Jiricny, J., and Nystrom-Lahti, M. (2000). "Mismatch repair defects in cancer." Curr Opin Genet Dev, 10(2), 157-61.

Johnson, L., Mercer, K., Greenbaum, D., Bronson, R. T., Crowley, D., Tuveson, D. A., and Jacks, T. (2001). "Somatic activation of the K-ras oncogene causes early onset lung cancer in mice." Nature, 410(6832), 1111-1116.

Kalitsis, P., Earle, E., Fowler, K. J., and Choo, K. H. (2000). "Bub3 gene disruption in mice reveals essential mitotic spindle checkpoint function during early embryogenesis." Genes Dev, 14(18), 2277-82.

Kim, S. H., Lin, D. P., Matsumoto, S., Kitazono, A., and Matsumoto, T. (1998). "Fission yeast Slp1: an effector of the Mad2-dependent spindle checkpoint." Science, 279(5353), 1045-7.

Kitagawa, R., and Rose, A. M. (1999). "Components of the spindle-assembly checkpoint are essential in Caenorhabditis elegans." Nat Cell Biolog, 1(8), 514-521.

Lee, H., Trainer, A. H., Friedman, L. S., Thistlethwaite, F. C., Evans, M. J., Ponder, B. A., and Venkitaraman, A. R. (1999). "Mitotic checkpoint inactivation fosters transformation in cells lacking the breast cancer susceptibility gene, Brca2." Mol Cell, 4(1), 1-10.

Lengauer, C., Kinzler, K. W., and Vogelstein, B. (1997). "Genetic instability in colorectal cancers." Nature, 386(6625), 623-7.

Lengauer, C., Kinzler, K. W., and Vogelstein, B. (1998). "Genetic instabilities in human cancers." Nature, 396(6712), 643-9.

Li, R., and Murray, A. W. (1991). "Feedback control of mitosis in budding yeast." Cell, 66(3), 519-31.

Li, R., Yerganian, G., Duesberg, P., Kraemer, A., Willer, A., Rausch, C., and Hehlmann, R. (1997). "Aneuploidy correlated 100% with chemical transformation of Chinese hamster cells." Proc Natl Acad Sci U S A, 94(26), 14506-11.

Li, Y., and Benezra, R. (1996). "Identification of a human mitotic checkpoint gene: hsMAD2." Science, 274(5285), 246-8.

Loeb, L. A. (1991). "Mutator phenotype may be required for multistage carcinogenesis." Cancer Res, 51(12), 3075-9.

Martinez-Exposito, M. J., Kaplan, K. B., Copeland, J., and Sorger, P. K. (1999). "Retention of the BUB3 checkpoint protein on lagging chromosomes." Proc Natl Acad Sci U S A, 96(15), 8493-8.

Michel, L. S., Liberal, V., Chatterjee, A., Kirchwegger, R., Pasche, B., Gerald, W., Dobles, M., Sorger, P. K., Murty, V.V., and Benezra, R. (2000). "MAD2 haplo-insufficiency causes premature anaphase and chromosome instability in mammalian cells." Nature, 409, 355-359.

Milas, L., Hunter, N. R., Kurdoglu, B., Mason, K. A., Meyn, R. E., Stephens, L. C., and Peters, L. J. (1995). "Kinetics of mitotic arrest and apoptosis in murine mammary and ovarian tumors treated with taxol." Cancer Chemother Pharmacol, 35(4), 297-303.

Mitleman, F., Johansson, B., and Mertens, F. (1994). Catalog of Chromosome Aberrations in Cancer, Wiley-Liss, New York.

Nicolaides, N. C., Papadopoulos, N., Liu, B., Wei, Y. F., Carter, K. C., Ruben, S. M., Rosen, C. A., Haseltine, W. A., Fleischmann, R. D., Fraser, C. M., and et al. (1994). "Mutations of two PMS homologues in hereditary nonpolyposis colon cancer." Nature, 371(6492), 75-80.

Nomoto, S., Haruki, N., Takahashi, T., Masuda, A., Koshikawa, T., Fujii, Y., and Osada, H. (1999). "Search for in vivo somatic mutations in the mitotic checkpoint gene, hMAD1, in human lung cancers." Oncogene, 18(50), 7180-3.

Nowell, P. C. (1976). "The clonal evolution of tumor cell populations." Science, 194(4260), 23-8.

Okamoto, A., Hussain, S. P., Hagiwara, K., Spillare, E. A., Rusin, M. R., Demetrick, D. J., Serrano, M., Hannon, G. J., Shiseki, M., Zariwala, M., and et al. (1995). "Mutations in the p16INK4/MTS1/CDKN2, p15INK4B/MTS2, and p18 genes in primary and metastatic lung cancer." Cancer Res, 55(7), 1448-51.

Papadopoulos, N., Nicolaides, N. C., Wei, Y. F., Ruben, S. M., Carter, K. C., Rosen, C. A., Haseltine, W. A., Fleischmann, R. D., Fraser, C. M., Adams, M. D., and et al. (1994). "Mutation of a mutL homolog in hereditary colon cancer." Science, 263(5153), 1625-9.

Parsons, R., Li, G. M., Longley, M., Modrich, P., Liu, B., Berk, T., Hamilton, S. R., Kinzler, K. W., and Vogelstein, B. (1995). "Mismatch repair deficiency in phenotypically normal human cells." Science, 268(5211), 738-40.

Peltomaki, P., and de la Chapelle, A. (1997). "Mutations predisposing to hereditary nonpolyposis colorectal cancer." Adv Cancer Res, 71, 93-119.

Rabinovitch, P. S., Reid, B. J., Haggitt, R. C., Norwood, T. H., and Rubin, C. E. (1989). "Progression to cancer in Barrett's esophagus is associated with genomic instability." Lab Invest, 60(1), 65-71.

Rehm, S., Ward, J. M., and Sass, B. (1994). "Tumors of the lungs." Pathology of tumours in laboratory animals, V. Turosov and U. Mohr, eds., IARC Scientific Publications, 324-39.

Reid, B. J., Blount, P. L., Rubin, C. E., Levine, D. S., Haggitt, R. C., and Rabinovitch, P. S. (1992). "Flow-cytometric and histological progression to malignancy in Barrett's esophagus: prospective endoscopic surveillance of a cohort." Gastroenterology, 102(4 Pt 1), 1212-9.

Rieder, C. L., Cole, R. W., Khodjakov, A., and Sluder, G. (1995). "The checkpoint delaying anaphase in response to chromosome monoorientation is mediated by an inhibitory signal produced by unattached kinetochores." J Cell Biol, 130(4), 941-8.

Rieder, C. L., Schultz, A., Cole, R., and Sluder, G. (1994). "Anaphase onset in vertebrate somatic cells is controlled by a checkpoint that monitors sister kinetochore attachment to the spindle." J Cell Biol, 127(5), 1301-10.

Shimkin, M. (1955). "Pulmonary Tumors in Experimental Animals." Advances in Cancer Research, J.P. Greenstein and A. Haddow, eds., Academic Press Inc. Publishers, 3, 233-267.

Smith, A. L., Hung, J., Walker, L., Rogers, T. E., Vuitch, F., Lee, E., and Gazdar, A. F. (1996). "Extensive areas of aneuploidy are present in the respiratory epithelium of lung cancer patients." Br J Cancer, 73(2), 203-9.

Strunnikov, A. V., Kingsbury, J., and Koshland, D. (1995). "CEP3 encodes a centromere protein of Saccharomyces cerevisiae." J Cell Biol, 128(5), 749-60.

Takahashi, T., Haruki, N., Nomoto, S., Masuda, A., Saji, S., and Osada, H. (1999). "Identification of frequent impairment of the mitotic checkpoint and molecular analysis of the mitotic checkpoint genes, hsMAD2 and p55CDC, in human lung cancers." Oncogene, 18(30), 4295-300.

Taylor, S. S., Ha, E., and McKeon, F. (1998). "The human homologue of Bub3 is required for kinetochore localization of Bub1 and a Mad3/Bub1-related protein kinase." J Cell Biol, 142(1), 1-11.

Taylor, S. S., and McKeon, F. (1997). "Kinetochore localization of murine Bub1 is required for normal mitotic timing and checkpoint response to spindle damage." Cell, 89(5), 727-35.

Tlsty, T. D., Margolin, B. H., and Lum, K. (1989). "Differences in the rates of gene amplification in nontumorigenic and tumorigenic cell lines as measured by Luria-Delbruck fluctuation analysis." Proc Natl Acad Sci U S A, 86(23), 9441-5.

Volm, M., Bak, M., Hahn, E. W., Mattern, J., and Weber, E. (1988). "DNA and S-phase distribution and incidence of metastasis in human primary lung carcinoma." Cytometry, 9(2), 183-8.

Wang, Y., and Burke, D. J. (1995). "Checkpoint genes required to delay cell division in response to nocodazole respond to impaired kinetochore function in the yeast Saccharomyces cerevisiae." Mol Cell Biol, 15(12), 6838-44.

Washimi, O., Nagatake, M., Osada, H., Ueda, R., Koshikawa, T., Seki, T., and Takahashi, T. (1995). "In vivo occurrence of p16 (MTS1) and p15 (MTS2) alterations preferentially in non-small cell lung cancers." Cancer Res, 55(3), 514-7.

Waters, J. C., Chen, R. H., Murray, A. W., and Salmon, E. D. (1998). "Localization of Mad2 to kinetochores depends on microtubule attachment, not tension." J Cell Biol, 141(5), 1181-91.

Weiss, E., and Winey, M. (1996). "The Saccharomyces cerevisiae spindle pole body duplication gene MPS1 is part of a mitotic checkpoint." J Cell Biol, 132(1-2), 111-23.

Weitzel, D. H., and Vandre, D. D. (2000). "Differential spindle assembly checkpoint response in human lung adenocarcinoma cells." Cell Tissue Res, 300(1), 57-65.

Winey, M., Goetsch, L., Baum, P., and Byers, B. (1991). "MPS1 and MPS2: novel yeast genes defining distinct steps of spindle pole body duplication." J Cell Biol, 114(4), 745-54.

Yu, H. G., Muszynski, M. G., and Kelly Dawe, R. (1999). "The maize homologue of the cell cycle checkpoint protein MAD2 reveals kinetochore substructure and contrasting mitotic and meiotic localization patterns." J Cell Biol, 145(3), 425-35.

Zieve, G. W., Turnbull, D., Mullins, J. M., and McIntosh, J. R. (1980). "Production of large numbers of mitotic mammalian cells by use of the reversible microtubule inhibitor nocodazole. Nocodazole accumulated mitotic cells." Exp Cell Res, 126(2), 397-405.

Zochbauer-Muller, S., Fong, K. M., Virmani, A. K., Geradts, J., Gazdar, A. F., and Minna, J. D. (2001). "Aberrant promoter methylation of multiple genes in non-small cell lung cancers." Cancer Res, 61(1), 249-55.

The work presented in this chapter is now being completed and prepared for publication. These experiments have been performed in collaboration with members of the Sorger lab. Stuart Levine performed the two-hybrid screen and analysis described in Figure 4-1 and 4-2. Robert Hagan performed the experiments shown in Figures 4-3, 4-4, 4-7, and 4-9a. Figures 4-3 and 4-4 are reproduced from the Master's Thesis of Robert Hagan.

Chapter 4: Identification of a common Mad2 binding site for Mad1, Cdc20, and two non-spindle checkpoint proteins

Abstract

The spindle assembly checkpoint ensures accurate chromosome segregation in eukaryotes by preventing anaphase initiation until the completion of mitotic spindle assembly. Mad2 is a key protein in the spindle checkpoint signaling pathway that has been shown to interact with several proteins, some of which have no known checkpoint role. We have used two-hybrid screening with Mad2 to identify the mouse homolog of Mad1. Mapping Mad2-binding peptides of Mad1, Cdc20, TNF α convertase, and the estrogen receptor β reveals that all share a short consensus sequence. A Mad1 peptide spanning this consensus sequence competed with the binding of Cdc20 to Mad2. Mutation of a single residue in the human Mad2 carboxyl-terminal tail, or of multiple conserved residues that are adjacent to the tail in the folded protein, prevents the binding of all four proteins. These results demonstrate that Mad1, Cdc20, and two proteins lacking known spindle checkpoint function interact with a common Mad2 binding site.

Introduction

The segregation of chromosomes by the mitotic spindle is a key event in the transmission of genetic information. Aneuploidy caused by missegregation results in developmental abnormalities and has also been linked to tumorigenesis (Mitleman et al. 1994; Reid et al. 1992). To prevent chromosome loss and gain during mitosis, all eukaryotic cells utilize a spindle assembly checkpoint to monitor the attachment of microtubules to chromosomes via kinetochores. Inhibition of microtubule-kinetochore attachment, via mutation of the yeast kinetochore genes Ctf13p and Cep3p, or treatment with anti-microtubule drugs such as taxol, benomyl, or nocodazole induces a mitotic

arrest that provides additional time for the spindle to assemble before anaphase initiation (Fuchs and Johnson 1978; Jacobs et al. 1988; Strunnikov et al. 1995; Wang and Burke 1995). The presence of even a single unattached kinetochore induces a mitotic arrest that is released by microtubule attachment or laser ablation of the unattached kinetochore (Rieder et al. 1995; Rieder et al. 1994).

Spindle checkpoint genes were originally identified in *S. cerevisiae* and include *MAD1-3* (mitotic arrest defective), *BUB1* and *3* (budding uninhibited by benomyl) and *MPS*1 (monopolar spindle). All are nonessential and are not required for accurate segregation during most mitoses except *MPS1* which is also required for spindle pole duplication (Hoyt et al. 1991; Li and Murray 1991; Weiss and Winey 1996; Winey et al. 1991). However, all are required for mitotic arrest in response to benomyl-induced spindle damage (Hoyt et al. 1991; Li and Murray 1991; Weiss and Winey 1996). Genetic disruption of *bub1* in *Drosophila*, *mdf-1* (*mad1*) in *C. elegans*, and *Mad2* and *Bub3* in mice demonstrates all are required for mitotic arrest in response to anti-microtubule drugs, thus revealing conservation of the checkpoint pathway in metazoans (Basu et al. 1999; Dobles et al. 2000; Kalitsis et al. 2000; Kitagawa and Rose 1999). Interestingly, disruption of checkpoint genes in metazoans results in embryonic lethality and a high rate of chromosome missegregation, indicating a requirement for checkpoint function even in the absence of exogenously induced spindle damage (Basu et al. 1999; Dobles et al. 2000; Kalitsis et al. 2000; Kitagawa and Rose 1999).

How checkpoint signaling links anaphase initiation to the completion of spindle assembly is an area of active investigation. All of the Mad and Bub proteins have been shown to localize specifically to unattached kinetochores during mitosis in mammalian

cells, consistent with a role in monitoring microtubule-kinetochore attachment (Jablonski et al. 1998; Jin et al. 1998; Li and Benezra 1996; Martinez-Exposito et al. 1999; Taylor and McKeon 1997). Immunodepletion of the kinetochore-localized microtubule motor protein CENP-E from *Xenopus* egg extracts prevents Mad1 and Mad2 recruitment and mitotic arrest in response to nocodazole treatment (Abrieu et al. 2000). This result suggests the checkpoint may sense microtubule-kinetochore attachment by monitoring CENP-E. How this information is then transduced through checkpoint proteins is poorly characterized, but it has been shown that checkpoint activation induces both formation of a Mad1p-Bub1p-Bub3p complex in *S. cerevisiae* and hyperphosphorylation of Mad1p in *S. cerevisiae* and mammalian cells (Brady and Hardwick 2000; Hardwick et al. 1996; Jin et al. 1998). In *S. cerevisiae* Mad1p phosphorylation requires Mps1p, and Mps1p has been shown to directly phosphorylate Mad1p *in vitro* (Hardwick et al. 1996). The checkpoint signaling pathway culminates in inhibition of Anaphase Promoting Complex (APC)-dependent ubiquination, thus inhibiting anaphase by preventing the degradation of Pds1p/Securin (Cohen-Fix et al. 1996; Hwang et al. 1998; Kim et al. 1998).

Mad2 has been shown to interact with Mad1 and with Cdc20, the protein that targets APC activity specifically against Pds1p/Securin (Chen et al. 1999; Hwang et al. 1998; Jin et al. 1998; Kim et al. 1998; Visintin et al. 1997). In *Xenopus* egg extracts, anti-Mad1 antibody blocks Mad2 localization to unattached kinetochores, suggesting Mad1 recruits Mad2 to kinetochores (Chen et al. 1998). Mad1p can be co-immunoprecipitated with Mad2p from *S. cerevisiae* extracts, and ten-residue amino or carboxyl-terminal Mad2p truncations that disrupt Mad1p binding also prevent Mad1p hyper-phosphorylation and mitotic arrest in response to benomyl (Chen et al. 1999). Mad2p-

Cdc20p interaction was first identified by two-hybrid interaction, and confirmed by finding *S. cerevisiae* and *S. pombe* Cdc20p mutants that both failed to bind Mad2p and failed to arrest in response to spindle damage (Hwang et al. 1998; Kim et al. 1998). Additionally, direct inhibition of APC-dependent ubiquination by bacterially expressed hMad2 has been demonstrated *in vitro* (Fang et al. 1998). Interestingly, deletion of the carboxyl-terminal unstructured tail of Mad2 prevents binding to both hCdc20 and *S. cerevisiae* Mad1p, suggesting both proteins may interact with Mad2 via this tail sequence (Chen et al. 1999; Luo et al. 2000).

Although Mad2 is the best characterized spindle checkpoint protein, there exists very little understanding of how it functions on a molecular level. The only recognizable feature in the 23kD protein is the HORMA domain, a motif with no known function shared only with the *S. cerevisae* proteins Hop1p and Rev7p (Aravind and Koonin 1998). The upstream signals that directly activate Mad2 to inhibit Cdc20-APC activity remain unclear, although regulation must exist as Mad2 is highly expressed and in *S. cerevisiae* remains associated with Mad1p through the entire cell cycle (Chen et al. 1999). The mechanism by which Mad2 then inhibits Cdc20-APC activity is also unknown, although identification of a Mad2-Cdc20-APC ternary complex *in vivo* suggests involvement of more than simple sequestration (Fang et al. 1998; Wassmann and Benezra 1998). Finally, numerous Mad2-interacting proteins have been identified that have no known connection to the spindle checkpoint. Whether these Mad2-interacting proteins such as TNF α convertase (TACE), estrogen receptor β (ERβ), and the insulin receptor play a role in Mad2 checkpoint function remains unknown (Nelson et al. 1999; O'Neill et al. 1997; Poelzl et al. 2000).

The work presented here describes the first phase of an investigation into the molecular function of Mad2. How checkpoint proteins detect the status of kinetochore attachment and relay this information to the APC remains poorly characterized. By focusing on Mad2 and the interaction with Mad1 and Cdc20, we hope to describe in detail molecular events in the checkpoint signaling pathway. Our approach is to first define the binding regions of each of the proteins, and then use this information to design mutants for analysis in cells. Most *in vivo* checkpoint studies to date have involved disruption of entire proteins (either via gene targeting or use of antibodies) – an excessively crude method for the investigation of signaling, especially in metazoans where these genes are essential (Basu et al. 1999; Chan et al. 1999; Dobles et al. 2000; Kalitsis et al. 2000; Kitagawa and Rose 1999). Design of subtle mutants, specifically deficient in interaction with one protein, should allow for much higher resolution dissection of the pathway. This approach should be especially valuable for proteins such as Mad2 that have several binding partners (Chen et al. 1999; Nelson et al. 1999; O'Neill et al. 1997; Poelzl et al. 2000).

To examine the molecular function of Mad2, we first utilized two-hybrid screening to clone the mouse homolog of Mad1. We then mapped the hMad2-binding region to a short peptide sequence for Mad1, Cdc20, TACE, and ERβ. Sequence similarity between these peptides, and the ability of the Mad1 peptide to compete with a large fragment of Cdc20 for Mad2 binding, suggested these proteins may bind to a common site of Mad2. Mutagenesis of individual residues in Mad2 identified a common binding surface for all four proteins. These findings provide an understanding of Mad2

interactions that will aid the design of mutants for sophisticated analysis of Mad2 function *in vivo*.

Results

Identification of Mad1 and a novel Mad2-interacting protein in mice

To identify Mad2 interacting genes, the complete coding sequence of rat Mad2 was used as bait in a two-hybrid screen with a murine T-cell lymphoma library. Of 50 clones that grew under nutritional selection, 45 induced lacZ expression with Mad2, but not with non-specific baits (p53, lamin, SNF, and CDK2). Sequencing 18 of these indicated they represented three distinct genes that we named Mad2 Binding Protein 1 (M2BP1, 11 clones), M2BP3 (6 clones), and M2BP4 (1 clone) (Fig 4-1). The putative translated sequence of M2BP1 possesses 16% identity (29% similarity) to *S. cerevisiae* Mad1p, and is perfectly homologous to residues 171-718 of the mouse Mad1 (mMad1) protein (Fig. 4-2). M2BP3 and M2BP4 lack homology to any genes of known function.

We confirmed the binding of mMad1 and M2BP3 to Mad2 using a biochemical interaction assay. [^{35}S]-Methionine labeled *in vitro*-translated mMad1 or M2BP3 was incubated with Mad2-GST fusion protein bound to glutathione-agarose beads, the beads washed, and the fraction of mMad1 and M2BP3 bound to beads determined via SDS-PAGE followed by autoradiography. Fig. 4-3 shows binding of both mMad1 and M2BP3 to mouse and human Mad2 (mMad2 and hMad2), but not to *S. cerevisiae* Mad2p, confirming the interaction of these proteins with Mad2, and demonstrating species specificity of the interaction.

Mapping the Mad2 binding site of Mad1

To define the Mad2-binding region of mMad1, we used the assay described above to investigate binding with progressively smaller fragments of Mad1. Carboxyl-terminal and central fragments that overlap between residues 522 and 592 both bound mMad2, whereas fragments lacking part of this region failed to bind (Fig. 4-4). We translated peptides from within this 71-residue region as Maltose Binding Protein fusions to create protein sufficiently large for resolution by SDS-PAGE. A 25-residue peptide from within this region (residues 534-558) binds mMad2 and shows no binding to *S. cerevisiae* Mad2p (Fig. 4-5). The interaction was confirmed by reversing the orientation of binding and pulling down *in vitro*-translated hMad2 with a 50-residue fragment of hMad1 (residues 521-571) immobilized on beads (Fig. 4-5).

To define the minimal Mad2-binding sequence, we used [^{35}S]-labeled *in vitro*-translated hMad2 to probe a membrane spotted with hMad1 peptides. The overlapping sequence between the only two hMad2-binding peptides suggests the minimal binding region is 19 residues long (538-556) (Fig. 4-6). To confirm this interaction we incubated the 19-residue hMad1 synthetic peptide with bacterially expressed hMad2 and analyzed hMad2 migration on a native gel. Fig. 4-7 shows that an equimolar concentration of hMad1 peptide is sufficient to induce a migration shift of virtually all the hMad2, thus demonstrating direct interaction of hMad2 with residues 538-556 of hMad1.

We then used our mapping results from mammalian Mad1 to aid in the identification of the Mad2-binding site of *S. cerevisiae* Mad1p. We mapped the Mad1p binding site to a 24-residue peptide (residues 575-598) that is homologous to the mammalian binding site (Fig. 4-8), although we have not determined the minimal

sequence required for binding. The efficiency of Mad1 pulldown by Mad2 appears similar for both yeast and human proteins, although the species specificity of interaction is more relaxed for Mad1p than for hMad1 (4-10). These results describe a conserved binding site between mammalian Mad1 and *S. cerevisiae* Mad1p that confers at least partial species specificity in the binding of Mad2.

Mapping the Mad2 binding site of Cdc20

The Mad2 binding region of hCdc20 was mapped using methods identical to those described above for Mad1. The first round of mapping demonstrated hMad2 binding to the amino-terminal 164 residues of hCdc20, but not the carboxyl-terminal WD-domain (residues 165-500) (Fig. 4-9). Reversing the orientation of binding by pulling down *in vitro*-translated hMad2 with bacterially expressed amino-terminal hCdc20 confirmed this interaction (Fig. 4-9). Identification of four point mutations in *S. cerevisiae* and *S. pombe* Cdc20p that abrogated Mad2p binding *in vivo* directed our further mapping efforts and lead us to utilize a peptide blot approach as described above (Hwang et al. 1998; Kim et al. 1998). Four 12-residue peptides showed hMad2 binding signals substantially stronger than adjacent peptides (Fig. 4-10). Further analysis with a second peptide membrane revealed that the nine residues from 129 to 137 bound hMad2 nearly as well as the strongest binding 12-residue peptide (Fig. 4-10).

To confirm this interaction, we performed a gel shift assay as described above for the hMad1 peptide. Preliminary hCdc20 mapping data lead us to attempt the assay with a fifteen-residue hCdc20 peptide that resulted in a slight increase in Mad2 mobility (data not shown). To determine whether the different mobility shifts caused by hMad1 and

hCdc20 peptides were due to differences in mass or charge, we synthesized a hCdc20 peptide with a similar mass and isoelectric point as the hMad1 peptide (Fig. 4-10e). This nineteen-residue hCdc20 peptide induced the same hMad2 mobility shift as the hMad1 peptide, thus demonstrating direct interaction of hMad2 with residues 129-147 of hCdc20 (Fig. 4-7).

To identify key Cdc20 residues involved in Mad2 binding, we used *in vitro*-translated hMad2 to probe a membrane spotted with mutant hCdc20 peptides. At least one amino acid substitution was tested for each of ten residues in a twelve-residue peptide. Single point mutations in five consecutive residues from K129 to L133 decreased Mad2 binding by 85-98%. Additionally, mutation of K136 decreased binding by over 75% (Fig. 4-11). These residues correspond to *S. cerevisiae* and *S. pombe* residues whose mutation also disrupts Mad2 binding and checkpoint function (Hwang et al. 1998; Kim et al. 1998).

Mapping the Mad2 binding sites of TNFα-convertase and estrogen receptor β

Previously published studies have identified several Mad2-interacting proteins that have no known involvement in the spindle assembly checkpoint (Nelson et al. 1999; Poelzl et al. 2000; O'Neill et al. 1997; Liu et al. 1999). For both human TNFα-convertase (TACE) and mouse estrogen receptor β (mERβ), the Mad2-binding sequence has been mapped to 33 and 34 residues, respectively (Nelson et al. 1999; Poelzl et al. 2000). To identify the minimal binding sequence in each protein, we used *in vitro*-translated hMad2 to probe a membrane spotted with peptides spanning the entire previously defined binding regions. Figure 4-12 shows that hMad2 binds to a series of sequential 12-residue

peptides from both proteins. TACE peptides exhibit stronger hMad2-binding than mERβ, although peptides from both proteins show considerably weaker binding than peptides from hCdc20.

Mad1, Cdc20, TACE, and ERβ interact with a common binding surface of Mad2

Alignment of Mad2-binding mammalian Mad1 and Cdc20 sequences reveals 44% homology (100% similarity) across nine residues (Fig. 4-13a). Comparison of these residues with the homologous sequences from *S. cerevisiae* and *S. pombe* indicate that the Cdc20 sequence exhibits a higher degree of homology with the Mad1 sequence in a given species than to the Cdc20 sequences in different species (Fig. 4-13b and c). This demonstrates that as the Mad2-binding site of Cdc20 has diverged through evolution, it has retained homology to the Mad2-binding site of Mad1. Finally, the strongest Mad2-interacting peptide from hMad1, hCdc20, TACE, and mERβ all share a four-residue consensus sequence starting at residue 3 (Fig. 4-13d). The conservation between these sequences suggests all may bind hMad2 at a common site. To investigate this possibility, I examined whether a hMad1 peptide could compete the binding of hMad2 to other proteins. Fig. 4-14 shows that a hMad1 peptide does indeed inhibit interaction of hMad2 with the hCdc20 amino-terminal domain, but that M2BP3 binding is unaffected by the hMad1 peptide. These results suggest that hMad1 and hCdc20 bind a common site of hMad2, or that the hMad1 peptide induces a conformational change in hMad2 that prevents additional binding.

To investigate the possibility that these proteins all bind to the same site of hMad2, I first examined the Mad2 carboxyl-terminal unstructured tail that is required for

Mad1 and Cdc20 binding (Chen et al. 1999; Luo et al. 2000). Four residues within this tail exhibit a dramatic change in NMR resonance upon binding a forty-residue fragment of hCdc20, suggesting involvement in the interaction (Luo et al. 2000). To test this hypothesis I individually mutated each of these four nonpolar residues (M196, V197, A198, and I201) to arginine, and used the *in vitro*-translated mutants in pulldown assays with bacterially expressed hMad1, hCdc20, TACE, and mERβ. Figure 4-15 shows that only mutation of Valine 197 significantly reduces binding, exhibiting a greater than 5-fold decrease in Mad1 and Cdc20 binding, and an approximately 50-fold decrease in binding to TACE and mERβ.

Comparing the hMad2 NMR structure with a multiple-species Mad2 sequence alignment revealed fourteen surface residues conserved across five species (Luo et al. 2000). Thirteen of these residues cluster in two faces of the folded protein (Fig. 4-17), with one proximal to the carboxyl-terminal tail (Face 1) and the other more distal (Face 2) (Luo et al. 2000). To test the hypothesis that these residues are involved in protein binding, I first mutated each residue by mutation to alanine, reversing the charge of a charged residue, or changing an uncharged residue to a charged residue. Mutations were made individually, or in combination with nearby residues in the same face. Each of the *in vitro*-translated mutants was then tested for binding to hMad1, hCdc20, TACE, and mERβ as described above, and the results summarized in Figure 4-16. Analysis of single alanine substitutions reveals only H191A showed a greater than two-fold reduction in binding to any protein, exhibiting a four-fold reduction in Cdc20 binding and at least a ten-fold reduction in TACE and mERβ binding. Interestingly, this mutant bound hMad1 with approximately 90% the efficiency of wildtype hMad2. Analysis of the double and

triple mutants revealed that none of the Face 2 mutations (i.e., those distant from the carboxyl-terminus) reduced binding to any protein by more than approximately two-fold, suggesting this region is relatively unimportant for interaction with these proteins. In contrast, all Face 1 double mutations reduced binding to all proteins by at least two-fold, and in some cases greater than ten-fold. These results suggest Face1 residues and the carboxyl-terminal tail of hMad2 form a common binding surface for both hMad1 and hCdc20, with residue H191 making a greater contribution to hCdc20 binding. Additionally, this analysis demonstrates that both TACE and mERβ use this same binding surface for Mad2 interaction.

Figure 4-1. Clones interacting with Mad2 in two-hybrid assay. (a) β-galactosidase units as tested in liquid culture assay for clones that did not test positive for β-galactosidase expression with non-specific baits (p53, lamin, SNF, and CDK2) in a filter lift assay. (b-d) DNA and protein sequences of Mad2 binding protein 1 (M2BP1), M2BP3, and M2BP4. All are partial clones that lack 5' translated sequence. (b) DNA sequence of M2BP1. Bases 1-2028 exhibit 100% homology to bases 595-2622 of Genbank sequence AF083812. Conceptual translation of this sequence is shown in Figure 4-2. (c) DNA sequence and conceptual translation of M2BP3. Bases 1-1176 exhibit 100% homology to bases 61-1236 of Genbank sequence NM 025649 (Mus musculus RIKEN cDNA 0610009D16), with the exception of a GC inversion at bases 133-134. The protein sequence initiates at the sixth residue of the conceptual translation of Genbank sequence NM 025649. (d) DNA sequence and conceptual translation of M2BP3. This sequence exhibits no homology with known genes.

a.

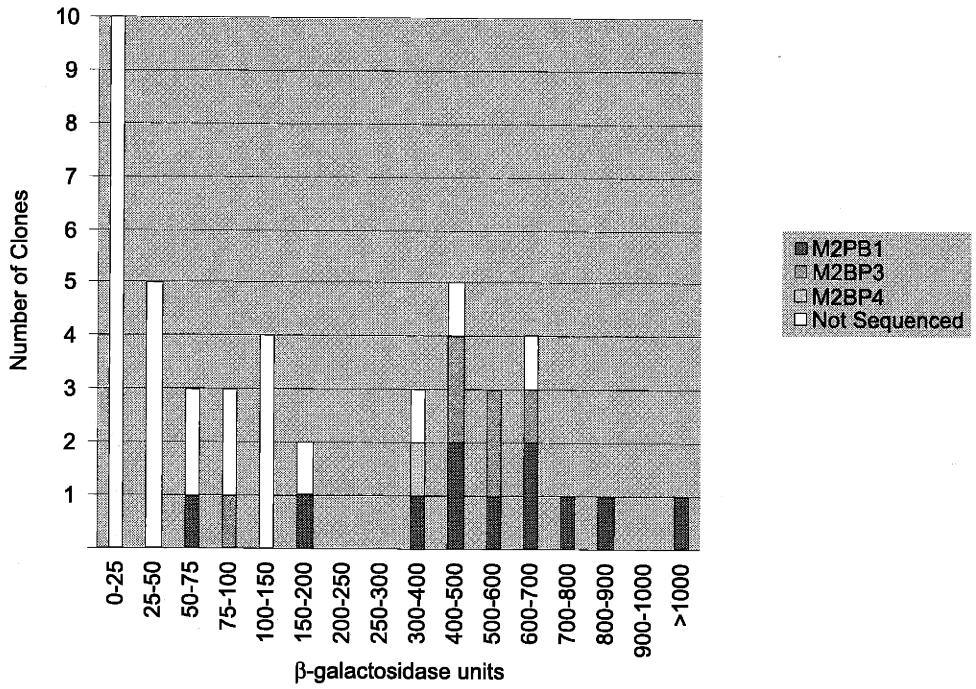

b. M2BP1

```
   1 AAGGTACAGGTCAAGCGGCT GGAGTCTGAAAAGCAGGAGC TGAAGGAGCAGCTGGAGCTG CAGCAGCGGAAATGGCAAGA
     GGCAAATCAGAAGATCCAGG AGCTGCAGGCCAGTCAAGAT GAGAGAGCTGAGCATGAGCA GAAGATTAAGGACCTGGAGC
 161 AGAAGCTGTGTCTACAAGAG CAGGATGCAGCTGTGGTGAA GAGCATGAAGTCTGAGCTGA TGCGGATGCCCAGGATGGAG
     CGTGAGCTGAAGAGGCTGCA TGAAGAGAACACTCATCTAA GGGAGATGAAGGAGACCAAT GGGCTGCTCACAGAGGAGCT
 321 GGAAGGTCTGCAGAGGAAAC TGAGCCGGCAGGAGAAGATG CAGGAGGCTCTGGTTGACCT GGAGTTGGAAAAGGAGAAGC
     TACTTGCAAAGCTGCAGAGC TGGGAGAACCTGGACCAGAC CATGGGCTTGAATCTCAGGA CTCCAGAGGACCTTTCTAGG
 481 TTCGTGGTTGAGCTACAGCA GCGAGAGCTCACCCTGAAGG AGAAGAATAACAGCATCACC AGCAGTGCCCGGGGTCTGGA
     GAAGGTCCAGCAGCAGCTCC AGGATGAGGTCCGGCAGGCC AATGCACAGCTGCTGGAGGA GCGGAAAAAGAGGGAGACAC
 641 ATGAGGCACTTGCCCGAAGG CTCCAGAAGCGCAATGCATT GCTGACCAAGGAGAGAGATG GCATGCGTGCCATCCTGGGA
     TCCTACGACAGTGAGCTGAC CCAAACTGAGTACTCAACCC AGCTGACACAGCGCCTGTGG GAGGCCGAGGACATGGTTCA
 801 GAAGGTACATGCCCACAGCT CGGAGATGGAGGCTCAGCTG TCTCAGGCCCTGGAGGAGCT TGGGGTTCAGAAGCAGAGAG
     CTGACACGCTGGAGATGGAG TTGAAGATGCTGAAGGCCCA GACAAGCTCAGCTGAATCTA GCTTCTCATTCTGCAAAGAG
 961 GAGGTGGATGCACTCAGGTT GAAGGTGGAGGAGCTGGAGG GTGAGCGGAGCCGTCTGGAA CAGGAAAAGCAGGTGCTGGA
     GATGCAGATGGAGAAACTAA CCCTACAGGGTGACTACAAC CAGAGTCGAACCAAAGTGCT ACACATGAGCCTTAACCCAA
1121 TCAGCATGGCCAGGCAACGC CAGCATGAGGACCATGACCG GCTGCAGGAGGAATGTGAGC GCTTACGGGGACTTGTGCAT
     GCCCTGGAGAGAGGGGGCCC CATCCCTGCTGACCTGGAGG CTGCCTCCAGTCTGCCCTCA TCAAAGGAGGTGGCAGAGCT
1281 GCGGAAGCAGGTGGAAAGTG CTGAGCTGAAGAACCAGCGG CTGAAGGAGGTTTTCCAGAC CAAGATCCAGGAGTTCCGCA
     AAGTTTGCTACACGCTGACC GGCTACCAGATTGACGTGAC CACGGAGAGCCAATACCGCC TCACCTCCCGATACGCTGAG
1441 CACCAGACGGACTGCCTCAT CTTCAAGGCCACAGGACCCT CGGGCTCCAAGATGCAGCTG CTGGAGACAGAGTTCTCACG
     GTCTGTGCCTGAGCTCATTG AACTGCACTTGCTGCAGCAG GACAGCATCCCTGCCTTCCT CAGTGCGCTCACCATAGAGC
1601 TGTTCAGCCGCCAGACCTCT ATCTAGCCTCTTCCCATGAG CATCTTCACTACAGCCGCTG GACCTCGGCCTAGCCTGTAC
     CTGCAGCTTCTCACATGCAG CCCCCAGACCTTGAGCTAGC TCTTGGTCTACAGTTGCCCA CATCATCCCCAGATCCCTTT
1761 GCCACCCATAGCTGCATCAT GTCACAAACACTAGCCGTGG CCTCTGCTCAAGCAGCCACT GTCTCTTGTCCCTGGCTAGG
     AGCAAGCTACTGGGGATGAC CAAGCCAGATCATACCCCAC TACTCTCCTCCCCACCCCAC CCCATTCTAGAGCCGCTCCA
1921 CGTACTGTCCCAAGGTGTAC CCCAGCCTCCAGTCCCATGC GCTGGTTGCTTAGGCTTCAG TGGCCAGACTGTAGCCTGTG
     TCCACAGTCTCAGACTAATG AAATAAAGGGTAAA 2034
```

C.

```
          10          20          30          40          50          60
GAT ATG TCC GAA CTG TCC CCT GCT GCT GCC CCA AAT TTG GAT TGG TAT GAG AAG CCG GAA
 D   M   S   E   L   S   P   A   A   A   P   N   L   D   W   Y   E   K   P   E>

          70          80          90         100         110         120
GAA ACT CAT GCT CCT GAA GTA GAT CTT GAG ACT GTC ATC CCG CCA GCC CAG GAA CCT TCC
 E   T   H   A   P   E   V   D   L   E   T   V   I   P   P   A   Q   E   P   S>

         130         140         150         160         170         180
AAT CCT GCG GAG CCC TTT TGC CCA AGA GAC CTG GTG CCG GTG GTG TTT CCC GGG CCT GTG
 N   P   A   E   P   F   C   P   R   D   L   V   P   V   V   F   P   G   P   V>

         190         200         210         220         230         240
AGC CAG GAA GAC TGC TGC CAG TTT ACT TGT GAA CTT CTC AAG CAT ATC CTG TAC CAG CGC
 S   Q   E   D   C   C   Q   F   T   C   E   L   L   K   H   I   L   Y   Q   R>

         250         260         270         280         290         300
CAT CAG CTC CCT CTG CCC TAT GAA CAG CTG AAG CAC TTC TAC CGG AAA GTT CCC CAG GCA
 H   Q   L   P   L   P   Y   E   Q   L   K   H   F   Y   R   K   V   P   Q   A>

         310         320         330         340         350         360
GAG GAC ACA GCA AGG AAG AAA GCT TGG CTC GCC ACG GAG GCG AGG AAC AGG AAG TGT CAG
 E   D   T   A   R   K   K   A   W   L   A   T   E   A   R   N   R   K   C   Q>

         370         380         390         400         410         420
CAG GCT TTG GCG GAG CTG GAG AGC GTC CTC AGT CAC CTA CGA GAC TTC TTT GCC CGG ACA
 Q   A   L   A   E   L   E   S   V   L   S   H   L   R   D   F   F   A   R   T>

         430         440         450         460         470         480
CTC GTA CCA CAA GTG TTG ATC CTT CTT GGA GGC AAT GCC CTC AGC CCT AAA GAA TTC TAT
 L   V   P   Q   V   L   I   L   L   G   G   N   A   L   S   P   K   E   F   Y>

         490         500         510         520         530         540
GAA CTT GAC CTG TCC AGG CTG GCT CCA TTC GGT GTG GAC CAG GGC CTG AAC ACA GCG GCT
 E   L   D   L   S   R   L   A   P   F   G   V   D   Q   G   L   N   T   A   A>

         550         560         570         580         590         600
TGC TTG CGT CGT CTC TTC AGA GCC ATC TTC TTG GCG GAT CCA TTT AGC GAA CTG CAG ACT
 C   L   R   R   L   F   R   A   I   F   L   A   D   P   F   S   E   L   Q   T>

         610         620         630         640         650         660
CCC CCG CTC ATG GGT ACC ATT GTC ATG GTT CAG GGC CAC CGT GAC TGT GGA GAA GAT TGG
 P   P   L   M   G   T   I   V   M   V   Q   G   H   R   D   C   G   E   D   W>

         670         680         690         700         710         720
TTT CAA CCG AAA CTG AAC TAC CGG GTG CCC AGC CGG GGC CAC AAA CTC ACC GTG ACA CTG
 F   Q   P   K   L   N   Y   R   V   P   S   R   G   H   K   L   T   V   T   L>

         730         740         750         760         770         780
TCA TGT GGC AGA CCT TCC GTC CCA GCC ATG GCT TCA GAG GAT TAC ATT TGG TTC CAG GCA
 S   C   G   R   P   S   V   P   A   M   A   S   E   D   Y   I   W   F   Q   A>

         790         800         810         820         830         840
CCA GTG ACA CTT AAA GGT TTC CAT GAG TGA AGG TAT AAG GAC AAT GGC TGA ATT CTC TCC
 P   V   T   L   K   G   F   H   E   *>

         850         860         870         880         890         900
CAT TCT CAT GCT AGG GCA CCC ATC TTC CCA CTG AGG GAG GAG GAA GGC TCT GTC CTG GCC

         910         920         930         940         950         960
ATG TGC CTT CTC TCC CCA GAC TTC CTG CTG ACT GAT GGT GTG TGG CTG GGG CTG TGA TAA

         970         980         990        1000        1010        1020
TTG TCA TCA AGC AAA GTC CCC CGA ATC AGT GAT TGG CTC CCA GAG GCC CCT GCG CCA GGA

        1030        1040        1050        1060        1070        1080
GGA TCT GTT TGG GAG TAG AAA GCA AGG CTG TGT CAG TAG ATC CCT CTA ATA ATG GAG GTG

        1090        1100        1110        1120        1130        1140
GTC CTT CCC TGC TTC ATG CTA TGG ATT TTC AGA ACT GTT ATC AGG ATG ATA ATG TGG GTG

        1150        1160        1170        1180
TTA CTC ATG ATT TTA AAT ATG ATG AGA TGA ATA AAG CGT GAA CT
```

d.

```
          10          20          30          40          50          60
ACA TGT GCT CCT AGG TTA CGT GTT AAT AAT GGG TAT AAG ATC TGG CAT TAT ACT GGC TCT
 T   C   A   P   R   L   R   V   N   N   G   Y   K   I   W   H   Y   T   G   S>

          70          80          90          100         110         120
CTT TTG CAT AAG TAT GAT GTG CCA TCA AAT GGA GAA TTA TGG CAG GTT TCT TGG CAG CCA
 L   L   H   K   Y   D   V   P   S   N   G   E   L   W   Q   V   S   W   Q   P>

          130         140         150         160         170         180
TTT TTG GAT GGA ATA TTT CCA GCA AAA ACG ATA AAG TAC CAA GCA GTT CCA AGT GAA GTG
 F   L   D   G   I   F   P   A   K   T   I   K   Y   Q   A   V   P   S   E   V>

          190         200         210         220         230         240
CCT AGT GAG GAG CCT AAA GTT GCA ACA GCT TAT AGA CCT CCA GCC TTA AGA AAT AAG CCA
 P   S   E   E   P   K   V   A   T   A   Y   R   P   P   A   L   R   N   K   P>

          250         260         270         280         290         300
GTC ACC AAT TCC AAA CTG CAT GAA GAG GAA CCT CCC CAG AAT ATG AAG CCA CAT CCA GGA
 V   T   N   S   K   L   H   E   E   E   P   P   Q   N   M   K   P   H   P   G>

          310         320         330         340         350         360
AGT GAC AAG CCA TTA TCA AAA ACA GCC CTT AAA AAT CAA AGG AAG CAT GAA GCT AAA AAA
 S   D   K   P   L   S   K   T   A   L   K   N   Q   R   K   H   E   A   K   K>

          370         380         390         400         410         420
GCT GCA AAC AGG AAG CAA GAA GTG ATG CGG CTC CTA CTC CTG TCC CAC AGA GTG CAC CAC
 A   A   N   R   K   Q   E   V   M   R   L   L   L   L   S   H   R   V   H   H>

          430         440         450         460         470         480
GGA ACA CGG TCA CCC AGT CTG CTT CTG GTG ATC CTG AAG TAG ACA AAA AAA TTA AGA ATC
 G   T   R   S   P   S   L   L   L   V   I   L   K   *>

          490         500         510         520         530         540
TAA AGA AGA AAC TGA AAG CCA TAG AGC AGC TAA AAG AGC AGG CAG CCG CCG GGA AAC AGC

          550         560         570         580         590         600
TAG AAA AAA ATC AGT TGG AGA AAA TTC AGA AAG AGA CAG CCC TTC TCC AAG AGC TTG AAG

ATT
```

Figure 4-2. Multiple species Mad1 alignment. Mad1 protein sequences from mouse, human, *Xenopus*, and *S. cerevisiae* aligned with MacVector (Oxford Molecular Group). Bold residues in dark boxes represent identity and light boxes represent similarity. Asterisk (*) indicates first residue of M2BP1. Genbank Accession numbers of mouse, *Xenopus*, and *S. cerevisiae* Mad1 are 4580768, 4583428, and 551091, respectively. The sequence of hMad1 is derived from our sequencing of pTXBP181.

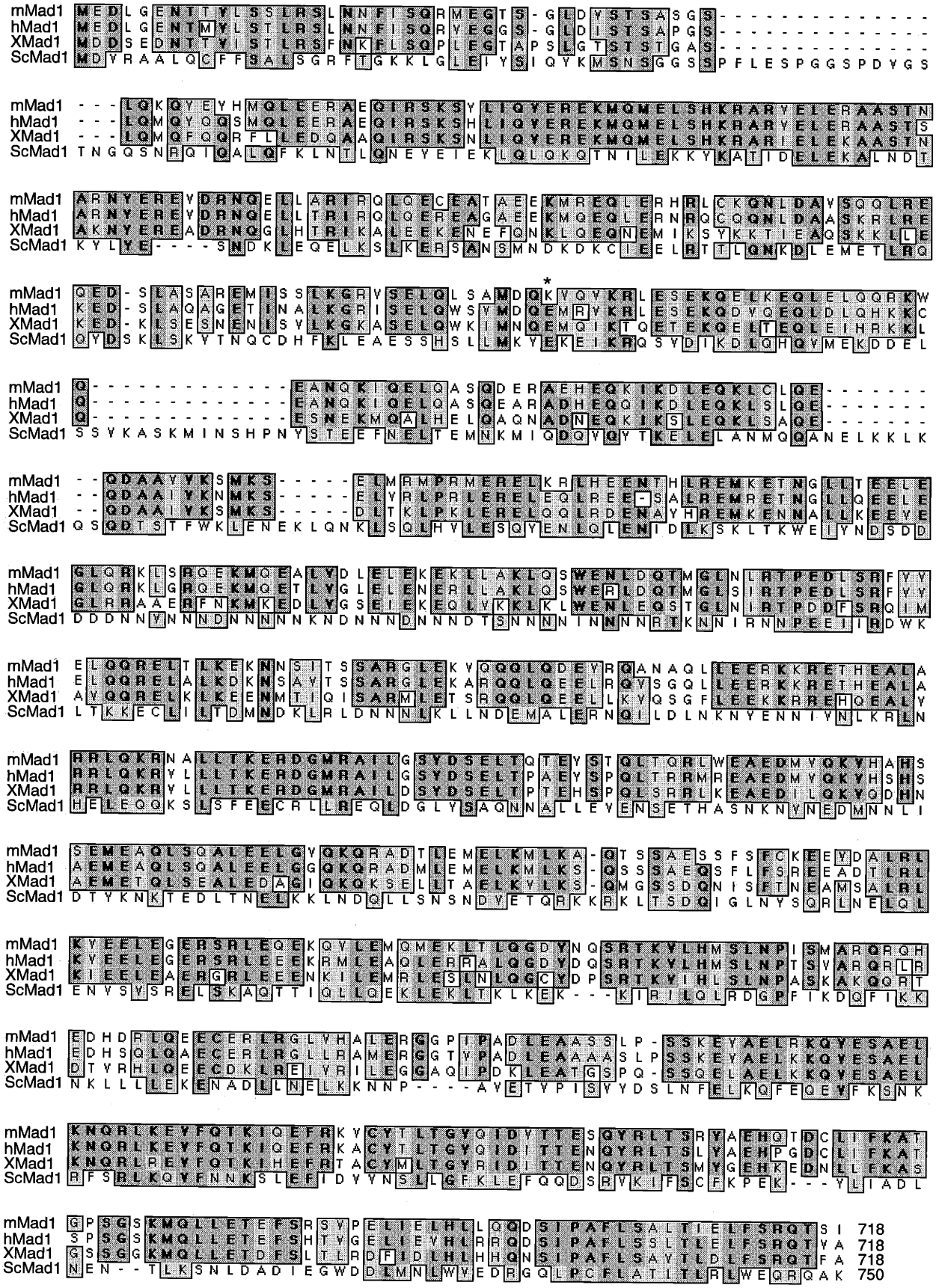
mMad1
hMad1
XMad1
ScMad1
718
718
718
750

Figure 4-3. Species specificity of mMad1 and M2BP3 binding to Mad2. (a-b) Binding of mMad1 and M2BP3 to Mad2. *In vitro*-translated [^{35}S]-labeled mMad1 or M2BP3 was incubated with *S. cerevisiae* (Y), mouse (M), or human (H) Mad2-GST fusion proteins immobilized on glutathione sepharose beads. Beads were spun down, washed and the bound Mad1 detected by SDS-PAGE and autoradiography. "Input" lanes represent 12.5% of the input in the binding reactions. (c) Analysis of Mad2 beads by SDS-PAGE and Coomassie staining shows equivalent concentrations of each protein used in binding reactions.

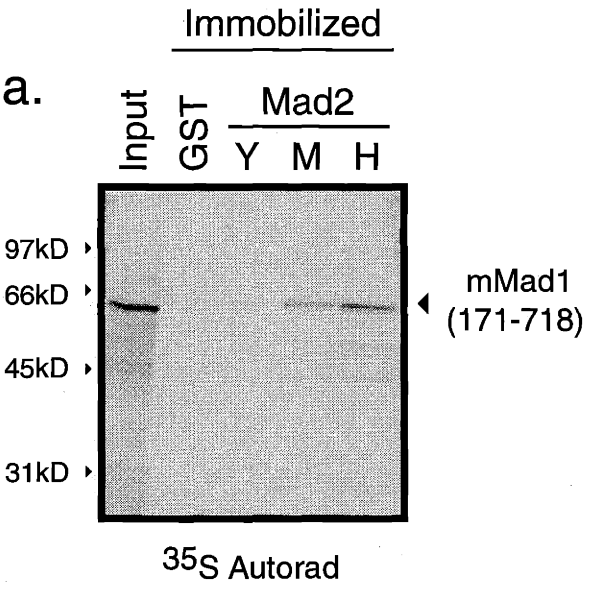
a.
Immobilized
Input
GST
Mad2
Y M H
97kD
66kD
45kD
31kD
mMad1
(171-718)
35S Autorad

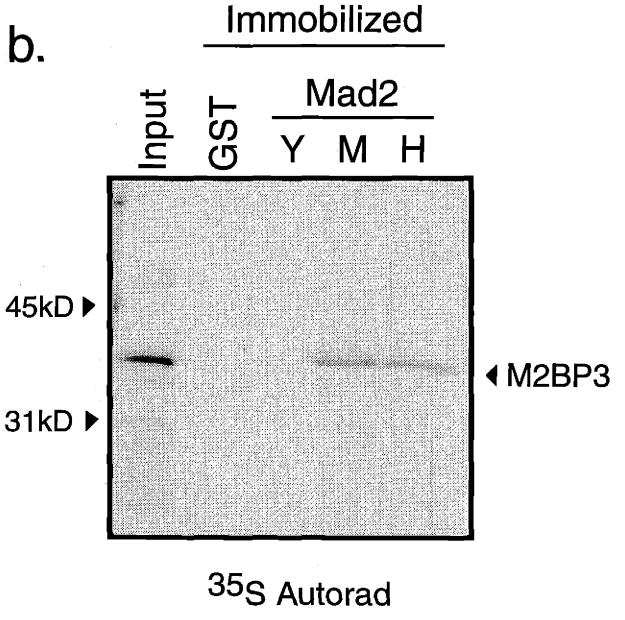
b.
Immobilized
Input
GST
Mad2
Y M H
45kD
31kD
M2BP3
35S Autorad

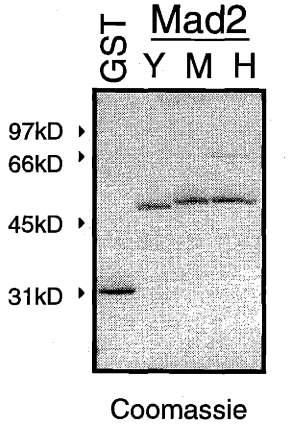
c.
GST
Mad2
Y M H
97kD
66kD
45kD
31kD
Coomassie

Figure 4-4. Mapping the Mad2 binding site of mMad1. (a-d) Analysis of mMad2 and *S. cerevisiae* Mad2p binding to mMad1 truncations as described in Figure 4-3. "Input" lanes represent 12.5% of input in binding reactions, except (b) represents 6.75% of the input. (e) Summary of mapping analysis.

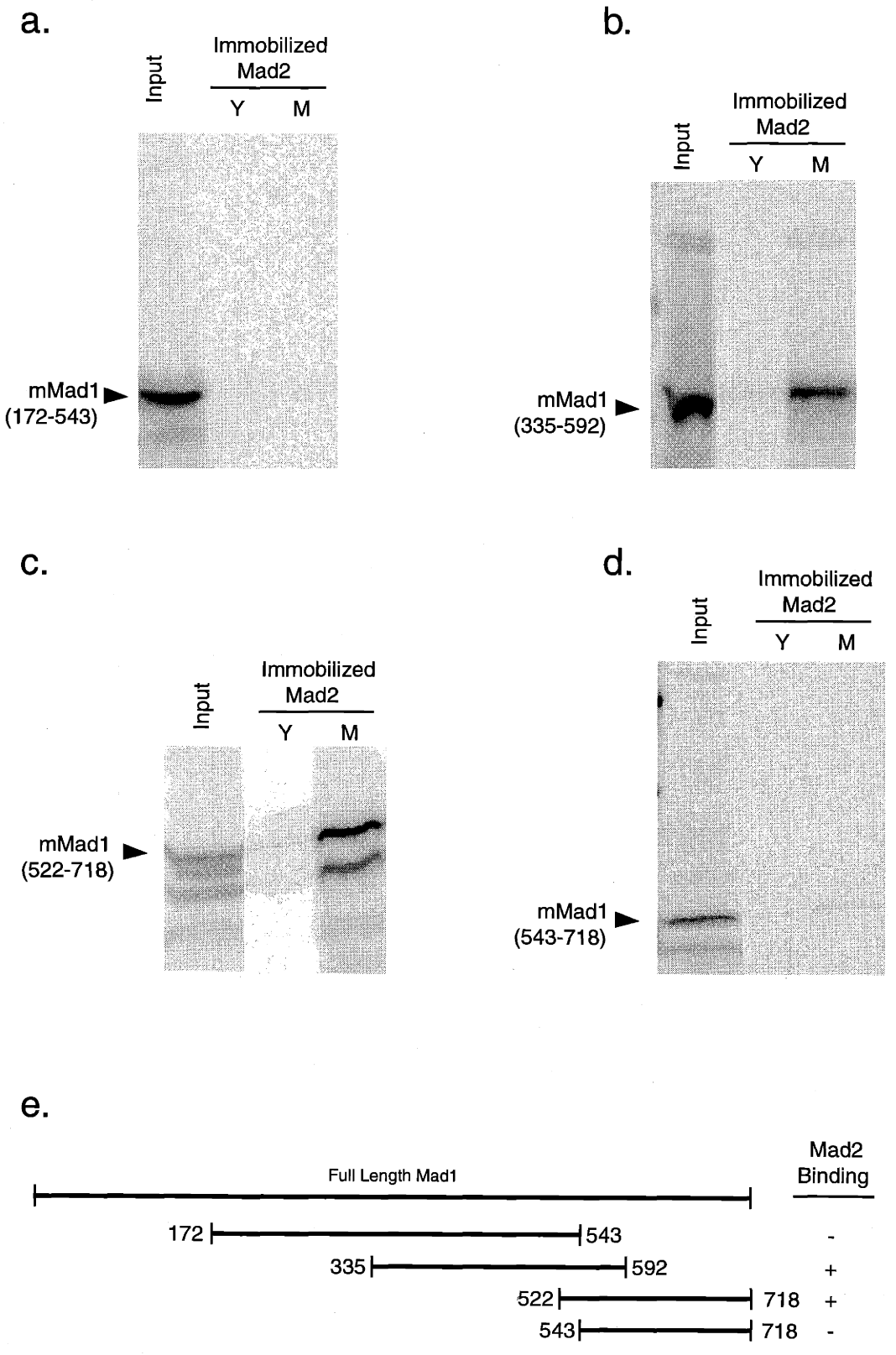
a.
Input
Immobilized Mad2
Y
M
mMad1 (172-543)
b.
Input
Immobilized Mad2
Y
M
mMad1 (335-592)
c.
Input
Immobilized Mad2
Y
M
mMad1 (522-718)
d.
Input
Immobilized Mad2
Y
M
mMad1 (543-718)
e.
Full Length Mad1
Mad2 Binding
172
543
-
335
592
+
522
718
+
543
718
-

Figure 4-5. High resolution mapping of the Mad2 binding site of mMad1. (a-b) Analysis of mMad2 and *S. cerevisiae* Mad2p binding to mMad1 truncations as described in Figure 4-3. mMad1 sequences were fused to the carboxyl-terminus of maltose binding protein. Equivalent concentrations of *in vitro*-translated mMad1 were used in each reaction. Bound fraction of the strongest interacting mMad1 fragment (residues 534-558) is equal to 18% of the input. (c) Reversed orientation hMad1 binding with hMad2. Binding of a 50-residue fragment of hMad1 (residues 521-571) expressed as a GST-fusion protein and immobilized on glutathione sepharose beads to *in vitro*-translated [^{35}S]-labeled hMad2.

a.

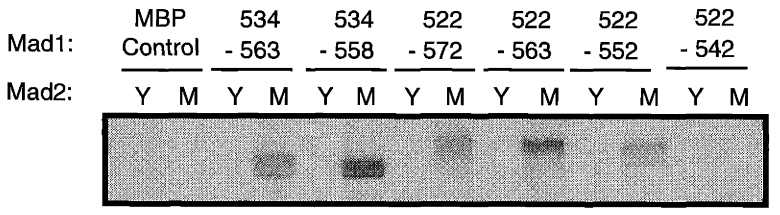
Mad1:
MBP Control
534 - 563
534 - 558
522 - 572
522 - 563
522 - 552
522 - 542
Mad2:
Y M Y M Y M Y M Y M Y M Y M

b.

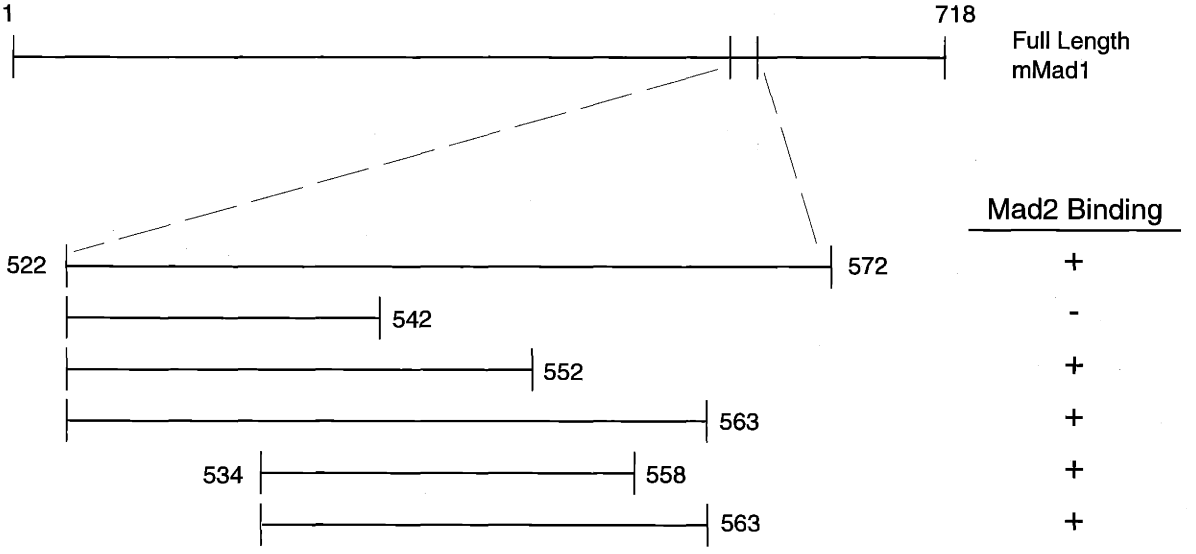
1
718
Full Length mMad1
Mad2 Binding
522
572
+
542
-
552
+
563
+
534
558
+
563
+

c.

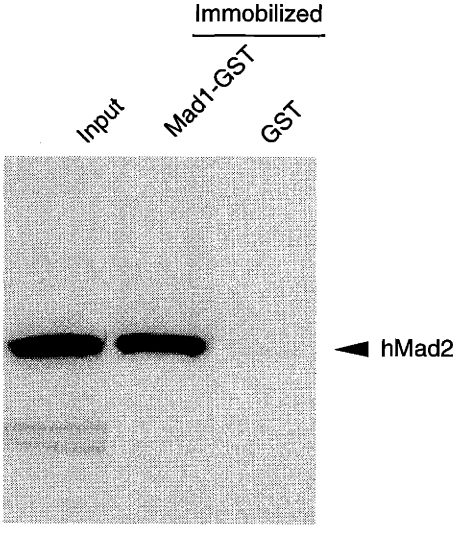
Immobilized
Input
Mad1-GST
GST
hMad2

Figure 4-6. Peptide mapping the hMad2-binding sequence of hMad1. (a) A membrane with 20-residue peptides scanning the hMad1 sequence shown in (c) were probed with *in vitro*-translated [^{35}S]-labeled hMad2. (b) Graphical representation of relative Mad2 binding to selected Mad1 peptides. y-axis is labeled in arbitrary units. (c) Mad1 sequence scanned on peptide blot. Bold type indicates the strongest binding peptide. Underlined residues are included in the fourth and fifth coiled-coils of Mad1 as predicted by PAIRCOIL analysis (Berger et al. 1995). The scanned sequence was derived from Mad1 sequence of Genbank Accession number U33822. Asterisk (*) represents an isoform-specific residue that is a histidine in our sequencing of hMad1.

a.

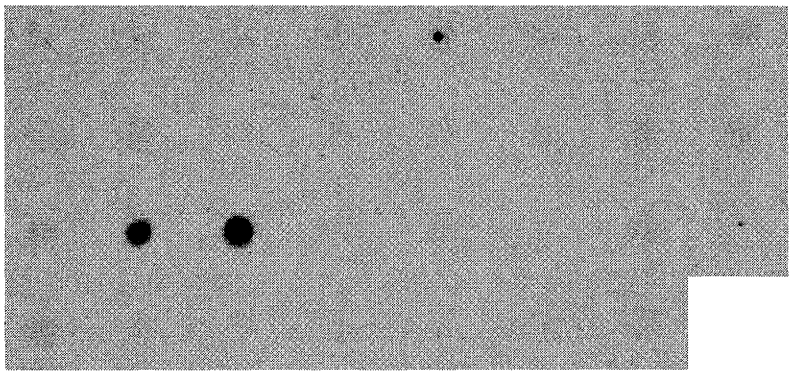

b.

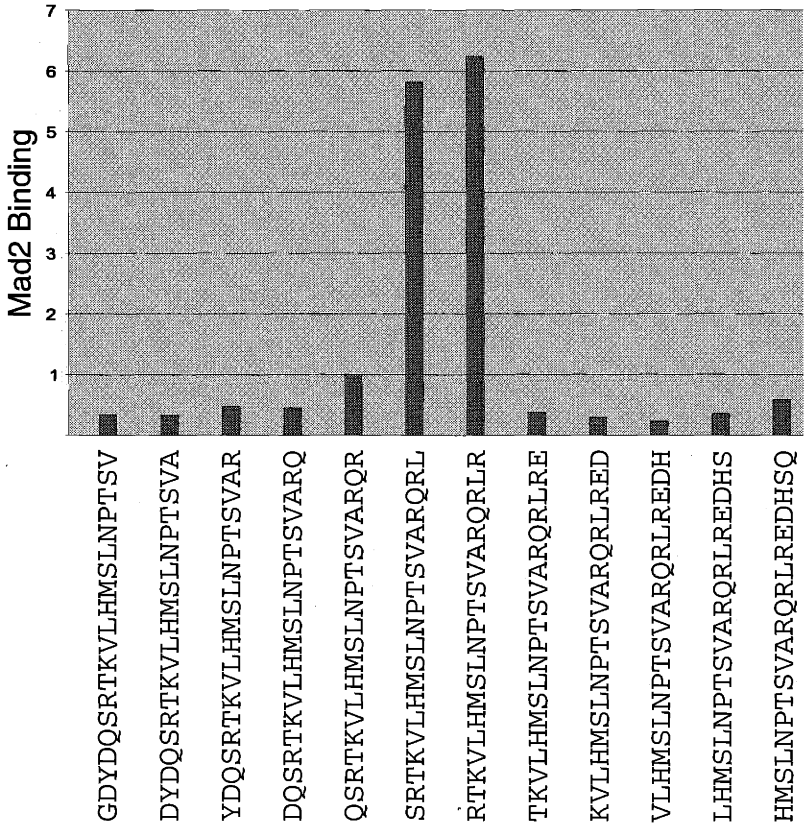
Mad2 Binding
7
6
5
4
3
2
1
GDYDQSRTKVLHMSLNPTSV
DYDQSRTKVLHMSLNPTSVA
YDQSRTKVLHMSLNPTSVAR
DQSRTKVLHMSLNPTSVARQ
QSRTKVLHMSLNPTSVARQR
SRTKVLHMSLNPTSVARQRL
RTKVLHMSLNPTSVARQRLR
TKVLHMSLNPTSVARQRLRE
KVLHMSLNPTSVARQRLRED
VLHMSLNPTSVARQRLREDH
LHMSLNPTSVARQRLREDHS
HMSLNPTSVARQRLREDHSQ

c.


520
569
*
MLEAQLERRALQGDYDQSRTKVLHMSLNPTSVARQRLREDHSQLQAECER
Coil IV
Coil V

Figure 4-7. Native gel mobility shift of hMad2 incubated with 0.1, 1, or 10 molar excess of 19-residue Mad1 or Cdc20 peptides. Control is a scrambled version of a 15-residue sequence spanning the minimal Cdc20 Mad2-binding sequence.

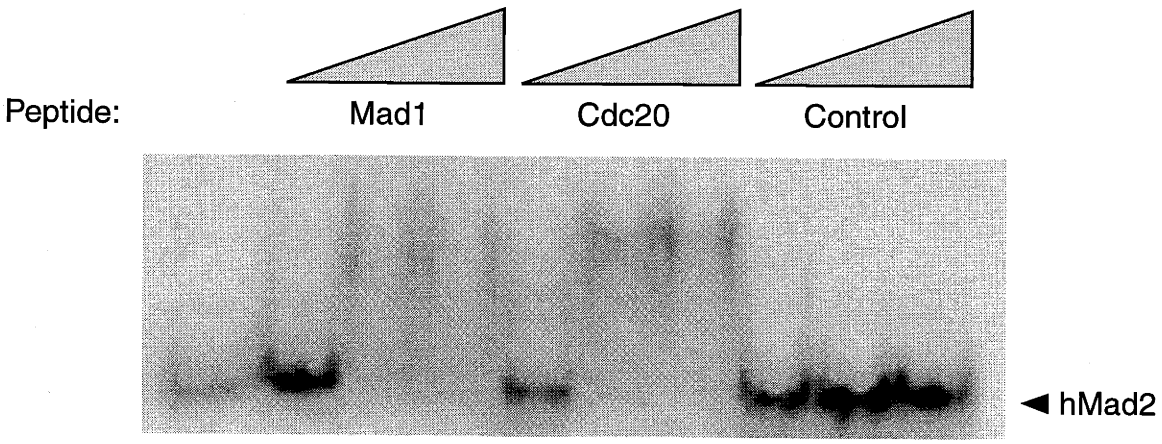
Peptide:
Mad1
Cdc20
Control
hMad2

Figure 4-8. Mapping the *S. cerevisiae* Mad2p-binding sequence of Mad1p. (a-c) *In vitro* translated [^{35}S]-labeled Mad1p was assayed for binding to mMad2 (m) or *S. cerevisiae* (y) Mad2p as described in Figure 4-3. Mad1p sequences in (c) were fused to the carboxyl-terminus of maltose binding protein. "Input" represents 30% of input in each binding reaction. (d) Alignment of the shortest Mad2p-binding Mad1p sequence with the minimal hMad2-binding sequence of hMad1. Dark boxes indicate identity and light boxes indicate similarity.

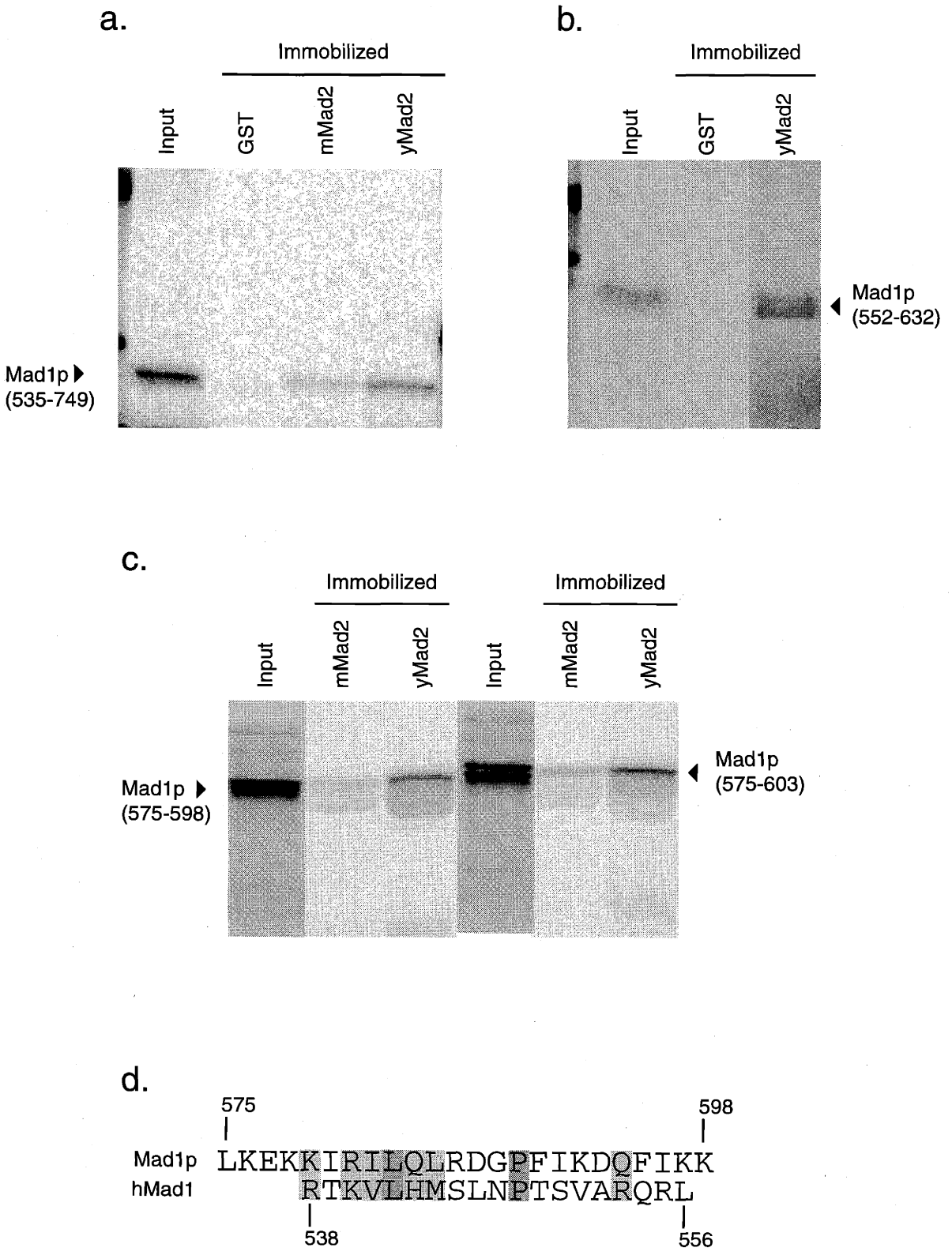
a.
Immobilized
Input
GST
mMad2
yMad2
Mad1p
(535-749)
b.
Immobilized
Input
GST
yMad2
Mad1p
(552-632)
c.
Immobilized
Immobilized
Input
mMad2
yMad2
Input
mMad2
yMad2
Mad1p
(575-598)
Mad1p
(575-603)
d.
575
598
Mad1p LKEKKIRILQLRDGPFIKDQFIKK
hMad1 RTKVLHMSLNPTSVARQRL
538
556

Figure 4-9. Mapping the hMad2 binding region of hCdc20. (a) Analysis of hMad2 and *S. cerevisiae* Mad2p binding to hCdc20 truncations as described in Figure 4-3. "Input" lanes represent approximately 15% of input in binding reactions. (b) Reversed orientation interaction of hCdc20 binding region with hMad2. Binding of *in vitro*-translated [^{35}S]-labeled hMad2 to the amino terminal 164 residues of hCdc20 expressed as a GST-fusion protein and immobilized on glutathione sepharose beads.

a.

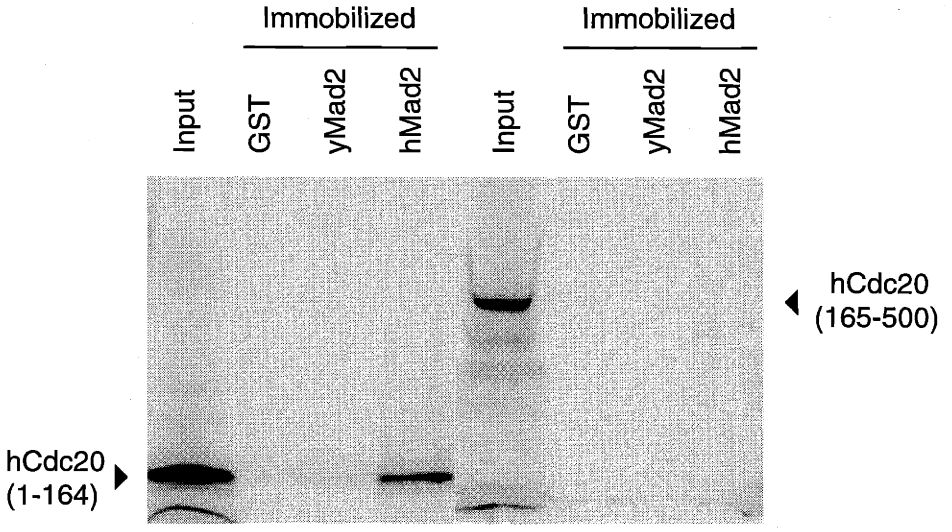
Immobilized
Immobilized
Input
GST
yMad2
hMad2
Input
GST
yMad2
hMad2
hCdc20
(165-500)
hCdc20
(1-164)

b.

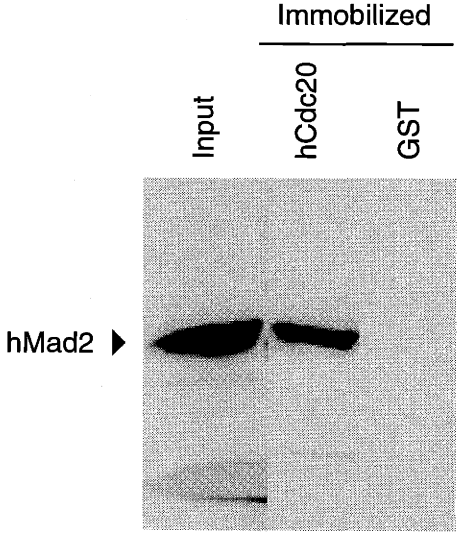
Immobilized
Input
hCdc20
GST
hMad2

Figure 4-10. Peptide mapping the hMad2-binding region of hCdc20. (a) A membrane with 12-residue peptides scanning the Cdc20 sequence shown in (e) probed with *in vitro*-translated [^{35}S]-labeled Mad2. (b) Graphical representation of relative Mad2 binding to each Mad1 peptide. Bold type indicates the strongest binding peptide. y-axis is labeled in arbitrary units. (c) Truncated versions of the 12-residue strongest binding peptide probed as in (a). Negative control is a scrambled version of the 12-residue peptide. The uneven signal in the nine-residue peptide most likely is the result of a scratch from the peptide applicator. The signal from this spot was calculated from a smaller region that did not include the scratched area. (d) Graphical representation of relative Mad2 binding to each Mad1 peptide in (c). Error bar for the 12-residue peptide represents one standard deviation for binding to four spots. (e) Cdc20 sequence scanned on peptide blot. Asterisk (*) indicate residues whose mutation in *S. cerevisiae* or *S. pombe* abrogates Mad2p-Cdc20p interaction and spindle checkpoint function (Hwang et al. 1998; Kim et al. 1998). Underlined sequence indicates synthetic peptide used in Mad2 gel shift assay described in Figure 4-7.

a.

b.

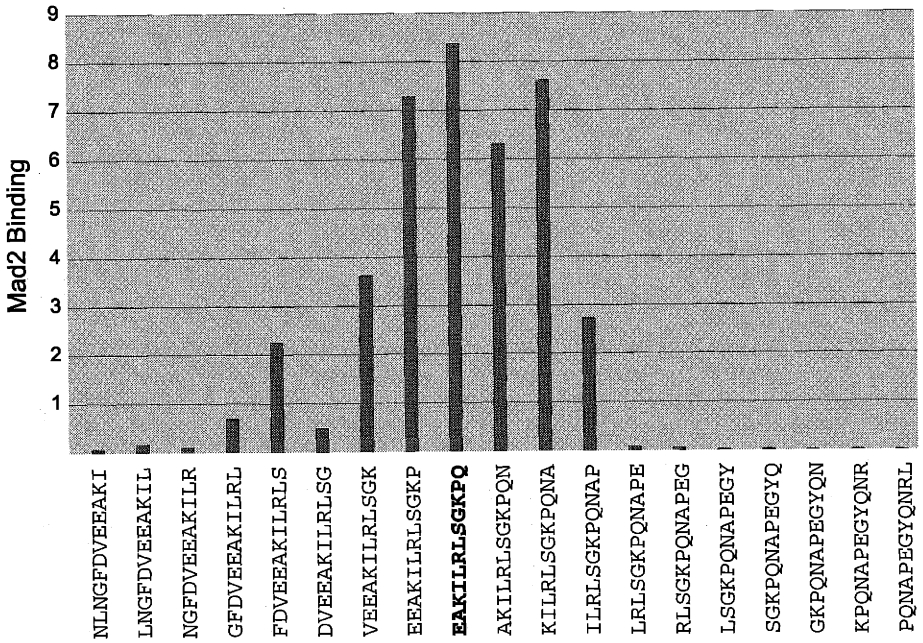
Mad2 Binding
9
8
7
6
5
4
3
2
1
NLNGFDVEEAKI
LNGFDVEEAKIL
NGFDVEEAKILR
GFDVEEAKILRL
FDVEEAKILRLS
DVEEAKILRLSG
VEEAKILRLSGK
EEAKILRLSGKP
EAKILRLSGKPQ
AKILRLSGKPQN
KILRLSGKPQNA
ILRLSGKPQNAP
LRLSGKPQNAPE
RLSGKPQNAPEG
LSGKPQNAPEGY
SGKPQNAPEGYQ
GKPQNAPEGYQN
KPQNAPEGYQNR
PQNAPEGYQNRL

c.

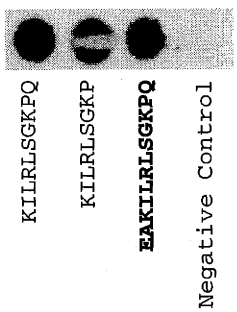
KILRLSGKPQ
KILRLSGKP
EAKILRLSGKPQ
Negative Control

d.

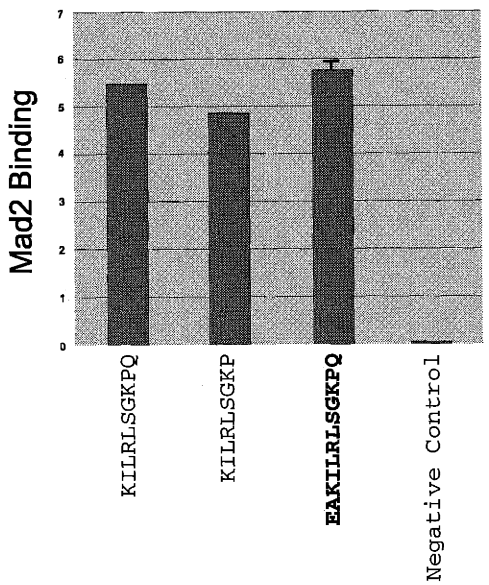
Mad2 Binding
7
6
5
4
3
2
1
0
KILRLSGKPQ
KILRLSGKP
EAKILRLSGKPQ
Negative Control

e.


119
148
NLNGFDVEEAKILRLSGKPQNAPEGYQNRL

Figure 4-11. Single residue mutations of a 12-residue Mad2-binding Cdc20 peptide probed with *in vitro* translated [^{35}S]-labeled Mad2. For each mutation, the wildtype residue is indicated in bold type (b). Error bar for the wildtype peptide represents one standard deviation for binding to four spots. Summary of mutant analysis is shown in (c). The 12-residue wildtype peptide is shown, with bold type indicating residues whose mutation reduced binding to less than 25% of wildtype binding. Asterisks (*) indicate residues whose mutation in *S. cerevisiae* or *S. pombe* abrogates Mad2p-Cdc20p interaction and spindle checkpoint function (Hwang et al. 1998; Kim et al. 1998).

a.

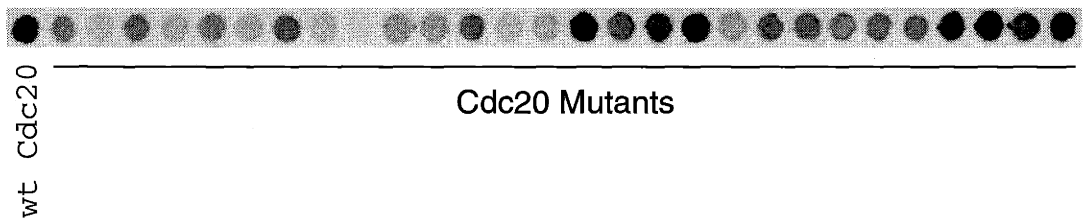

b.

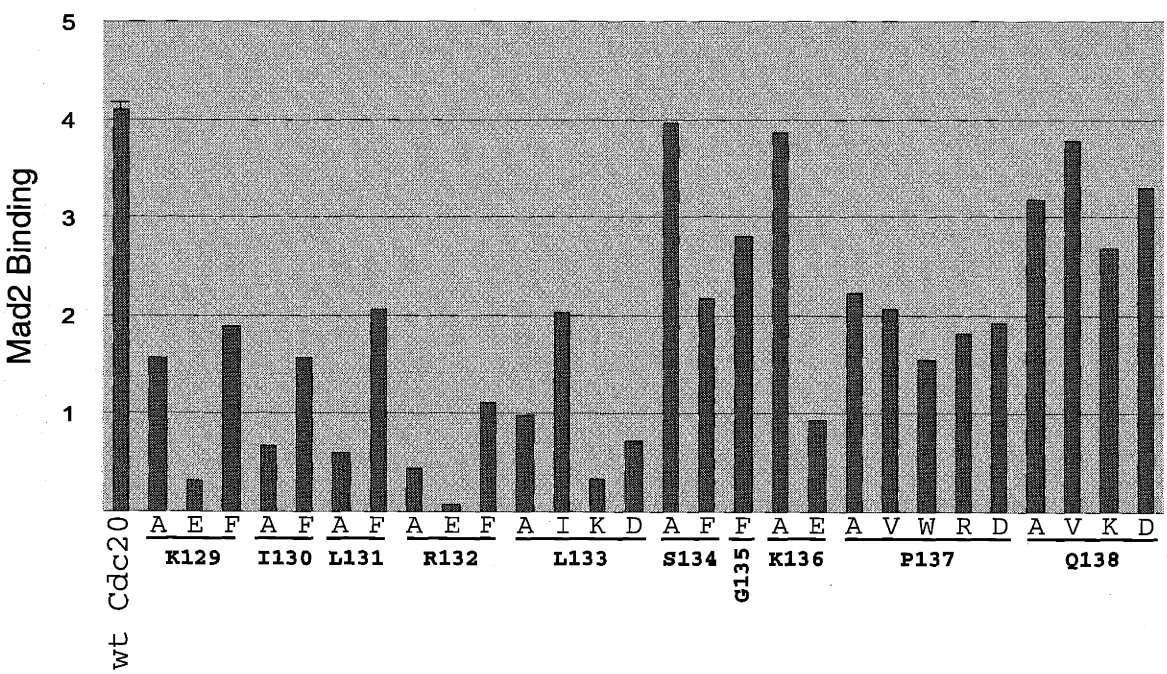

c.

EA**KILRL**SG**K**PQ

Figure 4-12. Peptide mapping the hMad2-binding regions of TACE and mERβ. (a-b) TACE peptides probed with *in vitro*-translated [^{35}S]-labeled Mad2. A hCdc20 peptide spanning residues 127-138 probed on the same membrane is shown for comparison. y-axis in (b) is labeled in arbitrary units. (c) TACE sequence scanned on peptide blot. Bold type indicates the strongest binding peptide. (d-f) Twelve-residue peptides scanning the Mad2-binding region of mERβ probed and analyzed as in (a-c).

a.

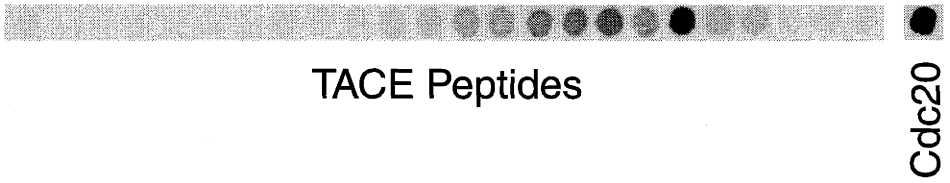
TACE Peptides
Cdc20

b.

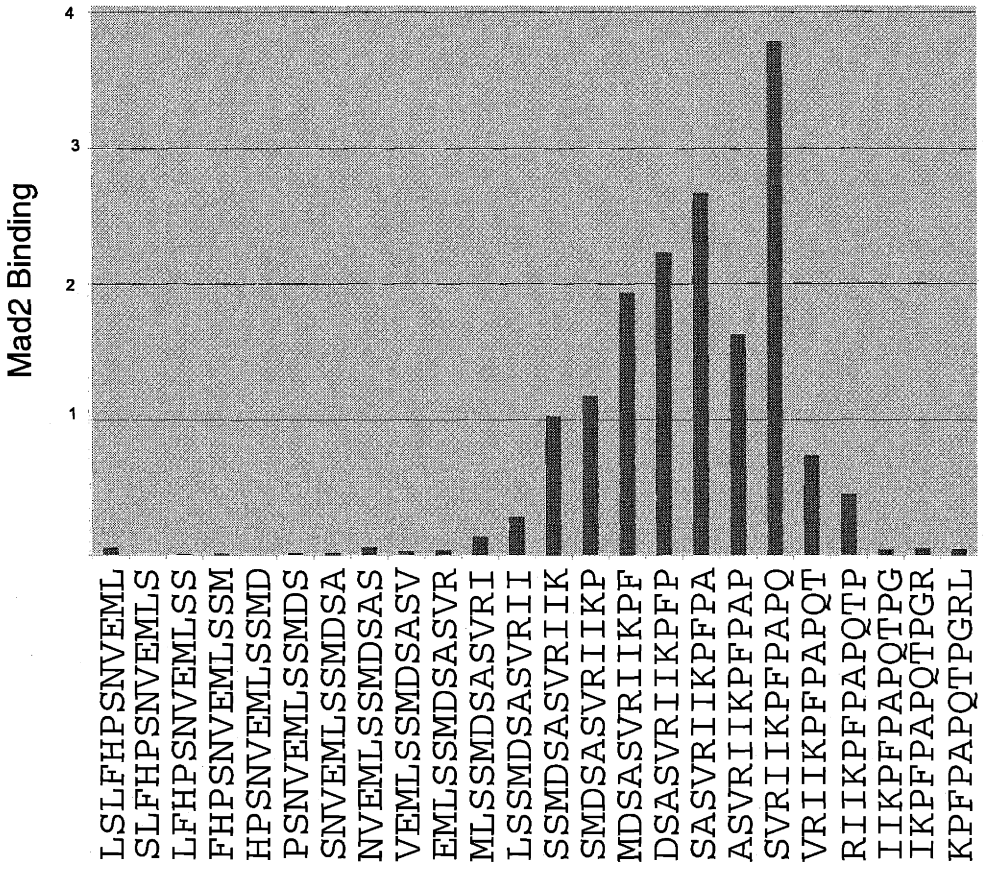
Mad2 Binding
4
3
2
1
LSLFHPSNVEML
SLFHPSNVEMLS
LFHPSNVEMLSS
FHPSNVEMLSSM
HPSNVEMLSSMD
PSNVEMLSSMDS
SNVEMLSSMDSA
NVEMLSSMDSAS
VEMLSSMDSASV
EMLSSMDSASVR
MLSSMDSASVRI
LSSMDSASVRII
SSMDSASVRIIK
SMDSASVRIIKP
MDSASVRIIKPF
DSASVRIIKPFP
SASVRIIKPFPA
ASVRIIKPFPAP
SVRIIKPFPAPQ
VRIIKPFPAPQT
RIIKPFPAPQTP
IIKPFPAPQTPG
IKPFPAPQTPGR
KPFPAPQTPGRL

c.


705
739
LSLFHPSNVEMLSSMDSA**SVRIIKPFPAPQ**TPGRL

d.

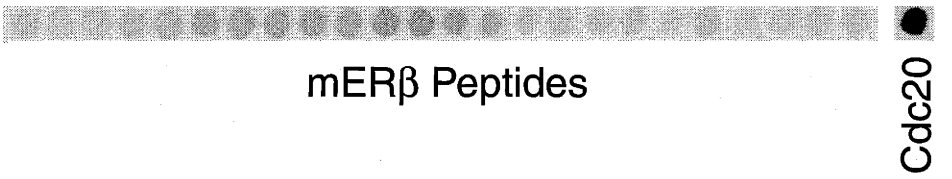
mERβ Peptides
Cdc20

e.

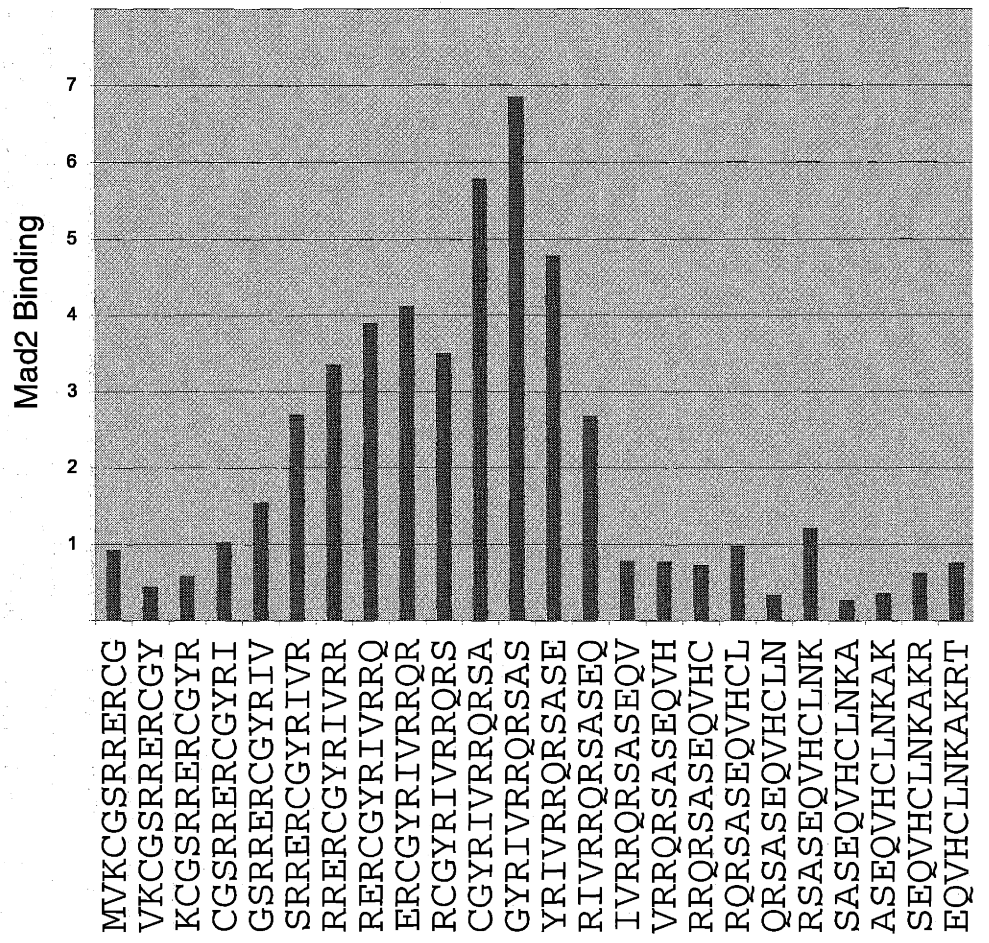
Mad2 Binding
1
2
3
4
5
6
7
MVKCGSRRERCG
VKCGSRRERCGY
KCGSRRERCGYR
CGSRRERCGYRI
GSRRERCGYRIV
SRRERCGYRIVR
RRERCGYRIVRR
RERCGYRIVRRQ
ERCGYRIVRRQR
RCGYRIVRRQRS
CGYRIVRRQRSA
GYRIVRRQRSAS
YRIVRRQRSASE
RIVRRQRSASEQ
IVRRQRSASEQV
VRRQRSASEQVH
RRQRSASEQVHC
RQRSASEQVHCL
QRSASEQVHCLN
RSASEQVHCLNK
SASEQVHCLNKA
ASEQVHCLNKAK
SEQVHCLNKAKR
EQVHCLNKAKRT

f.


169
203
MVKCGSRRERC**GYRIVRRQRSAS**EQVHCLNKAKRT

Figure 4-13. Alignment of Mad2-binding sequences. (a) Alignment of hMad1 and hCdc20 sequences spanning the hMad2-binding peptide of each along with mouse homologs. Dark boxes indicate identity and light boxes indicate similarity. (b) Alignment of conserved hMad1 and hCdc20 nine-residue Mad2-binding sequences with homologous sequences from *S. cerevisiae* and *S. pombe*. (c) Cross-species analysis of homology between predicted Mad2-binding sequences of Mad1 and Cdc20. Similarity was determined using the BLOSUM 62 matrix (Henikoff and Henikoff 1992). (d) Intra-species analysis of homology between predicted Mad2-binding sequences from Mad1 and Cdc20. (e) Alignment of binding sequences for all Mad2-binding proteins analyzed. For each mammalian protein the strongest binding peptide is shown. Only a portion of the 25-residue *S. cerevisiae* binding peptide is shown.

a.

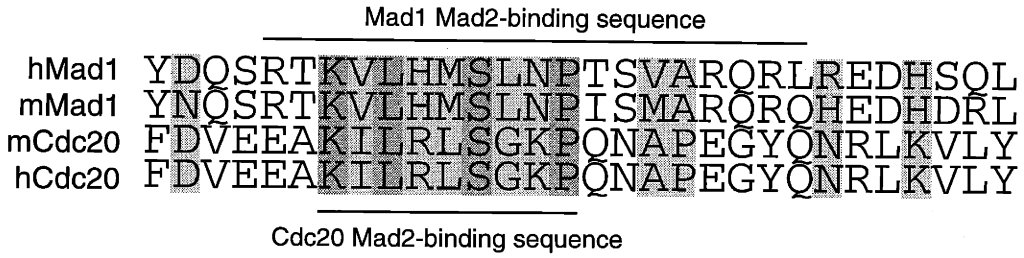

b.

c.

	Mad1 Similarity Score	Cdc20 Similarity Score
Human - S. cerevisiae	13	15
Human - S. pombe	18	2
S. cerevisiae - S. pombe	26	11
Average	19	9

d.

	Mad1-Cdc20 Similarity Score
Human	21
S. cerevisiae	20
S. pombe	9
Average	17

e.

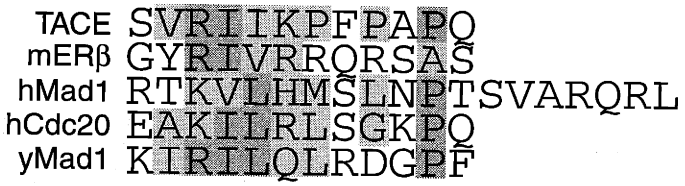

Figure 4-14. Mad1 peptide competition of Mad2 binding. Binding of *in vitro*-translated [^{35}S]–labeled hCdc20 (a) and M2BP3 (b) to hMad2-GST immobilized on glutathione beads as described in Figure 4-3. mMad1 peptide spans residues 534-558. Negative control (NC) peptide is a residue-scrambled version of the Mad1 peptide. Input lane represents 25% of translation product used in each reaction.

a.

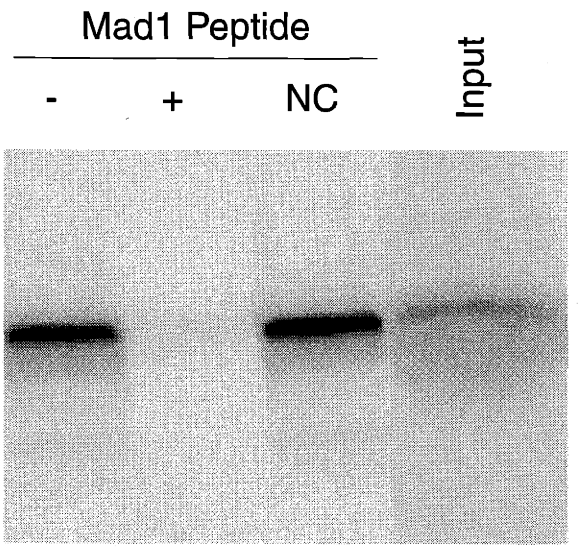

◀ hCdc20 (1-164)

b.

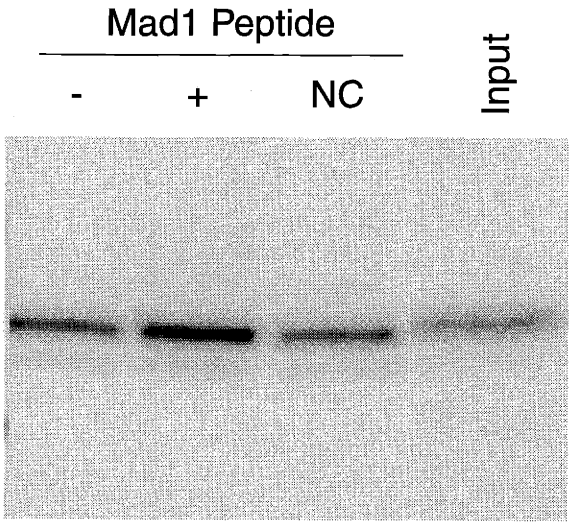

◀ M2BP3

Figure 4-15. Binding analysis of Mad2-interacting proteins with hMad2 mutated at carboxyl-terminal residues. (a) *In vitro* translated [^{35}S]–labeled Mad2 mutants assayed for binding to GST-fusion proteins immobilized on glutathione beads as in Figure 4-3. A standard Mad2 concentration was used in each binding reaction. M196R Mad2 has only one methionine, as compared to two in the wildtype protein. For each fusion protein, the wildtype Mad2 binding reaction was performed in triplicate. Bound fraction of wildtype Mad2 is equal to approximately 50% of the input. (b) Binding of each mutant expressed relative to wildtype Mad2 (wt Mad2) binding. Wildtype binding is expressed as the average of three binding reactions, and error bars represent one standard deviation. The representation of wildtype Mad2 binding to each protein has been normalized.

a.

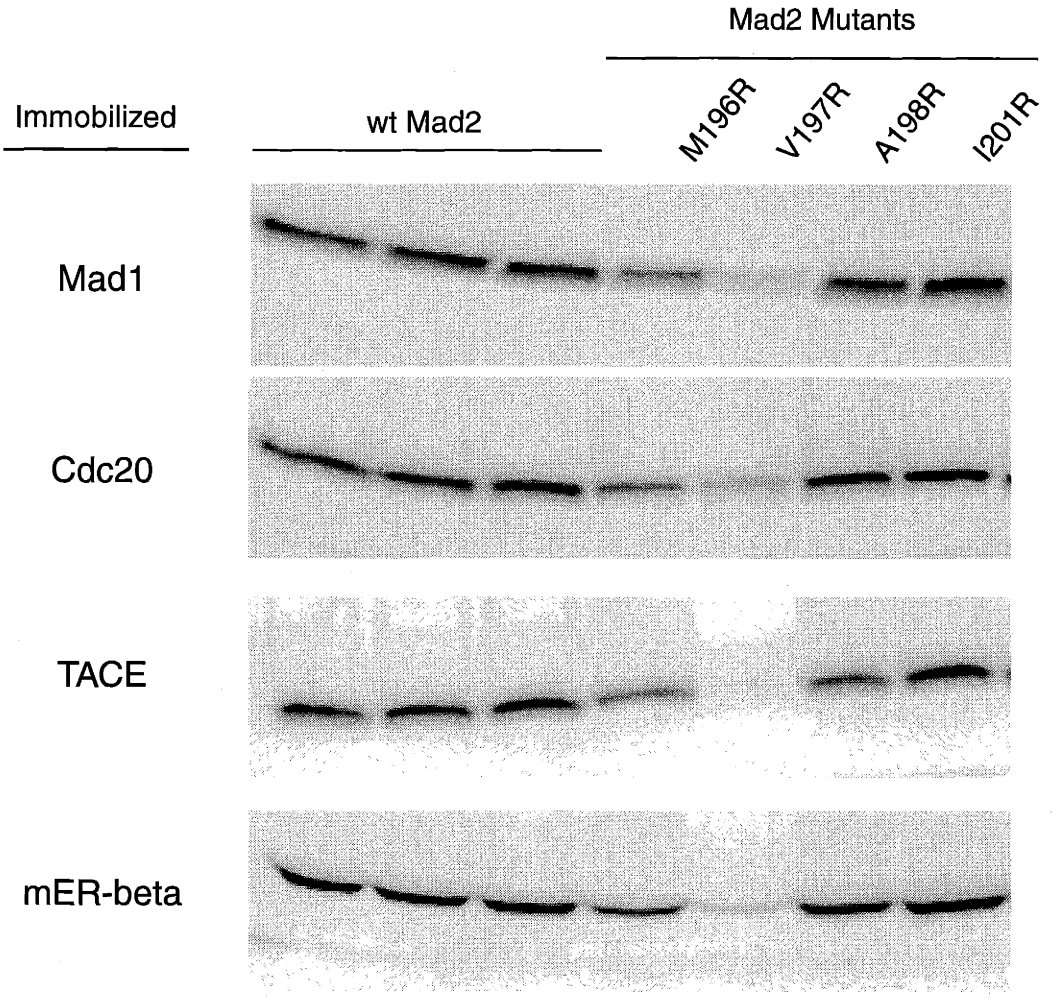
Mad2 Mutants
Immobilized
wt Mad2
M196R
V197R
A198R
I201R
Mad1
Cdc20
TACE
mER-beta

b.

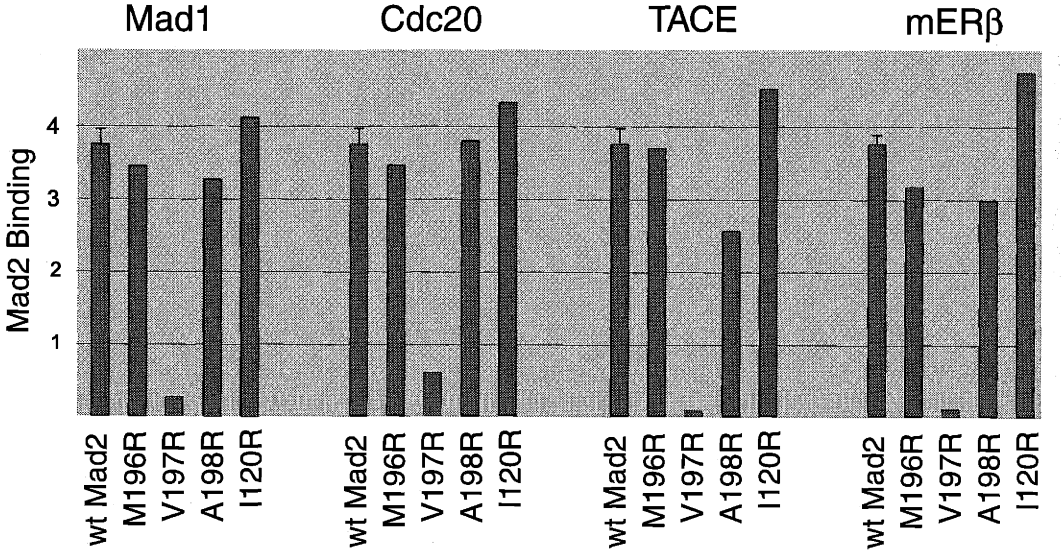
Mad1
Cdc20
TACE
mERβ
Mad2 Binding
4
3
2
1
wt Mad2
M196R
V197R
A198R
I120R

Figure 4-16. Binding analysis of Mad2-interacting proteins with hMad2 mutated at conserved residues. (a-b) *In vitro* translated [^{35}S]–labeled hMad2 mutant binding to Mad1 and Cdc20 (a) and TACE and mERβ (b) as in Figure 4-15. Wildtype binding is the average of three binding reactions, and error bars represent one standard deviation. All mutated residues localize to a surface near the carboxyl-terminal terminal tail (Figure 4-17). Light-colored bar indicates a residue not conserved between species. Asterisk (*) indicates a Mad2 mutant that differentially reduced Mad1 and Cdc20 binding. (c) Binding of Mad2 with mutations in residues distant from the carboxyl-terminal tail (Figure 4-17). Mutants were assayed as in Figure 4-15. Wildtype binding is the average of three binding reactions, and error bars represent one standard deviation.

a.

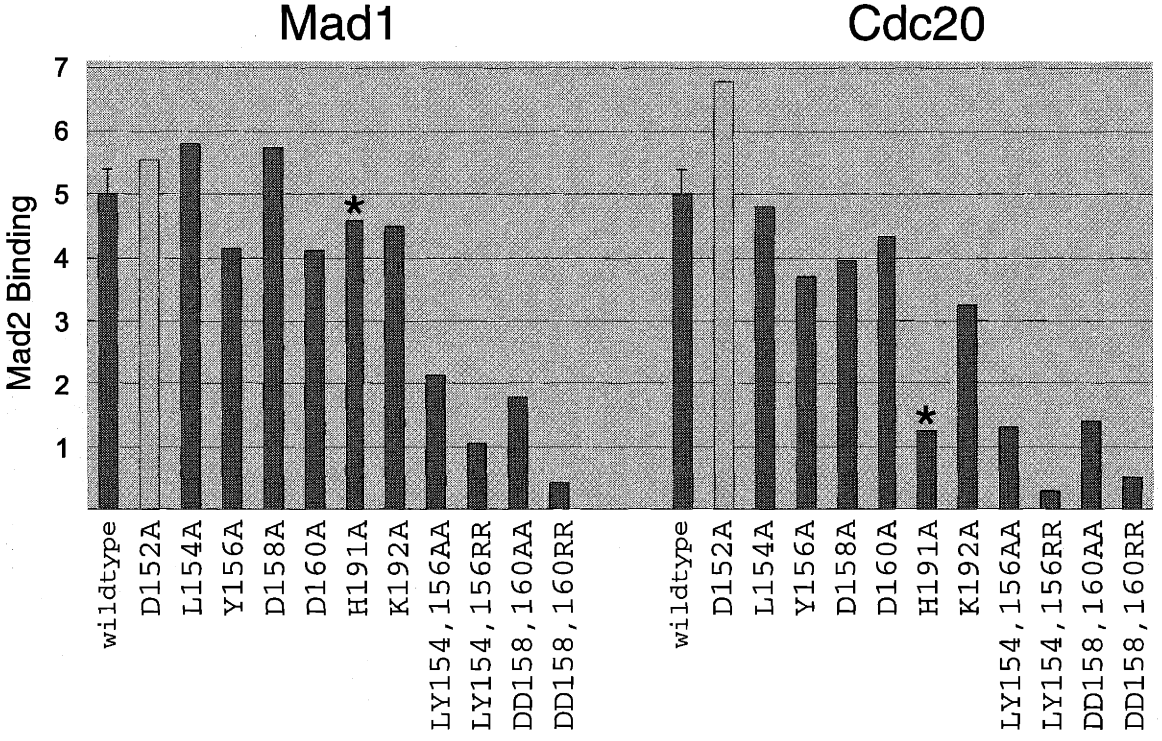
Mad1
Cdc20
Mad2 Binding
1
2
3
4
5
6
7
*
*
wildtype
D152A
L154A
Y156A
D158A
D160A
H191A
K192A
LY154,156AA
LY154,156RR
DD158,160AA
DD158,160RR

b.

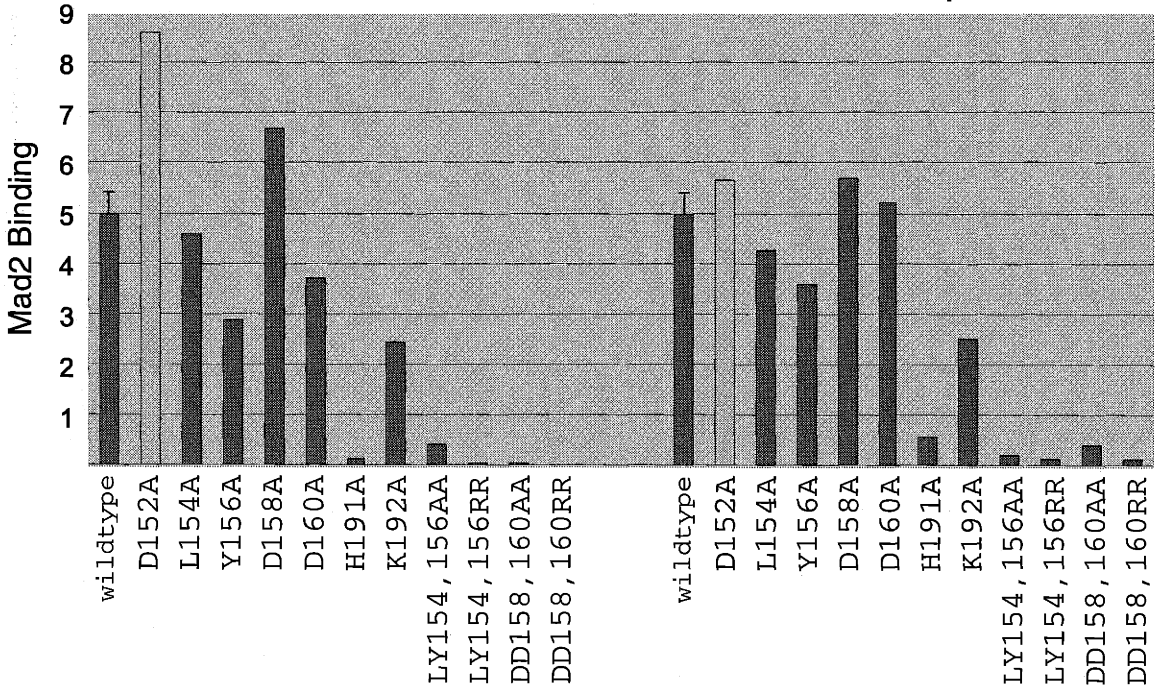
TACE
mERβ
Mad2 Binding
1
2
3
4
5
6
7
8
9
wildtype
D152A
L154A
Y156A
D158A
D160A
H191A
K192A
LY154,156AA
LY154,156RR
DD158,160AA
DD158,160RR

c.

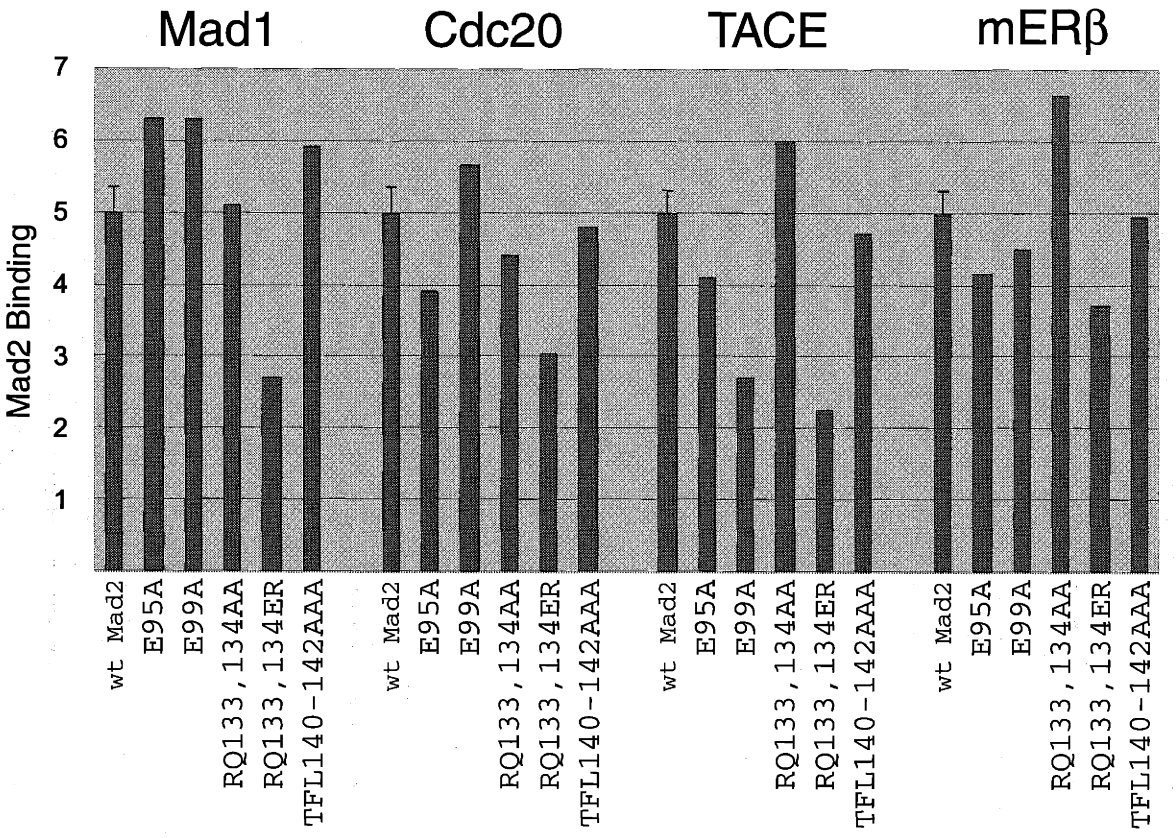
Mad1
Cdc20
TACE
mERβ
Mad2 Binding
7
6
5
4
3
2
1
wt Mad2
E95A
E99A
RQ133,134AA
RQ133,134ER
TFL140-142AAA
wt Mad2
E95A
E99A
RQ133,134AA
RQ133,134ER
TFL140-142AAA
wt Mad2
E95A
E99A
RQ133,134AA
RQ133,134ER
TFL140-142AAA
wt Mad2
E95A
E99A
RQ133,134AA
RQ133,134ER
TFL140-142AAA

Figure 4-17. Summary of hMad2 mutational analysis. Conserved surface residues are grouped in two faces (b) based on proximity to the carboxyl-terminus (arrow). Red indicates residues whose mutation (singly or in combination with other mutations) reduced hMad1 and hCdc20 binding greater than 2-fold. Green indicates residues whose mutation had a less than 2-fold affect on binding. Spacefill model (a) was generated with RasMol using the NMR structure data of Luo et al., 2000.

a.

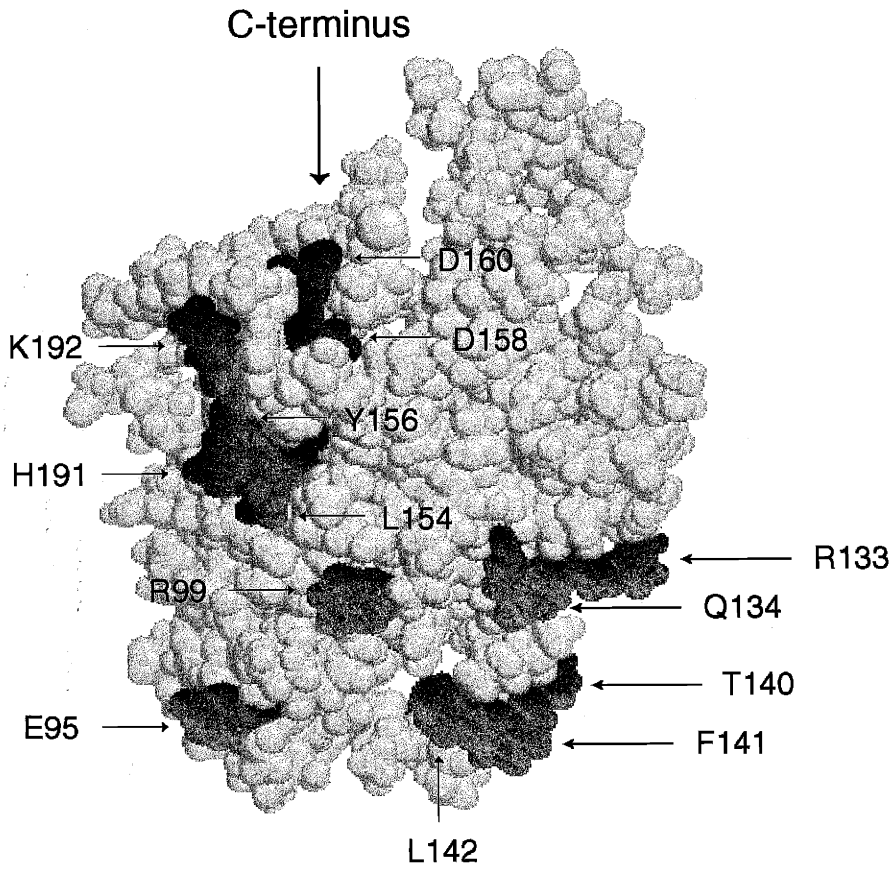

b.

Face1	Face2
L154	E95
Y156	R99
D158	R133
D160	Q134
H191	T140
K192	F141
	L142

Discussion

In this study we have cloned the mouse Mad1 gene and characterized the interaction of Mad2 with Mad1 and Cdc20. The Mad2-binding domains of hMad1 and hCdc20 have been defined to nine and nineteen residues, respectively. The binding of hMad1 and hCdc20 peptides to bacterially expressed hMad2 is the first demonstration of direct interaction of these proteins with Mad2. The hCdc20 peptide sequence we have identified spans four residues whose mutation in *S. cerevisiae* or *S. pombe* abrogates Mad2p-binding and checkpoint function (Hwang et al. 1998; Kim et al. 1998). Similarly, our Mad1 peptide is consistent with previous low resolution mapping of *S. cerevisiae* Mad1p and human Mad1 by 2-hybrid analysis and coimmunoprecipitation (Chen et al. 1999; Jin et al. 1998). However, *in vivo* analysis indicates additional Mad1p carboxyl-terminal sequence is also required for Mad2p interaction in *S. cerevisiae* (Chen et al. 1999). We do not understand why Mad2 binding requires additional sequence in Mad1 as compared to Cdc20. This is particularly surprising in view of the high degree of homology between mammalian Mad1 and Cdc20 across the entire nine residues of the Cdc20 peptide, although it is possible that the additional sequence is required for Mad1 secondary structure that enhances Mad2 interaction.

Mutational analysis of hMad2 demonstrates that both hMad1 and hCdc20 bind a common site of hMad2 that includes the carboxyl-terminal tail and an adjacent surface with 6 residues conserved in *S. cerevisiae*, *S. pombe*, *Xenopus*, and mammals (Luo et al. 2000). These results are consistent with previous demonstrations that truncation of this unstructured tail sequence abrogates binding to both hCdc20 and Mad1p. Mutation of residue H191 disrupts hCdc20 binding more severely than hMad1 binding, suggesting

that hMad1 and hCdc20 utilize differential interactions in binding to the same site of hMad2. A caveat to our results is that these mutations may exhibit reduced binding due to misfolding of hMad2. To rule out this possibility, we are currently expressing hMad2 mutants in *E. coli* for thermal melt analysis and to determine proteolytic stability. Additionally, we also plan to assay the binding of hMad2 mutants to M2BP3. As M2BP3-hMad2 binding is not competed by the Mad1 peptide, we believe M2BP3 binds to a different site of hMad2 and thus expect it will be relatively unaffected by mutations in and near the carboxyl-terminal tail. Finally, *in vivo* support for the relevance of this hMad2 binding surface is provided by demonstration that phosphorylation of Face1 residues negatively regulates hMad1 and hCdc20 binding and prevents checkpoint-mediated mitotic arrest in HeLa cells (per. comm., Katja Wassmann and Robert Benezra).

Although both Mad1 and Cdc20 bind Mad2, it is not known whether all three proteins form a ternary complex or whether Mad2 interacts with each protein separately. Our identification of a common Mad2 binding site for both proteins indicates that a single monomer of hMad2 cannot simultaneously bind both hMad1 and hCdc20. A ternary complex can form only if Mad2 is oligomerized. Both monomeric and oligomeric hMad2 are seen when expressed in *E. coli*, and only the oligomerized form inhibits APC-dependent ubiquination in *Xenopus* egg extracts and induces mitotic arrest when injected into two-cell *Xenopus* embryos (Fang et al. 1998). However, NMR analysis of hMad2 binding to a forty-residue fragment of hCdc20 reveals that these proteins interact only in a 1:1 complex, and that addition of hCdc20 to oligomeric hMad2 rapidly disrupts all hMad2 oligomers. The role of Mad2 oligomerization in the checkpoint signaling pathway thus remains unclear, but there is currently no evidence that Mad2 is oligomerized when

complexed with Cdc20. We thus favor a model in which monomeric or oligomeric Mad2 is first activated in a Mad1-dependent manner, and then monomeric Mad2 inhibits Cdc20-APC activity independently of Mad1 association.

In this study we have also examined the interaction of hMad2 with TACE and mERβ, two proteins with no known role in the spindle checkpoint. hMad2 binding to these proteins is disrupted by the same mutations that disrupt interaction with hMad1 and hCdc20, suggesting all bind a common site of Mad2. However, binding of TACE and mERβ is more sensitive to these mutations than hMad1 and hCdc20, suggesting hMad1 and hCdc20 may utilize additional residues for binding. This is consistent with the extended homology between hMad1 and hCdc20 as compared to that of all four proteins (nine residues vs. four residues). The role of Mad2 interaction with TACE and mERβ is unknown. One possibility is that Mad2 is involved in non-checkpoint functions. The binding of Mad2 to a proline rich sequence of TACE suggests Mad2 may negatively regulate binding of SH3 domain proteins (Nelson et al. 1999). Alternatively, TACE and ERβ may sequester Mad2 to reduce the effective concentration in the cell when it is not required. A final possibility is that these receptors are involved in the spindle checkpoint. Our finding that both TACE and mERβ bind the same site of hMad2 that binds hMad1 and hCdc20 is consistent with this hypothesis, although other interpretations are equally likely.

The *in vitro* mapping data presented here provide information for the design of mutations to disrupt spindle checkpoint protein interaction *in vivo*. We plan to make point mutations in Mad1 to specifically disrupt Mad1-Mad2 interaction without directly interfering with other protein interactions or affecting protein stability. This will allow

examination of the requirement for Mad1-Mad2 interaction in checkpoint function. Ultimately, the goal will be to move beyond mitotic arrest or chromosome loss assays, and instead to use these mutants for the investigation of molecular events in checkpoint signaling. For example, a GFP-tagged Mad2 could be examined in cells to determine whether it translocates along microtubules. Additionally, these mutations may have subtle checkpoint phenotypes that are nonetheless compatible with viability, allowing cell biology experiments that are currently very difficult in the embryonically-lethal knockout mice.

Materials and Methods

Yeast two-hybrid screen

Rat Mad2 was used to screen for interacting proteins in a mouse T-cell lymphoma two-hybrid library (Clonetech ML4001AD) with an estimated complexity of 1.5-2X10^6 clones. The Y190 yeast strain (MATa gal4 gal80 his3 trp1-901 ade2-101 ura3-52 leu2-3, -112 + URA3::GAL→lacZ, LYS2::GAL→HIS3 cyh^r) was cotransformed with the library and rat Mad2 bait plasmid (pMD130, see below). Library clones expressing Mad2-interacting proteins were selected by virtue of growth after 5 days on histidine-free media in the presence of 50mM 3-aminotriazole (SIGMA A8056). A filter lift assay (Breeden and Nasmyth 1985) to detect β-galactosidase expression was also used to confirm the interaction of Mad2 with each library clone.

To confirm specific interactions, clones were grown in the presence of cyclohexamide to lose the Mad2 plasmid, and then mated to four separate yeast strains expressing negative control bait genes in a pAS1 vector (p53, SNF1, lamin, and CDK2).

All clones not expressing β-galactosidase with negative control baits in the filter lift assay were assayed using a β-galactosidase liquid assay (Clontech PT3024-1) with Mad2 bait plasmid . Because we encountered difficulty with plasmid isolation from the library clones, we recovered interacting genes via PCR amplification from DNA preps, and used the PCR products for sequencing.

Plasmids

Mad2. A plasmid expressing rat Mad2 (dbEST ID 294792) fused to the GAL4-binding domain was generated by PCR subcloning into the NdeI-SalI sites of pASII (pMD130).

mMad2 for expression in bacteria was generated by first PCR subcloning a *Mad2* cDNA clone (pMD143, (Dobles et al. 2000)) into pBlueScriptII. This construct (pMD173) was sequenced to confirm no PCR mutations had been introduced, and a BamHI-SalI fragment including the entire Mad2 protein as well as a Kozak consensus sequence was cloned into pGEX-4T-2 to create a GST-fusion protein (pSL8-3).

hMad2 for expression in bacteria was generated by first PCR subcloning an EST clone (GenbankID R10991) into FASTBAC (GIBCO BRL) (pRH1), and then transferring the BamHI-SalI fragment into pGEX-4T-2 (pRH2). This BamHI-SalI fragment was also transferred into pGEX-6P-2 (pRH4), and this clone used for protein preparations in which Mad2 was cleaved from the GST protein.

S. cerevisiae MAD2 for expression in bacteria was generated by first PCR amplifying Mad2 from genomic DNA to add 5' NdeI and 3' SalI restriction sites, and subcloning into pMIT-3 (a variant of the pFASTBAC vector (GIBCO BRL)) to create

pMD133. A BamHI-SalI fragment of pMD133 was cloned into pGEX-4T-2 to create the GST-fusion plasmid pSL4.

Mad1. A full-length *hMad1* BamHI-EcoRI cDNA fragment in pGEX-5X-2 (pTXBP181) was obtained as a kind gift of Dong-Yan Jin and Kuan-Teh Jeang. Sequencing the translated region indicated identity to Genbank sequence U33822 with the following changes: D189E, V190L, E260K, an extra histidine between residues A267 and L268, R556→H557, and a conservative A→G third base change in codon A267. Residues L521-R571 were PCR amplified to add BamHI-SalI sites and subcloned into pGEX-5X-3 to create a GST-fusion protein (pMD239) that was then sequenced to confirm no PCR mutations had been introduced. The terminating codon of the fusion protein is provided by the pGEX vector sequence.

M2BP1 clone pSLO11 was generated by PCR subcloning the longest identified M2BP1 clone from the two-hybrid screen (A1) into the EcoRI-XhoI restriction sites of pACT2.2.

ScMAD1 genomic clone pKH130 was obtained as a kind gift of Kevin Hardwick and Andrew Murray (Hardwick and Murray 1995).

Cdc20. A full-length human *Cdc20* cDNA clone was obtained as a kind gift of Edgar Kramer and Jan-Michael Peters (Kramer et al. 1998). The amino-terminal 164 codons were PCR amplified to add BamHI-SalI restriction sites and then subcloned into pGEX-6P-2 to create a GST fusion protein (pMD229). Sequencing revealed a K163N mutation.

TACE. The Mad2-interacting cytotail of TNF α convertase fused to GST (pGST-TACE cytotail / pIP220) was obtained as a kind gift of Johannes Schlondorff and Carl Blobel (Nelson et al. 1999).

mERβ. The carboxyl-terminal Mad2-interacting domain of mERβ fused to GST (GST-mERβ 173-208 / pIP225) was obtained as a kind gift of Howard Surks and Michael Mendelsohn (Poelzl et al. 2000).

Protein Expression

All GST-fusion proteins were expressed in BL21(DE3) *E. coli.* Overnight cultures in Luria-Bertani broth (LB) with 0.1mg/ml Ampicillin were diluted 1:100 in LB with Ampicillin and grown at 37°C with shaking to an A_{600} of 2.0. Bacteria were then diluted 10-fold by centrifugation (4,600Xg, 10 min, 4°C) and resuspension of the entire pellet in fresh LB with Ampicillin, grown at room temperature for 3 hr with shaking, induced with 1-2mM IPTG and grown for another 5 hr at room temperature with shaking. (The bacteria expressing TACE fusion protein were simply induced and grown for 3 hr at 37°C immediately following the 10-fold dilution.) Bacteria were harvested by centrifugation (4,600Xg, 15 min, 4°C), and the pellets frozen to –20°C.

Frozen pellets were resuspended in 3X w/v Breakage Buffer (50mM Hepes [pH 8.0], 150mM NaCl, 2mM EDTA, 1mM DTT, 1mM PMSF, 10% glycerol), and the bacteria lysed by sonication. Lysates were recovered from a 12,000Xg centrifugation (15 min, 4°C) aliquoted, frozen in liquid nitrogen, and stored at –80°C.

In vitro Translations

DNA templates for *in vitro* translation were made by two rounds of PCR amplification to add a T7 promoter to the 5' end, and to improve translational yield at least 12 bases were added 3' to the STOP codon. The 5' added sequence includes 10 bases to improve translational yield, a T7 promoter (bold, see MOL246), a BamHI site (underlined), a Kozak consensus sequence (italicized), and an HA epitope (double underlined). Gene fragments were first amplified with a primer that added part of the HA epitope to the 5' end (CTTATgATgTTCCAgATTACgCN). (Note the final "N" is a "place holder", as all GCN codons encode Valine.) This product was then reamplified with MOL246.

MOL246: C ggA CTC AgA **TgT AAT ACg ACT CAC TAT Agg** ggA TCC *gCC ACC ATg* ggA TAC CCT TAT gAT gTT CCA gAT TAC gC

PCR products were electro-eluted from an agarose gel, extracted with phenol-chloroform, purified over a Sephadex G-50 (SIGMA G-50-300) spin column, EtOH-precipitated, and resuspend to approximately 100mg/ml in nuclease-free water. Coupled transcription/translation was carried out with 8µl DNA, 2µl 10mCi/ml L-[^{35}S]-Methionine (NEN Life Science Products NEG-009A), and 40µl rabbit reticulocyte lysate mix (PROMEGA L1170) at 30°C for 90 min.

For some experiments, the translation yield for each protein was quantitated by electropheresis followed by autoradiography, and a standard concentration of translated product used in each binding reaction. Undiluted rabbit reticulocyte lysate mix was used

to bring each sample to a constant volume. For experiments in which the concentrations of translation products were not normalized, a fraction of the translation product is shown for comparison.

Binding Assay

In vitro binding assays were performed with [^{35}S]-Methionine labeled *in vitro*-translated protein and GST-fusion protein immobilized on glutathione sepharose beads (Pharmacia 17-0756-01). Glutathione beads were first washed three times by repeated suspension in 1ml Breakage buffer (see above) followed by a short spin (<4sec) in an Eppendorf microfuge and removal of supernatant using an aspirator with a 26-gauge needle. Beads were incubated with fusion protein lysates (see above) in the presence of 1% Triton-X 100 at 4°C with gentle rocking for 60 min. (Breakage buffer was used if necessary to raise the volume to 200µl.) The beads were then pelleted, the supernatant removed, and the beads washed 3 times with 1ml IP buffer (50mM Hepes [pH 8.0], 150mM NaCl, 50mM β-glycerophosphate, 50mM NaF, 1mM EDTA, 10% glycerol, 1% Triton-X 100) buffer as described above.

200µl binding reactions in IP buffer with a final concentration of 1mM DTT were carried out at 4°C with 20µl of protein-bound beads and 5-15µl of *in vitro* translate in 1.7ml Low Binding Tubes (Marsh T6050G). After a 5hr incubation with rocking, the beads were pelleted and the supernatant removed as described above. The beads were then washed 3 times with 1ml IP buffer (without vortexing), using a "succulator". (A succulator is an aspirator attachment for removing supernatants from 32 eppendorf tubes

simultaneously. The 100µl sample remaining in each tube after use of the succulator was not removed except for after the final wash.)

The bead pellets were resuspended in 20µl 2X SDS-PAGE loading buffer, vortexed, boiled 1 min, vortexed again, pelleted, and the supernatant run on a 10% acrylamide SDS-PAGE gel. Gels were fixed in 20% MeOH/7% Acetic acid, dried, and exposed on a Phosphorimager (Molecular Dynamics). Signals from [^{35}S]-labeled *in vitro* translates were quantified using Moleculare Dynamics software.

Peptide Mapping

Cdc20, TACE and mERβ peptides were synthesized on a PEG 500-modified cellulose membrane (AbiMed AC01-12) via coupling to β-Alanine residues. A membrane spotted with Mad1 peptides was obtained through the Research Genetics service "Peptides on Paper".

Membranes were moistened 30 sec in MeOH, washed 3X5 min in TBS-T (25mM Tris [pH8.0], 137mM NaCl, 13.4mM KCl, 0.1% Tween-20), and blocked overnight at 4°C in TBS-T with 2% BSA. The next day membranes were briefly washed in TBS-T (1-3 min) and each probed with 50µl [^{35}S]-labeled *in vitro*-translated hMad2 (purified on a Sephadex G-25 spin column pre-washed with Breakage buffer (see above)) in 1.5-3ml TBS-T with 1% BSA for 60 min at room temperature without rocking. Membranes were quickly rinsed with TBS-T and then washed at room temperature for 5 min each in the following solutions: TBS-T, TBS-T with 0.5M NaCl, TBS-T with 0.5% Triton-X 100, and TBS-T. After thorough drying, membranes were exposed on a PhosphorImager, and binding assessed using Molecular Dynamics software to quantitate [^{35}S] signals.

Synthetic Peptides

hMad1 and hCdc20 nineteen-residue peptides were synthesized by Biosynthesis, Inc (Lewisville, Texas), HPLC purified, and aliquots pooled to yield a final purity of greater than 85%. The hMad1 twenty-five-residue peptide and hCdc20 fifteen-residue peptide were synthesized and HPLC purified (fractions pooled to yield approximately 75% purity) by the Center for Cancer Research BioPolymers Lab (MIT). All peptides were resuspended to 25mg/ml in DMSO (Aldrich 67-68-5) and stored at –70°C.

Gel Shift Assay

330pmol of bacterially expressed hMad2 was incubated with peptides in IP buffer (see above) in a total reaction volume of 10μ. After a 45 min incubation on ice, samples were diluted into 15μ loading buffer and immediately loaded onto a non-denaturing gel. Gels were run at room temperature, and then Coomassie stained and scanned.

Acknowledgments

I would like to thank Kim Simons for assistance in database analysis of Mad2-binding sequences. The contributions of Dirk Godshalk to this project are also appreciated.

References

Abrieu, A., Kahana, J. A., Wood, K. W., and Cleveland, D. W. (2000). "CENP-E as an essential component of the mitotic checkpoint in vitro." Cell, 102(6), 817-26.

Aravind, L., and Koonin, E. V. (1998). "The HORMA domain: a common structural denominator in mitotic checkpoints, chromosome synapsis and DNA repair." Trends Biochem Sci, 23(8), 284-6.

Basu, J., Bousbaa, H., Logarinho, E., Li, Z., Williams, B. C., Lopes, C., Sunkel, C. E., and Goldberg, M. L. (1999). "Mutations in the essential spindle checkpoint gene bub1 cause chromosome missegregation and fail to block apoptosis in Drosophila." J Cell Biol, 146(1), 13-28.

Berger, B., Wilson, D. B., Wolf, E., Tonchev, T., Milla, M., and Kim, P. S. (1995). "Predicting coiled coils by use of pairwise residue correlations." Proc Natl Acad Sci U S A, 92(18), 8259-63.

Brady, D. M., and Hardwick, K. G. (2000). "Complex formation between Mad1p, Bub1p and Bub3p is crucial for spindle checkpoint function." Curr Biol, 10(11), 675-8.

Breeden, L., and Nasmyth, K. (1985). "Regulation of the yeast HO gene." Cold Spring Harb Symp Quant Biol, 50(3), 643-50.

Chan, G. K., Jablonski, S. A., Sudakin, V., Hittle, J. C., and Yen, T. J. (1999). "Human BUBR1 is a mitotic checkpoint kinase that monitors CENP-E functions at kinetochores and binds the cyclosome/APC." J Cell Biol, 146(5), 941-54.

Chen, R. H., Brady, D. M., Smith, D., Murray, A. W., and Hardwick, K. G. (1999). "The spindle checkpoint of budding yeast depends on a tight complex between the Mad1 and Mad2 proteins." Mol Biol Cell, 10(8), 2607-18.

Chen, R. H., Shevchenko, A., Mann, M., and Murray, A. W. (1998). "Spindle checkpoint protein Xmad1 recruits Xmad2 to unattached kinetochores." J Cell Biol, 143(2), 283-95.

Cohen-Fix, O., Peters, J. M., Kirschner, M. W., and Koshland, D. (1996). "Anaphase initiation in Saccharomyces cerevisiae is controlled by the APC-dependent degradation of the anaphase inhibitor Pds1p." Genes Dev, 10(24), 3081-93.

Dobles, M., Liberal, V., Scott, M. L., Benezra, R., and Sorger, P. K. (2000). "Chromosome missegregation and apoptosis in mice lacking the mitotic checkpoint protein Mad2." Cell, 101, 635-645.

Fang, G., Yu, H., and Kirschner, M. W. (1998). "The checkpoint protein MAD2 and the mitotic regulator CDC20 form a ternary complex with the anaphase-promoting complex to control anaphase initiation." Genes Dev, 12(12), 1871-83.

Fuchs, D. A., and Johnson, R. K. (1978). "Cytologic evidence that taxol, an antineoplastic agent from Taxus brevifolia, acts as a mitotic spindle poison." Cancer Treat Rep, 62(8), 1219-22.

Hardwick, K. G., and Murray, A. W. (1995). "Mad1p, a phosphoprotein component of the spindle assembly checkpoint in budding yeast." J Cell Biol, 131(3), 709-20.

Hardwick, K. G., Weiss, E., Luca, F. C., Winey, M., and Murray, A. W. (1996). "Activation of the budding yeast spindle assembly checkpoint without mitotic spindle disruption." Science, 273(5277), 953-6.

Henikoff, S., and Henikoff, J. G. (1992). "Amino acid substitution matrices from protein blocks." Proc Natl Acad Sci U S A, 89(22), 10915-9.

Hoyt, M. A., Totis, L., and Roberts, B. T. (1991). "S. cerevisiae genes required for cell cycle arrest in response to loss of microtubule function." Cell, 66(3), 507-17.

Hwang, L. H., Lau, L. F., Smith, D. L., Mistrot, C. A., Hardwick, K. G., Hwang, E. S., Amon, A., and Murray, A. W. (1998). "Budding yeast Cdc20: a target of the spindle checkpoint." Science, 279(5353), 1041-4.

Jablonski, S. A., Chan, G. K., Cooke, C. A., Earnshaw, W. C., and Yen, T. J. (1998). "The hBUB1 and hBUBR1 kinases sequentially assemble onto kinetochores during prophase with hBUBR1 concentrating at the kinetochore plates in mitosis." Chromosoma, 107(6-7), 386-96.

Jacobs, C. W., Adams, A. E., Szaniszlo, P. J., and Pringle, J. R. (1988). "Functions of microtubules in the Saccharomyces cerevisiae cell cycle." J Cell Biol, 107(4), 1409-26.

Jin, D. Y., Spencer, F., and Jeang, K. T. (1998). "Human T cell leukemia virus type 1 oncoprotein Tax targets the human mitotic checkpoint protein MAD1." Cell, 93(1), 81-91.

Kalitsis, P., Earle, E., Fowler, K. J., and Choo, K. H. (2000). "Bub3 gene disruption in mice reveals essential mitotic spindle checkpoint function during early embryogenesis." Genes Dev, 14(18), 2277-82.

Kim, S. H., Lin, D. P., Matsumoto, S., Kitazono, A., and Matsumoto, T. (1998). "Fission yeast Slp1: an effector of the Mad2-dependent spindle checkpoint." Science, 279(5353), 1045-7.

Kitagawa, R., and Rose, A. M. (1999). "Components of the spindle-assembly checkpoint are essential in Caenorhabditis elegans." Nat Cell Biolog, 1(8), 514-521.

Kramer, E. R., Gieffers, C., Holzl, G., Hengstschlager, M., and Peters, J. M. (1998). "Activation of the human anaphase-promoting complex by proteins of the CDC20/Fizzy family." Curr Biol, 8(22), 1207-10.

Li, R., and Murray, A. W. (1991). "Feedback control of mitosis in budding yeast." Cell, 66(3), 519-31.

Li, Y., and Benezra, R. (1996). "Identification of a human mitotic checkpoint gene: hsMAD2." Science, 274(5285), 246-8.

Liu, Y. C., Pan, J., Zhang, C., Fan, W., Collinge, M., Bender, J. R., and Weissman, S. M. (1999). "A MHC-encoded ubiquitin-like protein (FAT10) binds noncovalently to the spindle assembly checkpoint protein MAD2." Proc Natl Acad Sci U S A, 96(8), 4313-8.

Luo, X., Fang, G., Coldiron, M., Lin, Y., Yu, H., Kirschner, M. W., and Wagner, G. (2000). "Structure of the Mad2 spindle assembly checkpoint protein and its interaction with Cdc20." Nat Struct Biol, 7(3), 224-9.

Martinez-Exposito, M. J., Kaplan, K. B., Copeland, J., and Sorger, P. K. (1999). "Retention of the BUB3 checkpoint protein on lagging chromosomes." Proc Natl Acad Sci U S A, 96(15), 8493-8.

Mitleman, F., Johansson, B., and Mertens, F. (1994). Catalog of Chromosome Aberrations in Cancer, Wiley-Liss, New York.

Nelson, K. K., Schlondorff, J., and Blobel, C. P. (1999). "Evidence for an interaction of the metalloprotease-disintegrin tumour necrosis factor alpha convertase (TACE) with mitotic arrest deficient 2 (MAD2), and of the metalloprotease-disintegrin MDC9 with a novel MAD2-related protein, MAD2beta." Biochem J, 343 Pt 3(44), 673-80.

O'Neill, T. J., Zhu, Y., and Gustafson, T. A. (1997). "Interaction of MAD2 with the carboxyl terminus of the insulin receptor but not with the IGFIR. Evidence for release from the insulin receptor after activation." J Biol Chem, 272(15), 10035-40.

Poelzl, G., Kasai, Y., Mochizuki, N., Shaul, P. W., Brown, M., and Mendelsohn, M. E. (2000). "Specific association of estrogen receptor beta with the cell cycle spindle assembly checkpoint protein, MAD2." Proc Natl Acad Sci U S A, 97(6), 2836-9.

Reid, B. J., Blount, P. L., Rubin, C. E., Levine, D. S., Haggitt, R. C., and Rabinovitch, P. S. (1992). "Flow-cytometric and histological progression to malignancy in Barrett's esophagus: prospective endoscopic surveillance of a cohort." Gastroenterology, 102(4 Pt 1), 1212-9.

Rieder, C. L., Cole, R. W., Khodjakov, A., and Sluder, G. (1995). "The checkpoint delaying anaphase in response to chromosome monoorientation is mediated by an inhibitory signal produced by unattached kinetochores." J Cell Biol, 130(4), 941-8.

Rieder, C. L., Schultz, A., Cole, R., and Sluder, G. (1994). "Anaphase onset in vertebrate somatic cells is controlled by a checkpoint that monitors sister kinetochore attachment to the spindle." J Cell Biol, 127(5), 1301-10.

Strunnikov, A. V., Kingsbury, J., and Koshland, D. (1995). "CEP3 encodes a centromere protein of Saccharomyces cerevisiae." J Cell Biol, 128(5), 749-60.

Taylor, S. S., and McKeon, F. (1997). "Kinetochore localization of murine Bub1 is required for normal mitotic timing and checkpoint response to spindle damage." Cell, 89(5), 727-35.

Visintin, R., Prinz, S., and Amon, A. (1997). "CDC20 and CDH1: a family of substrate-specific activators of APC- dependent proteolysis." Science, 278(5337), 460-3.

Wang, Y., and Burke, D. J. (1995). "Checkpoint genes required to delay cell division in response to nocodazole respond to impaired kinetochore function in the yeast Saccharomyces cerevisiae." Mol Cell Biol, 15(12), 6838-44.

Wassmann, K., and Benezra, R. (1998). "Mad2 transiently associates with an APC/p55Cdc complex during mitosis." Proc Natl Acad Sci U S A, 95(19), 11193-8.

Weiss, E., and Winey, M. (1996). "The Saccharomyces cerevisiae spindle pole body duplication gene MPS1 is part of a mitotic checkpoint." J Cell Biol, 132(1-2), 111-23.

Winey, M., Goetsch, L., Baum, P., and Byers, B. (1991). "MPS1 and MPS2: novel yeast genes defining distinct steps of spindle pole body duplication." J Cell Biol, 114(4), 745-54.

Chapter 5: Conclusions and future directions

When I initiated this project, very little was known about how mammalian cells link the initiation of anaphase to microtubule-kinetochore attachment. Our molecular understanding of the spindle assembly checkpoint was limited to recognition that the *S. cerevisiae MAD* and *BUB* genes were required for mitotic arrest in response to spindle damage (Hoyt et al. 1991; Li and Murray 1991). No metazoan genes involved in the process, or even homologous to the *MAD* and *BUB* genes, had been identified. However, the mammalian spindle assembly checkpoint was viewed as a promising area of research, as errors in chromosome segregation had long been hypothesized to play a role in tumorigenesis (Hartwell and Kastan 1994; Nowell 1976). In the past five years, mammalian homologs of all the known *S. cerevisiae* spindle checkpoint genes have been identified, and considerable progress has been made in describing a broad outline of a conserved eukaryotic checkpoint pathway. My research has contributed to understanding the role of the spindle checkpoint in metazoans, how checkpoint proteins interact to signal the status of spindle assembly, and has also provided the first causal link between mutations in this pathway and tumorigenesis. This chapter presents the results of my research in context of the entire field of spindle checkpoint research, and follows with suggestions for approaches and directions for future investigation of the mammalian spindle checkpoint.

Conclusions

Genetic Analysis of the Spindle Checkpoint in Metazoans

Mad2 was the first metazoan gene identified having homology to an *S. cerevisiae MAD* or *BUB* gene. Experiments in *Xenopus* egg extracts and HeLa cells showing that

anti-Mad2 antibodies blocked mitotic arrest in response to nocodazole demonstrated a Mad2 role in spindle checkpoint function (Chen et al. 1996; Li and Benezra 1996). My use of homologous recombination to generate *Mad2*-null mouse embryos was the first genetic disruption of *Mad2* in metazoans, and the first genetic disruption of any spindle checkpoint protein in mammalian cells. Failure of *Mad2*-null embryonic cells to arrest in response to nocodazole-induced spindle damage confirms the spindle checkpoint function of Mad2 in mammals. Additional genetic disruptions of checkpoint proteins in mice, *Drosophila*, and *C. elegans* support the model that the spindle checkpoint pathway is largely conserved across all eukaryotes (Basu et al. 1999; Kalitsis et al. 2000; Kitagawa and Rose 1999).

Spindle Checkpoint Requirement for Normal Mitosis in Metazoans

Despite confirmation of metazoan Mad and Bub protein function in the spindle checkpoint, the results described above do not address whether the spindle checkpoint falls within the classical definition of checkpoints as a monitoring system invoked only in the rare event of a problem, or whether it operates in every mitosis to regulate the timing of anaphase initiation. Localization of checkpoint proteins to kinetochores during prophase of every cell cycle is consistent with the idea that the checkpoint regulates anaphase initiation in normal mitoses (Chen et al. 1996; Jin et al. 1998; Li and Benezra 1996; Martinez-Exposito et al. 1999; Taylor and McKeon 1997). However, previous analysis in yeast had provided ambiguous results. Although *mad2* mutation in *S. cerevisiae* caused a 10-fold increase in chromosome loss, the loss rate was still only about 1 chromosome per 10^4 cell divisions (Li and Murray 1991). In contrast, genetic

disruption of *BUB1* in *S. pombe* resulted in missegregation in approximately half of all mitoses, suggesting checkpoint involvement in ensuring proper segregation even in the absence of exogenously induced spindle damage (Bernard et al. 1998).

Disruption of the spindle checkpoint in mammalian cells via anti-Mad2 antibody injection or expression of a dominant negative Bub1 fragment shortens the length of mitosis (Gorbsky et al. 1998; Taylor and McKeon 1997). Although these experiments suggest that the checkpoint functions during normal mitoses to prevent premature segregation, they suffer from the caveat that the exogenous proteins may disrupt function of other proteins involved in mitotic timing. We have shown a high rate of chromosome missegregation in *Mad2*-null embryos, providing clear evidence that Mad2 is required for accurate chromosome segregation during normal mitosis. This finding is consistent with the chromosome missegregation caused by mutation of *Drosophila bub1*, *C. elegans mdf-1* (*mad1*), and mouse *Bub3* (Basu et al. 1999; Kalitsis et al. 2000; Kitagawa and Rose 1999). Support for the model that the missegregation is the result of premature anaphase initiation is provided by an experiment showing that delaying anaphase initiation with an *apc4* mutation in *C. elegans* rescues the viability of *mdf-1* mutant embryos (Furuta et al. 2000). Providing a definitive resolution to this issue in mammalian cells will require developing reagents for following chromosome dynamics in individual cells.

The differential requirement between metazoans and *S. cerevisiae* for Mad and Bub genes in viability and segregation fidelity suggests a fundamental difference in how the checkpoint operates. However, it appears that in both cases the checkpoint functions during every mitosis to prevent premature anaphase initiation, and that the different responses to checkpoint gene mutation may reflect differences in the timing of spindle

assembly. In cultured PtK_1 cells, anti-Mad2 antibody injection results in anaphase initiation approximately fifteen minutes after nuclear envelope breakdown (NEB) (Gorbsky et al. 1998). Because spindle assembly initiates at NEB, and requires an average of about thirty minutes in these cells, the antibody injection causes a high rate of missegregation (Gorbsky et al. 1998; Rieder et al. 1994). In *S. cerevisiae*, *mad2* mutation results in anaphase initiation ten minutes earlier than in wildtype cells (Shonn et al. 2000). However, there usually remains sufficient time to complete spindle assembly, probably because assembly begins during S-phase in *S. cerevisiae*. In *S. pombe,* the timing of spindle assembly is more similar to that of metazoans than *S. cerevisiae*. Although it has not been determined whether *bub1* mutation results in shortened mitosis in *S. pombe*, the missegregation observed in these cells is consistent with the model that the spindle checkpoint functions to prevent premature anaphase in both metazoans and fungi (Bernard et al. 1998). Under normal conditions this function is usually not required for accurate segregation in *S. cerevisiae*, whereas the relative timing of spindle assembly and anaphase initiation makes the checkpoint essential for high segregation fidelity in metazoans and *S. pombe*.

Lethality of Spindle Checkpoint Mutation in Metazoans

In contrast to findings in both *S. cerevisiae* and *S. pombe*, all genetic disruptions of spindle checkpoint genes are lethal in metazoans (Basu et al. 1999; Dobles et al. 2000; Kalitsis et al. 2000; Kitagawa and Rose 1999). Our observation that murine non-mitotic *Mad2*-null trophoblast giant cells survive and continue to cycle after the mitotic embryonic cells have died strongly suggests that the lethality is due to a mitotic defect.

Viability of *apc4-mdf-1* compound mutant *C. elegans* embryos supports the model that the lethality of checkpoint mutants is a consequence of premature anaphase that results in chromosome missegregation (Furuta et al. 2000). It will be very interesting to determine whether the checkpoint is required for viability in non-embryonic cells. Normal development is highly sensitive to aneuploidy (see Chapter 1), and thus it is possible embryos are unusual in their checkpoint requirement for viability. Viability of $Mad2^{+/-}$ human cells that exhibit a comparatively low rate of chromosome missegregation suggests non-embryonic cells have the potential to survive some checkpoint defects that result in missegregation (Michel et al. 2001).

Embryonic lethality in both *Mad2*-null embryos and *bub1*-mutant *Drosophila* is associated with widespread apoptosis (Basu et al. 1999; Dobles et al. 2000). Although it has not yet been possible to address whether apoptosis occurs in the same cells that missegregate chromosomes, this would be consistent with the apoptosis of cultured mammalian cells treated with anti-microtubule drugs (Jordan et al. 1996; Woods et al. 1995). However, this does not rule out the possibility that some apoptotic pathways may be checkpoint-dependent. For example, there may be one pathway in response to prolonged delay of spindle assembly, and a second pathway activated in response to aneuploidy. Also, it is possible that the apoptosis observed in these studies is activated by components of the spindle checkpoint pathway not disrupted by mutation of *Bub1* or *Mad2*.

The apoptosis in *Drosophila* and murine checkpoint gene mutants clearly contradicts a model suggested by analysis of HeLa cells expressing a dominant negative fragment of Bub1. A significant reduction of nocodazole-induced apoptosis in these cells,

as compared to nocodazole-treated normal HeLa cells, suggests that checkpoint function is required for missegregation-induced apoptosis (Taylor and McKeon 1997). One explanation for the discrepancy between these results and those from the *Drosophila* and murine mutants is that it reflects differences between embryonic cells and non-embryonic cells. Another possibility is that the interpretation of the HeLa cell experiment is complicated by genetic modifications in this transformed cell line. Reduced apoptosis in response to missegregation may in fact be the very explanation as to how HeLa cells became aneuploid and transformed. This possibility underscores the dangers of using established cell lines in studies of checkpoints and apoptosis. Suggested below are approaches for creating reagents that more accurately reflect checkpoint function in normal cells.

Spindle Checkpoint Genes as Tumor Suppressors

The finding of lung tumors in *Mad2* heterozygous mice provides the first evidence for a causal connection between spindle checkpoint gene mutation and cancer. We have not yet characterized the tumor cells, but we expect they will exhibit checkpoint defects and aneuploidy. The checkpoint defects and increased missegregation in $Mad2^{+/-}$ mouse embryonic fibroblasts are consistent with the hypothesis that aneuploidy develops in lung cells even before the initiation of tumorigenesis. Validation of this hypothesis would confirm the widely cited view that increased chromosome missegregation may play a causative role in cancer (Hartwell and Kastan 1994; Nowell 1976). Still, sequencing of spindle checkpoint genes in human tumors has identified few mutations, and thus the explanation for the aneuploidy common in human cancers remains unknown.

One possibility is that we simply lack sufficient knowledge of the checkpoint signaling pathway to identify the tumor suppressors. Recent work in our lab has identified a connection between the spindle checkpoint and the Adenomatous Polyposis Coli (APC) protein that is commonly mutated in human colon cancer. APC forms a complex with Bub1 and Bub3 in mitotic HeLa cells, and truncation of the APC gene increases chromosome missegregation in mouse embryonic stem cells (Kaplan et al. 2001). As we learn more about the spindle checkpoint and the regulation of chromosome segregation we should arrive at a better explanation for the causes of aneuploidy in human cancers.

Future Directions

While the phenomenon of mitotic arrest in response to problems with spindle assembly has been known for nearly fifty years, identification of spindle checkpoint genes began only in the last decade (Hoyt et al. 1991; Li and Murray 1991; Weiss and Winey 1996). Identification of these genes has allowed genetic experiments revealing the consequence of checkpoint loss of function, and some insight into how the checkpoint pathway operates. Although informative and occasionally surprising, these analyses so far have largely only confirmed our expectations of checkpoint function. A complete molecular description of how cells links anaphase to spindle assembly remains distant. We have a preliminary understanding of the event monitored by the checkpoint (microtubule-kinetochore attachment) and the output of checkpoint signaling (Cdc20-APC inhibition), but the details of these events remain unclear. Despite knowledge of some of the protein interactions and phosphorylation events during checkpoint signaling, how the complete signaling pathway connects the input and output events is unknown.

While additional knockouts of the checkpoint genes and examination of interactions between known checkpoint proteins will no doubt prove informative, significant progress in describing the molecular events of spindle checkpoint signaling in mammalian cells will require some fundamentally different approaches.

Understanding checkpoint signaling will ultimately require knowledge of how the proteins interact *in vivo*. Although several interactions have been identified, we know very little about their physiological relevance, what protein complexes form in cells, and how these complexes are modified under different conditions. Recent identification of Bub1p-Bub3p-Mad1p association in nocodazole-treated *S. cerevisiae* cells provided the first evidence for checkpoint-dependent complex formation (Brady and Hardwick 2000). Furthermore, all the *S. cerevisiae* Mad proteins interact with Cdc20p in two-hybrid assays (Hwang et al. 1998), and Mad1-Mad2 and Bub1-Bub3 complexes have been identified in both *S. cerevisiae* and metazoans (Chen et al. 1999; Chen et al. 1998; Jin et al. 1998; Roberts et al. 1994; Taylor et al. 1998). It will be informative to purify these complexes from cells, identify all the proteins, and determine how the components, stoichiometry, and modification of the complexes vary throughout the cell cycle and when cells are exposed to microtubule drugs. This approach should both reveal physiologically relevant protein-protein interactions and also be useful in identifying novel checkpoint genes.

Despite the utility of this biochemical approach, the spindle checkpoint is a complex phenomenon that cannot be understood merely in terms of a linear pathway of protein-protein interactions and enzymatic reactions. The spindle checkpoint signaling pathway utilizes structural features of the cell, such as kinetochores for protein recruitment and microtubules for kinetochore-to-spindle translocation (Chen et al. 1996;

Howell et al. 2000; Li and Benezra 1996). Thus, obtaining a full understanding of checkpoint function will also require analysis of live cells. Analysis of live cells will both directly contribute to the elucidation of checkpoint function, and provide the means to test the physiological relevance of findings discovered via biochemical approaches. However, significant progress will dependent on technical advances to move the field beyond simple observation and studies in which anti-microtubule drugs are used to cause massive spindle damage. Among the advances required are physiologically relevant means of activating the checkpoint, sophisticated assays to monitor the status of checkpoint activation, and more subtle mechanisms for checkpoint disruption.

The only method currently available for checkpoint activation in mammalian cells is treatment with drugs that disrupt microtubule dynamics. These compounds create an unnatural context for checkpoint signaling by potentially interfering with activities such as microtubule-dependent transport of Mad2 from kinetochores to spindle poles. Furthermore, the wholesale disruption of microtubules they cause is not even a feature of endogenous spindle assembly problems. In fact, most naturally occurring checkpoint-induced mitotic arrests are probably not caused by any defect at all (as opposed to the arrest induced by DNA damage), but rather are a response to the natural variation in time required for the stochastic process of spindle assembly. Thus, the key to inducing physiologically relevant checkpoint activation lies in delaying spindle assembly with minimum disruption to the cell.

In *S. cerevisiae*, non-drug induced checkpoint activation has been achieved by mutation of kinetochore proteins and centromeric DNA, and by overloading the spindle with a high number of minichromosomes (Spencer and Hieter 1992; Wang and Burke

1995; Wells and Murray 1996). As more is learned about microtubule-kinetochore attachment in mammalian cells, it may be possible to design kinetochore mutations that lower the efficiency of microtubule attachment and thus slow spindle assembly. Most useful would be to put a mutated kinetochore gene under a promoter that allows for regulated expression. Also, compounds that directly block microtubule-kinetochore binding could be used to similar effect. However, the necessity that these mutations or chemical inhibitors not interfere with checkpoint protein function at kinetochores clearly presents a challenge. An alternative approach is suggested by experiments showing *S. cerevisiae MPS1* overexpression induces Mad1p phosphorylation and mitotic arrest (Hardwick et al. 1996). It may be possible to similarly activate the checkpoint in mammalian cells by overexpression of the *MPS1* homolog *Esk/TTK*. Although upstream proteins would be ignored, this approach could be extremely useful both for live cell analysis and in biochemical studies to follow changes in downstream proteins upon checkpoint activation.

Fully understanding the consequences of checkpoint activation in mammalian cells will require more sophisticated assays than currently available. *In vivo* analysis of checkpoint activity or malfunction generally involves use of fixed or dead cells, such as in the examination of protein localization to kinetochores, chromosome missegregation, and apoptosis. However, spindle assembly and chromosome segregation are dynamic processes, and thus require examination over time in live cells. This is currently feasible only in cells with intractable genetics, such as PtK_1 cells, or on a population level, as in the use of FACS analysis to follow changes in ploidy. Tagging chromosomes with a visible marker would provide a way to visualize chromosome dynamics and thus to

follow the timing of spindle assembly and anaphase initiation. The use of GFP-tagged chromosomes in *S. cerevisiae* has yielded surprising insights into chromosome dynamics and lead to rapid progress in revealing the roles of kinetochore proteins and understanding the consequences of their mutation (Goshima and Yanagida 2000; He et al. 2000; Straight et al. 1997). It is expected that transgenic mice with GFP-tagged chromosomes now in development in our lab will be similarly valuable for following the timing of mitosis in checkpoint-activated cells and understanding the consequences of checkpoint gene mutations.

Significant progress in mammalian spindle checkpoint research will also require more sophisticated and subtle methods for disrupting the spindle checkpoint. The knockouts of murine *Mad2* and *Bub3* have proven useful for studying the consequences of complete loss of function, but not as reagents for dissecting the pathway. One problem with these knockouts is that they result in such early embryonic lethality that they provide few cells for analysis. Because cells outside the context of an embryo may survive loss of checkpoint function, use of Cre-lox technology to delay gene disruption until after development or harvest of cells from mice may provide one solution to the problem (Kuhn et al. 1995). Alternatively, use of cell-permeable dominant negative peptides or chemical inhibitors offer the opportunity to induce rapid disruption of the pathway in culture. Cell based assays are now in progress to screen for such inhibitors (per. comm., Randall King) and may yield extremely powerful reagents for dissecting the checkpoint pathway.

The second problem with the current murine checkpoint mutants is that both involve the loss of a complete protein. The spindle checkpoint pathway involves

assembly of multi-protein complexes, and the loss of one component may directly disrupt the functions and interactions of several other proteins (Brady and Hardwick 2000; Chen et al. 1999; Roberts et al. 1994). This makes epistatic data difficult to interpret and thus, even if viable, checkpoint gene mutations that cause the loss of a whole protein are probably of limited value for the analysis of checkpoint signaling. Use of dominant negative peptides or chemical inhibitors described above may interfere with a particular function or interaction without causing complete disruption of whole complexes. Also, as more is learned from the biochemical analysis of checkpoint protein interactions, mutations can be introduced into kinase active sites, phosphorylation sites, and protein-binding sites. Use of mutations and inhibitors in conjunction with live cell assays should be useful both for dissecting the spindle checkpoint pathway and examining the cellular consequences of less severe checkpoint damage than that caused by complete gene knockouts.

Summary

The work presented in this thesis describes a significant contribution to the mammalian spindle checkpoint field. The *Mad2* knockout mouse represents the first genetic disruption of a spindle checkpoint gene in mammals. Analysis of this mouse has established a requirement for *Mad2* function in mammalian development and accurate chromosome segregation. Additionally, the increased incidence of lung tumors in the $Mad2^{+/-}$ mice demonstrates the first causal link between spindle checkpoint gene mutation and cancer. Despite the value of these results, this work also reveals the limitations of this approach. Recognition that *Mad2* is required for viability suggests that

it will not be possible to make significant progress in understanding the checkpoint pathway by analysis of conventional knockout mice. Furthermore, the limited tumor spectrum of *Mad2*$^{+/-}$ mice is consistent with the finding of few mutations in known checkpoint genes in human tumors. I believe the next phase of spindle checkpoint research in mammals should focus on approaches for identifying additional factors involved, and investigating the complexities of checkpoint signaling *in vivo*. The biochemical study of Mad2 protein interactions presented here describes an initial step towards a high resolution dissection of checkpoint signaling. As we obtain a fuller molecular description of checkpoint function we should arrive at a better understanding of the role of missegregation in human disease and syndromes, and eventually learn to exploit this understanding for treatments.

References

Basu, J., Bousbaa, H., Logarinho, E., Li, Z., Williams, B. C., Lopes, C., Sunkel, C. E., and Goldberg, M. L. (1999). "Mutations in the essential spindle checkpoint gene bub1 cause chromosome missegregation and fail to block apoptosis in Drosophila." J Cell Biol, 146(1), 13-28.

Bernard, P., Hardwick, K., and Javerzat, J. P. (1998). "Fission yeast bub1 is a mitotic centromere protein essential for the spindle checkpoint and the preservation of correct ploidy through mitosis." J Cell Biol, 143(7), 1775-87.

Brady, D. M., and Hardwick, K. G. (2000). "Complex formation between Mad1p, Bub1p and Bub3p is crucial for spindle checkpoint function." Curr Biol, 10(11), 675-8.

Chen, R. H., Brady, D. M., Smith, D., Murray, A. W., and Hardwick, K. G. (1999). "The spindle checkpoint of budding yeast depends on a tight complex between the Mad1 and Mad2 proteins." Mol Biol Cell, 10(8), 2607-18.

Chen, R. H., Shevchenko, A., Mann, M., and Murray, A. W. (1998). "Spindle checkpoint protein Xmad1 recruits Xmad2 to unattached kinetochores." J Cell Biol, 143(2), 283-95.

Chen, R. H., Waters, J. C., Salmon, E. D., and Murray, A. W. (1996). "Association of spindle assembly checkpoint component XMAD2 with unattached kinetochores." Science, 274(5285), 242-6.

Dobles, M., Liberal, V., Scott, M. L., Benezra, R., and Sorger, P. K. (2000). "Chromosome missegregation and apoptosis in mice lacking the mitotic checkpoint protein Mad2." Cell, 101, 635-645.

Furuta, T., Tuck, S., Kirchner, J., Koch, B., Auty, R., Kitagawa, R., Rose, A. M., and Greenstein, D. (2000). "EMB-30: an APC4 homologue required for metaphase-to-anaphase transitions during meiosis and mitosis in Caenorhabditis elegans." Mol Biol Cell, 11(4), 1401-19.

Gorbsky, G. J., Chen, R. H., and Murray, A. W. (1998). "Microinjection of antibody to Mad2 protein into mammalian cells in mitosis induces premature anaphase." J Cell Biol, 141(5), 1193-205.

Goshima, G., and Yanagida, M. (2000). "Establishing biorientation occurs with precocious separation of the sister kinetochores, but not the arms, in the early spindle of budding yeast." Cell, 100(6), 619-33.

Hardwick, K. G., Weiss, E., Luca, F. C., Winey, M., and Murray, A. W. (1996). "Activation of the budding yeast spindle assembly checkpoint without mitotic spindle disruption." Science, 273(5277), 953-6.

Hartwell, L. H., and Kastan, M. B. (1994). "Cell cycle control and cancer." Science, 266(5192), 1821-8.

He, X., Asthana, S., and Sorger, P. K. (2000). "Transient sister chromatid separation and elastic deformation of chromosomes during mitosis in budding yeast." Cell, 101(7), 763-75.

Howell, B. J., Hoffman, D. B., Fang, G., Murray, A. W., and Salmon, E. D. (2000). "Visualization of Mad2 dynamics at kinetochores, along spindle fibers, and at spindle poles in living cells." J Cell Biol, 150(6), 1233-50.

Hoyt, M. A., Totis, L., and Roberts, B. T. (1991). "S. cerevisiae genes required for cell cycle arrest in response to loss of microtubule function." Cell, 66(3), 507-17.

Hwang, L. H., Lau, L. F., Smith, D. L., Mistrot, C. A., Hardwick, K. G., Hwang, E. S., Amon, A., and Murray, A. W. (1998). "Budding yeast Cdc20: a target of the spindle checkpoint." Science, 279(5353), 1041-4.

Jin, D. Y., Spencer, F., and Jeang, K. T. (1998). "Human T cell leukemia virus type 1 oncoprotein Tax targets the human mitotic checkpoint protein MAD1." Cell, 93(1), 81-91.

Jordan, M. A., Wendell, K., Gardiner, S., Derry, W. B., Copp, H., and Wilson, L. (1996). "Mitotic block induced in HeLa cells by low concentrations of paclitaxel (Taxol) results in abnormal mitotic exit and apoptotic cell death." Cancer Res, 56(4), 816-25.

Kalitsis, P., Earle, E., Fowler, K. J., and Choo, K. H. (2000). "Bub3 gene disruption in mice reveals essential mitotic spindle checkpoint function during early embryogenesis." Genes Dev, 14(18), 2277-82.

Kaplan, K. B., Burds, A. A., Swedlow, J. R., Bekir, S. S., Sorger, P. K., and Nathke, I. S. (2001). "A role for the Adenomatous Prolyposis Coli protein in chromosome segregation." Nat Cell Biolog, 3(4), 429-32.

Kitagawa, R., and Rose, A. M. (1999). "Components of the spindle-assembly checkpoint are essential in Caenorhabditis elegans." Nat Cell Biolog, 1(8), 514-521.

Kuhn, R., Schwenk, F., Aguet, M., and Rajewsky, K. (1995). "Inducible gene targeting in mice." Science, 269(5229), 1427-9.

Li, R., and Murray, A. W. (1991). "Feedback control of mitosis in budding yeast." Cell, 66(3), 519-31.

Li, Y., and Benezra, R. (1996). "Identification of a human mitotic checkpoint gene: hsMAD2." Science, 274(5285), 246-8.

Martinez-Exposito, M. J., Kaplan, K. B., Copeland, J., and Sorger, P. K. (1999). "Retention of the BUB3 checkpoint protein on lagging chromosomes." Proc Natl Acad Sci U S A, 96(15), 8493-8.

Michel, L.S., Liberal, V., Chatterjee, A., Kirchwegger, R., Pasche, B., Gerald, W., Dobles, M., Sorger, P.K., Murty, V.V., Benezra, R. (2001). "MAD2 haplo-insufficiency causes premature anaphase and chromosome instability in mammalian cells." Nature 409, 355-9.

Nowell, P. C. (1976). "The clonal evolution of tumor cell populations." Science, 194(4260), 23-8.

Rieder, C. L., Schultz, A., Cole, R., and Sluder, G. (1994). "Anaphase onset in vertebrate somatic cells is controlled by a checkpoint that monitors sister kinetochore attachment to the spindle." J Cell Biol, 127(5), 1301-10.

Roberts, B. T., Farr, K. A., and Hoyt, M. A. (1994). "The Saccharomyces cerevisiae checkpoint gene BUB1 encodes a novel protein kinase." Mol Cell Biol, 14(12), 8282-91.

Shonn, M. A., McCarroll, R., and Murray, A. W. (2000). "Requirement of the spindle checkpoint for proper chromosome segregation in budding yeast meiosis." Science, 289(5477), 300-3.

Spencer, F., and Hieter, P. (1992). "Centromere DNA mutations induce a mitotic delay in Saccharomyces cerevisiae." Proc Natl Acad Sci U S A, 89(19), 8908-12.

Straight, A. F., Marshall, W. F., Sedat, J. W., and Murray, A. W. (1997). "Mitosis in living budding yeast: anaphase A but no metaphase plate." Science, 277(5325), 574-8.

Taylor, S. S., Ha, E., and McKeon, F. (1998). "The human homologue of Bub3 is required for kinetochore localization of Bub1 and a Mad3/Bub1-related protein kinase." J Cell Biol, 142(1), 1-11.

Taylor, S. S., and McKeon, F. (1997). "Kinetochore localization of murine Bub1 is required for normal mitotic timing and checkpoint response to spindle damage." Cell, 89(5), 727-35.

Wang, Y., and Burke, D. J. (1995). "Checkpoint genes required to delay cell division in response to nocodazole respond to impaired kinetochore function in the yeast Saccharomyces cerevisiae." Mol Cell Biol, 15(12), 6838-44.

Weiss, E., and Winey, M. (1996). "The Saccharomyces cerevisiae spindle pole body duplication gene MPS1 is part of a mitotic checkpoint." J Cell Biol, 132(1-2), 111-23.

Wells, W. A., and Murray, A. W. (1996). "Aberrantly segregating centromeres activate the spindle assembly checkpoint in budding yeast." J Cell Biol, 133(1), 75-84.

Woods, C., Zhu, J., McQueney, P.A., Bollag, D., Lazarides, E. (1995). "Taxol-induced mitotic block triggers rapid onset of a p53-independent apoptotic pathway." Molecular Medicine, 1, 506-526.